SYNTHESIS AND CHARACTERIZATION OF ORTHO-PHENYLENEETHYNYLENES AND DIPHENYLAMINE POLYMERS

A Dissertation
Presented to
The Academic Faculty

by

Sandra Leigh Shotwell

In Partial Fulfillment
of the Requirements for the Degree
Doctorate of Philosophy in the
School of Chemistry and Biochemistry

Georgia Institute of Technology
May 2006

SYNTHESIS AND CHARACTERIZATION OF ORTHO-PHENYLENEETHYNYLENES AND DIPHENYLAMINE POLYMERS

Approved by:

Dr. Uwe H. F. Bunz, Advisor
School of Chemistry and Biochemistry
Georgia Institute of Technology

Dr. Laren Tolbert
School of Chemistry and Biochemistry
Georgia Institute of Technology

Dr. Joseph Perry
School of Chemistry and Biochemistry
Georgia Institute of Technology

Dr. Anselm Griffin
PTFE
Georgia Institute of Technology

Dr. David Collard
School of Chemistry and Biochemistry
Georgia Institute of Technology

Date Approved: January 13, 2006

To my father, Robert Ray Shotwell
And my sister, Dr. Mary Beth Shotwell Hillhouse

And in memory of my mother,
Marilyn Grace Stovall Shotwell

ACKNOWLEDGEMENTS

I would like to thank my advisor Dr. Uwe Bunz for a very interesting and unpredictable graduate experience. Also thank you to my committee, Dr. David Collard, Dr. Anselm Griffin, Dr. Joseph Perry, and Dr. Laren Tolbert.

I would like to thank the members of the Bunz Group for their support over the last few years. Thanks goes to Dr. Selma Bakbak and Dr. Belma Erdogan for all of their support, Turkish language and cooking lessons, and fashion advice. Also I would like to thank Dr. Carlito Bangcuyo for helping me with columns and iodinations and conversations over Chicken Philly Specials. Thanks is also due to Dr. Paul M. Windscheif for getting me acclimated to the lab and helping me with my chemistry, and to Dr. Glen Brizius for helping me set up my station in an empty room. I would also like to thank current Bunz group members Jake Leech and Ronnie Phillips for giving me a home after I had moved away. Thanks to Wang for helping me during my last few months in the Bunz lab. Dr. Shaobin Miao, thank you for helping me on my presentations. Thanks to AJ Zuccherro and Brad Carson for filling the other side of my lab and being great labmates. I would like to thank Anna Dunkhorst and Dr. Stefan Scholz for all of their help. Thanks to Dr. Ik-Bum Kim for the conversations. Thank you and good luck the new members, Scott Brombosz and Psarus McGrier. Thanks goes to former Bunz Group Members, Dr. James Wilson, Dr. Winni Steffen, Dr. Neil Pschirer, Dr. Shane Waybright, Dr. Matt Laskoski, Dr. Holly Ricks, and Dr. Ruta Bly,

During my research I have been fortunate enough to collaborate with Dr. zur Loye's group at the University of South Carolina. I had a fruitful collaboration with Dr. Jeffery

Fiscus and Andrea Goforth who formed metal coordination compounds with my ligands. Also I was fortunate to have the help of an excellent crystallographer, Dr. Mark Smith, who determined all of the crystal data seen here in this thesis.

I would like to thank my family. Thank you to my sister, Dr. Mary Beth Shotwell Hillhouse, for offering me healthy competition during my childhood and into my adult life. My mother, Marilyn Shotwell always valued education and spent hours after teaching her own students helping me with my studies. I would not be where I am today without her help. I want to thank my father Ray Shotwell for giving me guidance and advice during my life and academic career.

Finally I would like to thank my husband, Dr. Michael Bleiweiss, for his continuous support during my time in graduate school.

TABLE OF CONTENTS

LIST OF TABLES

LIST OF FIGURES

LIST OF SCHEMES

LIST OF SYMBOLS AND ABBREVIATIONS

DMF	dimethylformamide
DPA	diphenyl amine
GPC	gel-permeation chromatography
IR	infrared spectroscopy
LED	light-emitting diode
Mp	melting point
MS	mass spectrometry
NMR	nuclear magnetic resonance
OPE	*ortho*-phenyleneethynylene
PAE	poly(arylene ethynylene)
PPE	poly(para-phenyleneethynylene)
TPA	triphenyl amine
THF	tetrahydrofuran
TMS	trimethylsilyl
TMSA	trimethylsilylacetylene
Uv-vis	ultra-violet visible
Φ	quantum yield

SUMMARY

In the first part of this thesis, the synthesis, characterization and investigation of *ortho*-phenyleneethynylenes containing heterocycles, are presented. These compounds display changes in absorption and emission spectra varying with their functionalization and size. These compounds also have the ability to coordinate with metals. The synthesis of coordination compounds and their crystallographic data are reported. The synthesis and characterization of tetraethynyl thiophene compounds containing pyridines are also presented. These compounds exhibit differences in absorption and emission spectra upon exposure to various metal salts. The final topic to be discussed is the synthesis and characterization of diphenyl amine polymers. These polymers could in principle be used in NLO applications or light emitting devices.

CHAPTER 1

INTRODUCTION

This work presents the synthesis and characterization of *ortho*-phenyleneethynylenes, thiophene ligands, and diphenyl amine (DPA) polymers. All of these compounds demonstrate interesting characteristics in absorption and emission spectra in solution, solid state and with the addition of trifluoroacetic acid or metals. These compounds also show promise in the use of LEDs and metal sensing.

This synthesis of *ortho*-phenyleneethynylenes, thiophene ligands, and diphenyl amine (DPA) polymers are constructed using the Heck-Cassar-Sonogashira-Hagihara palladium catalyzed reaction. This coupling reaction of terminal akynes to aromatic bromides or iodides has been known since 1975.[1-3] The catalytic cycle can be seen in Scheme 1.[4] In the first step, the alkyne is treated with CuI and an amine to form the cuprated alkyne **A** which then undergoes transmetallation with the palladium catalyst to form a dialkyne and the active Pd(0) species **C**. The active catalyst, **C**, undergoes oxidative addition with an aryl bromide or iodide to form the intermediate **D**. This intermediate **D** then participates in transmetallation with **A** to give the diorgano-Pd species **E**, which then undergoes reductive elimination to form the product, **F**. The Pd(0) catalyst, **C**, is regenerated in the final step.

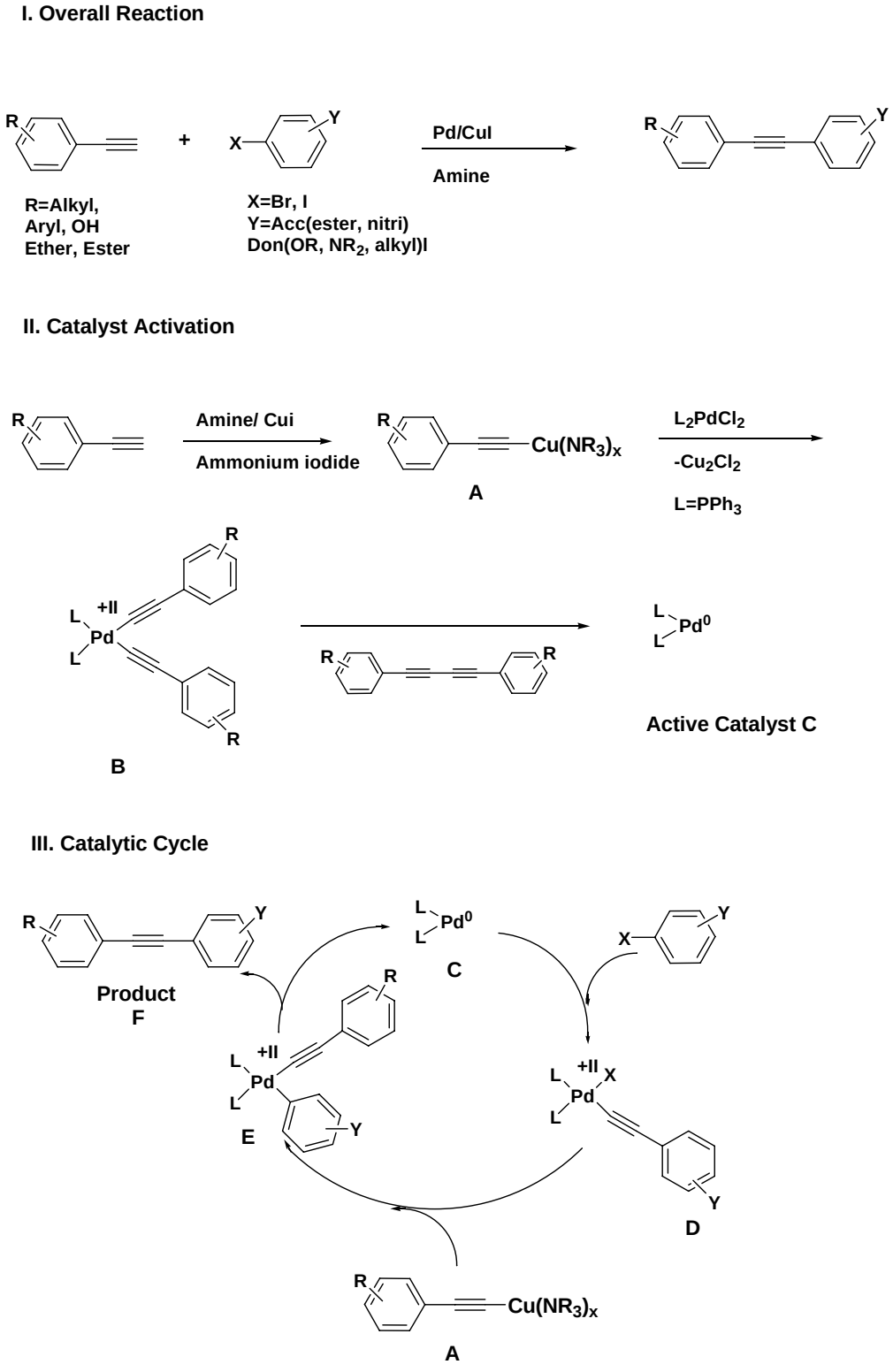

Figure 1.1: Catalytic coupling scheme for the Heck-Cassar-Sonogashira-Hagihara Reaction

The first compounds to be presented are *ortho*-phenylene ethynylenes. Chapter 2 presents the synthesis, absorption and emission spectra, and solid state crystal data for a series of six trimeric OPE's containing pyridine, pyrimidines, and pyrazines. In Chapter 3 the focus is turned towards synthesizing longer OPEs from trimer through heptamer (Figure 2.2).[5] It is of importance to design compounds which are both flexible, easily processed, yet do not require the presence of side chains. OPEs may fulfill these requirements. These types of compounds have a large outside surface, and almost no accessible interior cavity which is similar to α-helical protein structures. OPEs promise ample discoveries with respect to solid-state ordering and supramolecular nano engineering, materials properties, and applications in solid state devices such as LEDs.

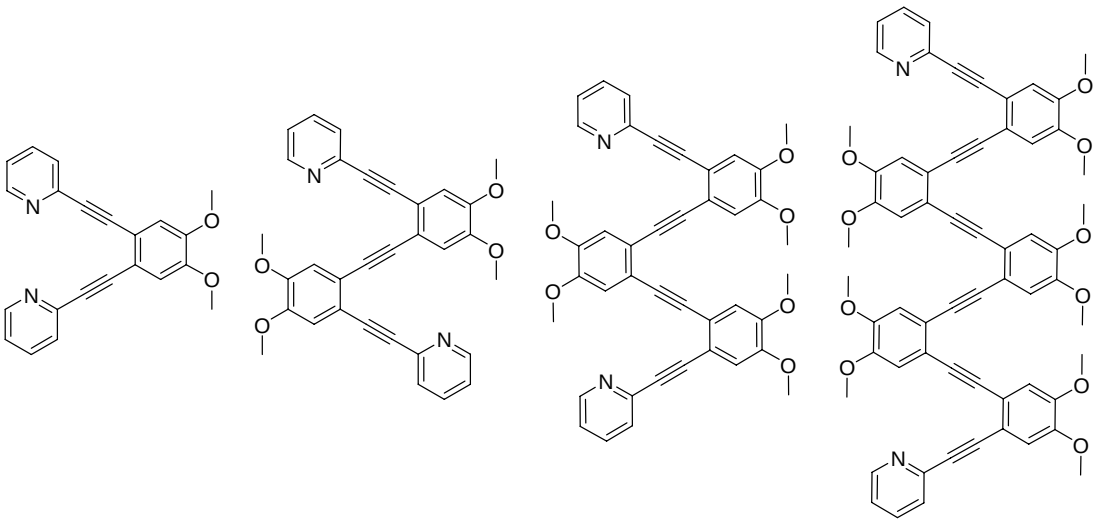

Figure 1.2: Pyridine capped OPEs

It was of interest to determine what sort of conformations could be obtained around a metal center utilizing OPEs as a ligand. Chapter 4 demonstrates the various conformations formed by using an OPE trimer with various metals to form a ring, a dimer, and a polymer (Figure 1.3)[6,7]. These such compounds can be used in supramolecular assembly of conjugated organic ligands toward novel photonic, electroactive, and structural materials[8-10]. Here the crystal data and synthesis of such compounds are described.

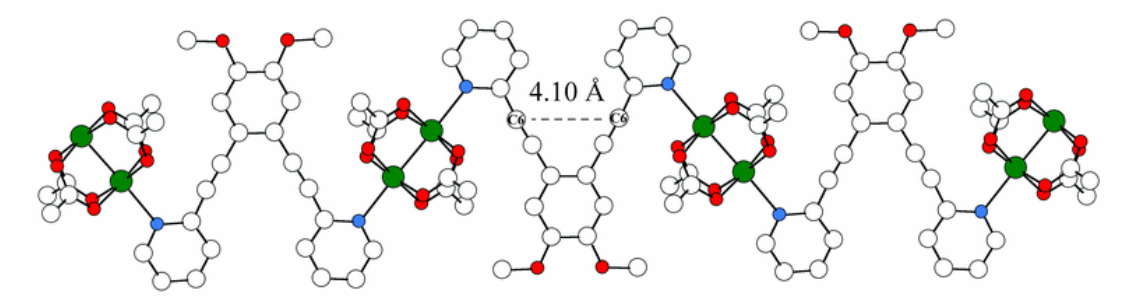

Figure 1.3: OPE polymer containing $Rh_2(OAc)_2$

Chapter 5 presents the synthesis of thiophene containing ligands which contain four pyridyl rings. The synthesis, absorption and emission spectra are presented as well as studies on the effect of metals on these compounds in solution. (Figure 1.4). By using different pyridines, the sensing ability for various metals is changed. These four metal binding sites demonstrate bathocrhomic shifts in absorption and emission based on the equivalents of metals used. These compounds show promise in future use in metal sensing.

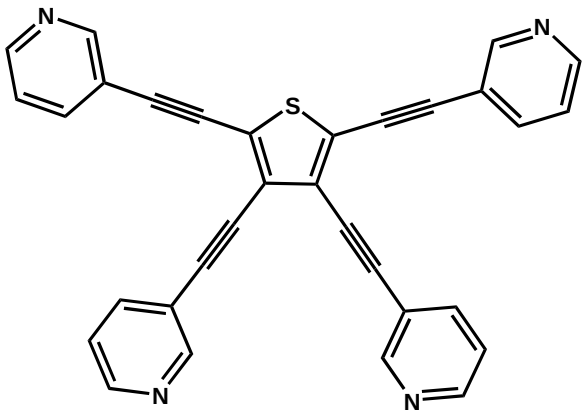

Figure 1.4: A thiophene containing ligand

The final chapter discusses the synthesis and characterization of polyaryleneethynylenes (PAEs) which contain diphenyl amines with various comonomers. Tertiary amines have been known to be suitable hole-transporting layers in the construction of organic LEDs. [11-13] Incoorperating a tertiary amine into the polymer backbone show a low threshold voltage compared with other polymers. One cause for this low threshold voltage is the π-electron delocalization between the nitrogen lone pair and the π-electrons in the conjugated units. In the case of the polymers presented in this thesis, the aromatic units are composed of one of the following: alkyl or alkoxy benzene, alkyl fluorene, or fluorenone. These types of polymers could be valuable in the area of polymeric electroluminescent devices because flat thin-film devices can be manufactured with reduced cost and weight.

2.5 References

1. Dieck, H. A.; Heck, R. F. *J Organnomet. Chem*. **1975**, *94*, 259.

2. Cassar, I. *J. Organnomet. Chem*. **1975**, *93*, 253.

3. Sonogashira, K.; Tohda, Y.; Hagihara, N. *Tetrahedron Lett*. **1975**, *16*, 4467.

4. Bunz, U. H. F. *Chem. Rev.* **2000**, *100*, 1605-1644.

5. Shotwell, S.; Windscheif, P. M.; Smith, M. D.; Bunz, U. H. F., *Org. Lett*. **2004**, *6*, 4151.

6, Fiscus, J. E.; Shotwell, S.; Layland, R. C.; Smith, M. D.; zur Loye, H.-C.; Bunz, U. H. F., *Chem. Commun*. **2001**, 2674.

7. Shotwell, S.; Ricks, H. L.; Morton, J.; Laskoski, M.; Fiscus, J.; Smith, M. D.; Shimizu, K. D.; zur Loye, H, C.; Bunz , U. H. F.; *J. Organomet. Chem.* **2003**, *671*, 43-51.

8. Kitamura, H.; Ozawa, T.; Jitsukawa, K.; Masuda, H.; Aoyama, Y.; Einaga, H., *Inorg. Chem*. **2000**, *39*, 3294.

9. Fiscus, J. E.; Shotwell, S.; Layland, R. C.; Smith, M. D.; zur Loye, H.-C.; Bunz, U.H. F., *Chem. Commun*. **2001**, 2674.

10. Roh, S.-G.; Nah, M.-K.; Oh, J. B.; Baek, N. S.; Park, K.-M.; Kim, H. K., Polyhedron **2005**, 24, 137

11. C.W. Tang, S.A. Van slyke, Appl. Phys. Lett. 51 1987 913

12. C. Adachi, T. Tsutsui, S. Aito. Appl. Phys. Lett. 55 1989 1489.

13. C. Adachi, S. Tokito. T. Tsutsui. S. Sait. Jpn. J. Appl. Phys. 27 1988 L269.

CHAPTER 2

ORTHO-PHENYLENEETHYNYLENE TRIMERS CONTAINING PYRIDINE, PYRIMIDINE AND PYRAZINE

2.1 Introduction

The synthesis and characterization of six *ortho*-phenyleneethynylene trimeric ligands consisting of various nitrogen containing heterocycles (pyridines, pyrimidines, and pyrazines) with a benzene center are presented. The absorption and emission spectra exhibit a pH dependency. Ligands of this type have been studied for their uses in metal coordination by the groups of Bosch, Bunz and others.[1-6] Metal coordination to ligands such as these will be discussed in the next chapter. More recently compounds containing enediyne scaffolding have been studied due to their similarities to families of molecules which display biological functions. These compounds, which are similar to the ones presented in this chapter, demonstrated inhibition of the growth of 60 different cancers. These molecules are stable, relatively facile to synthesize, blue emitting in solution and yellow emitting in the solid state and show promise for use in organic displays.

2.2 Results and Discussion

The synthesis of OPE trimers begins with synthesis of a halogenated centerpiece from 1,2-dimethoxybenzene **2.1** to form **2.2** by utilizing standard iodination conditions[9]. The two nitrogen containing heterocyclic arms are produced by the alkynylation of the halogenated pyridines **2.3**, **2.5**, **2.7** and pyrimidines **2.9** and **2.11** using the Heck-Cassar-Sonogashira-Hagihara (HCSH)[7,8] coupling reaction to form the corresponding compounds **2.4**, **2.6**, **2.8**, and **2.10**. Due to the fact that chloro-heterocycles are not as reactive under HCSH conditions, it was necessary to perform a halogen exchange using chloropyrazine **2.13** to obtain iodopyrazine **2.14** using NaI, H_2SO_4, acetic acid and acetonitrile. From **2.14** the production of the alkynylated species **2.15** was feasible in a 72% yield.

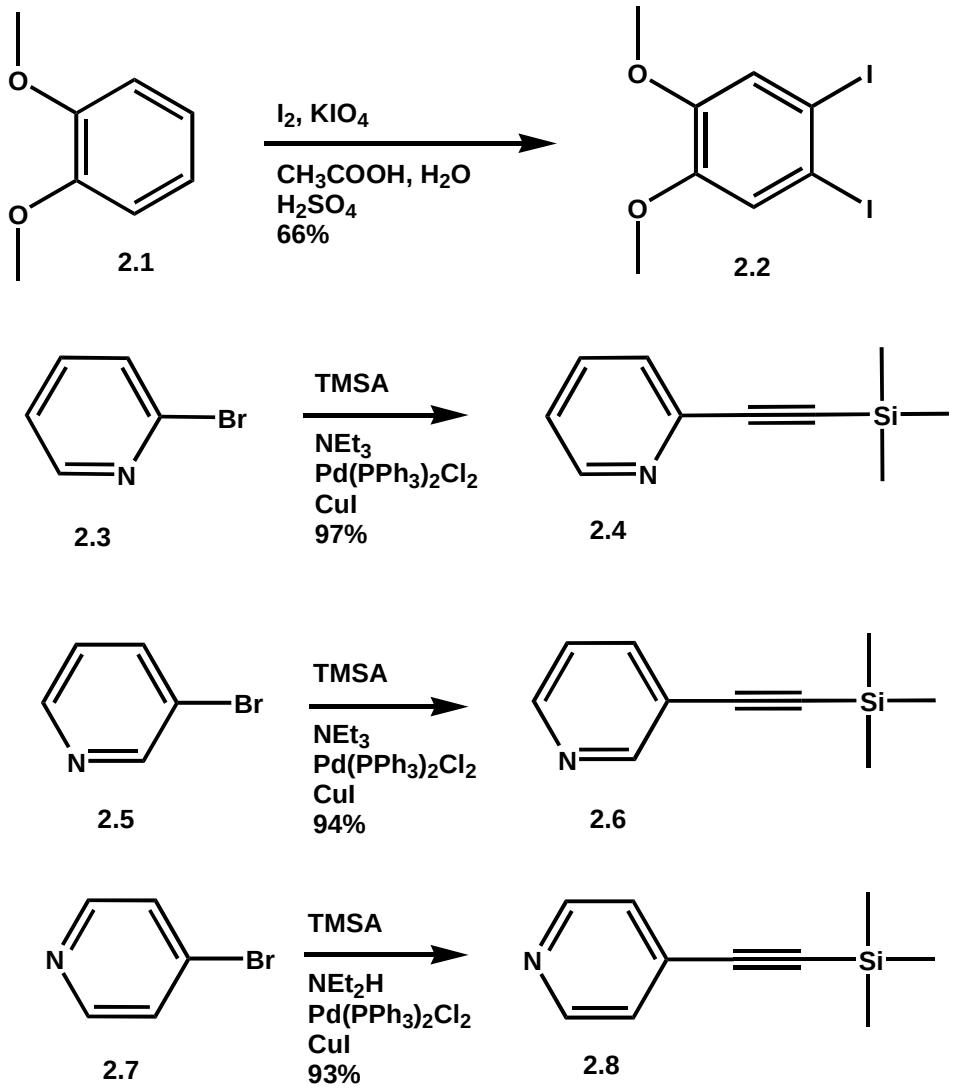

Scheme 2.1: Synthesis of heterocyclic arms and centerpiece.

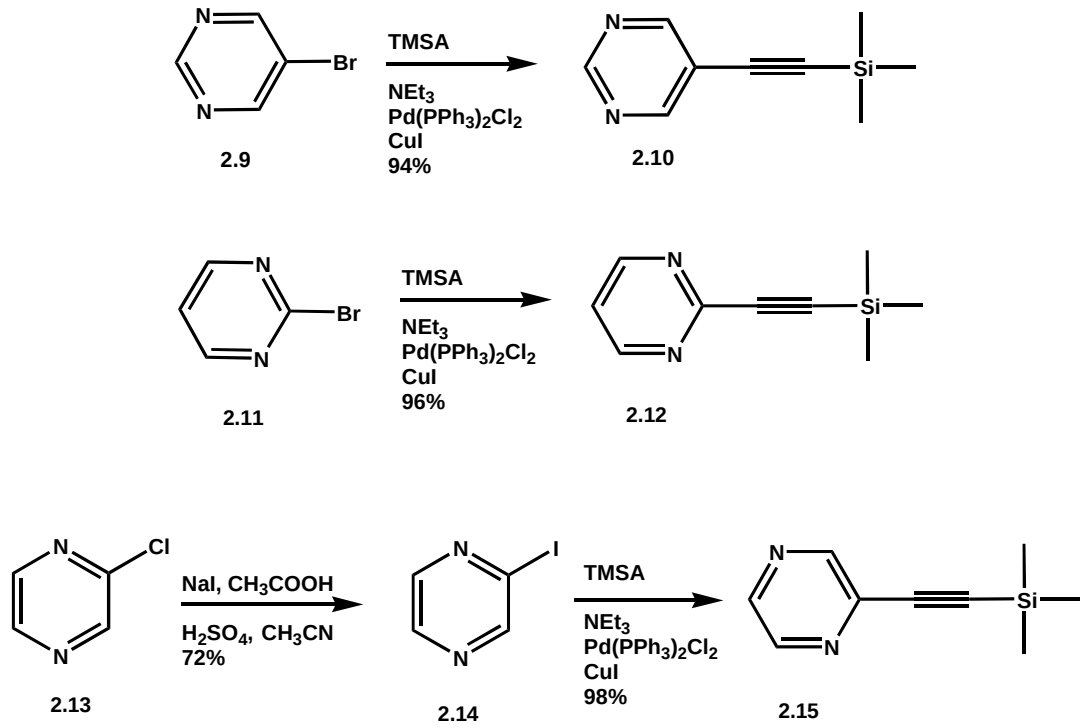

Scheme 2.2: Synthesis of alkynylated heterocyclic arms.

As seen in Scheme 2.1 and Scheme 2.2 the arms are attached to the centerpiece by coupling **2.2** using the *in situ* deprotection and coupling reaction developed by Waybright.[10] The synthesis begins with the *in situ* deprotection and coupling reaction 2-trimethylsilylethynyl pyridine **2.4** with the diiodo compound **2.2,** using 0.5 equivalents of the diiodo compound**.** (Scheme 2.1) The trimethylsilyl group of **2.4** is cleaved *in situ*, while coupling by the addition of KOH in ethanol to the reaction mixture. The Pd-catalyst does not appear to be affected by the presence of the hydroxide. This reaction yields the trimer **2.16** in a 73% yield. This ligand is proved to be valuable in coordination chemistry as will be seen in Chapter 3. The synthesis of five additional

ligands, **2.17**-**2.21**, of this type can be seen in Scheme 2.2. The synthesis is similar to the synthesis of **2.16** and the yields are reasonable.

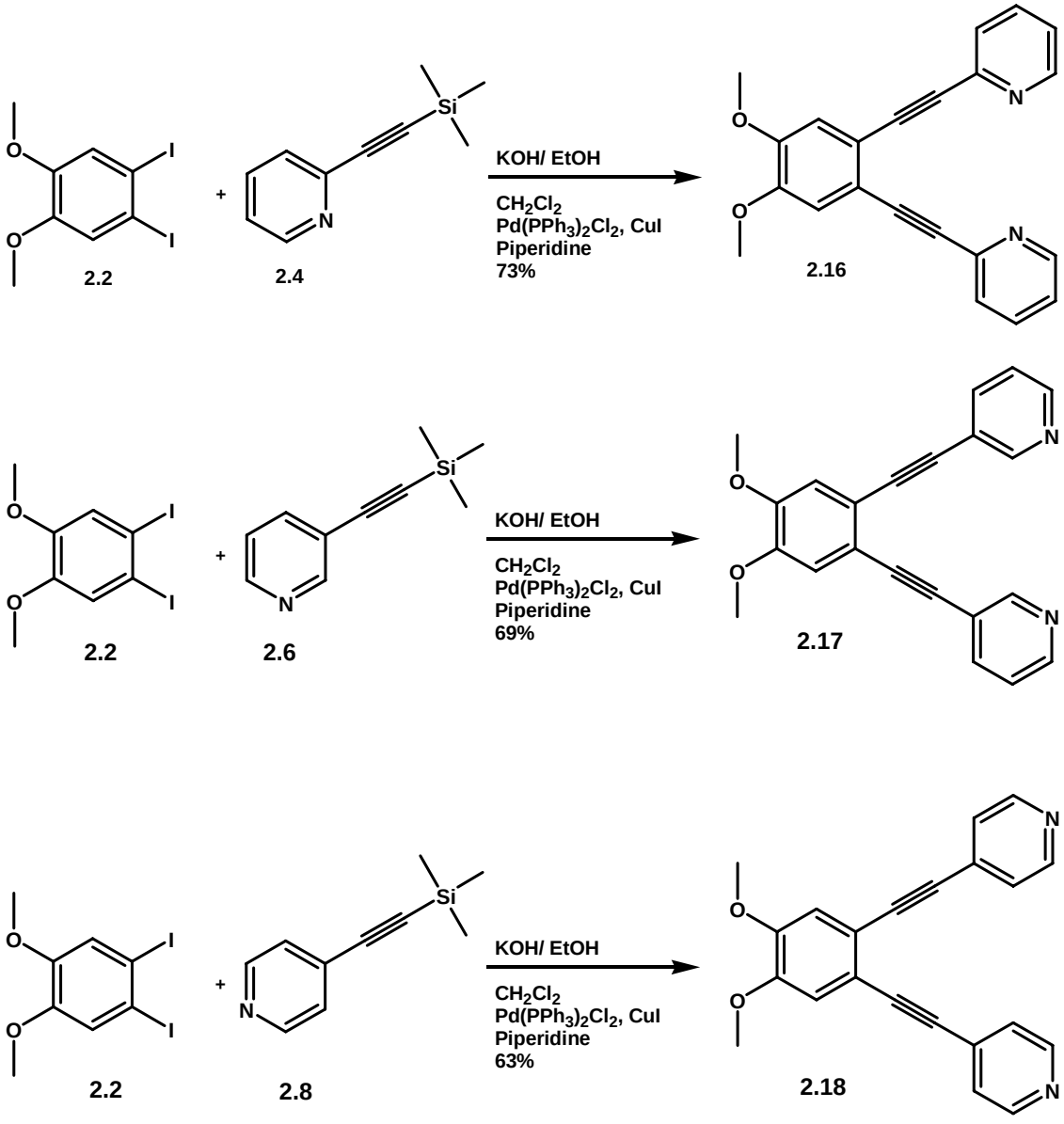

Scheme 2.3: Synthesis of trimeric ligands (cont.).

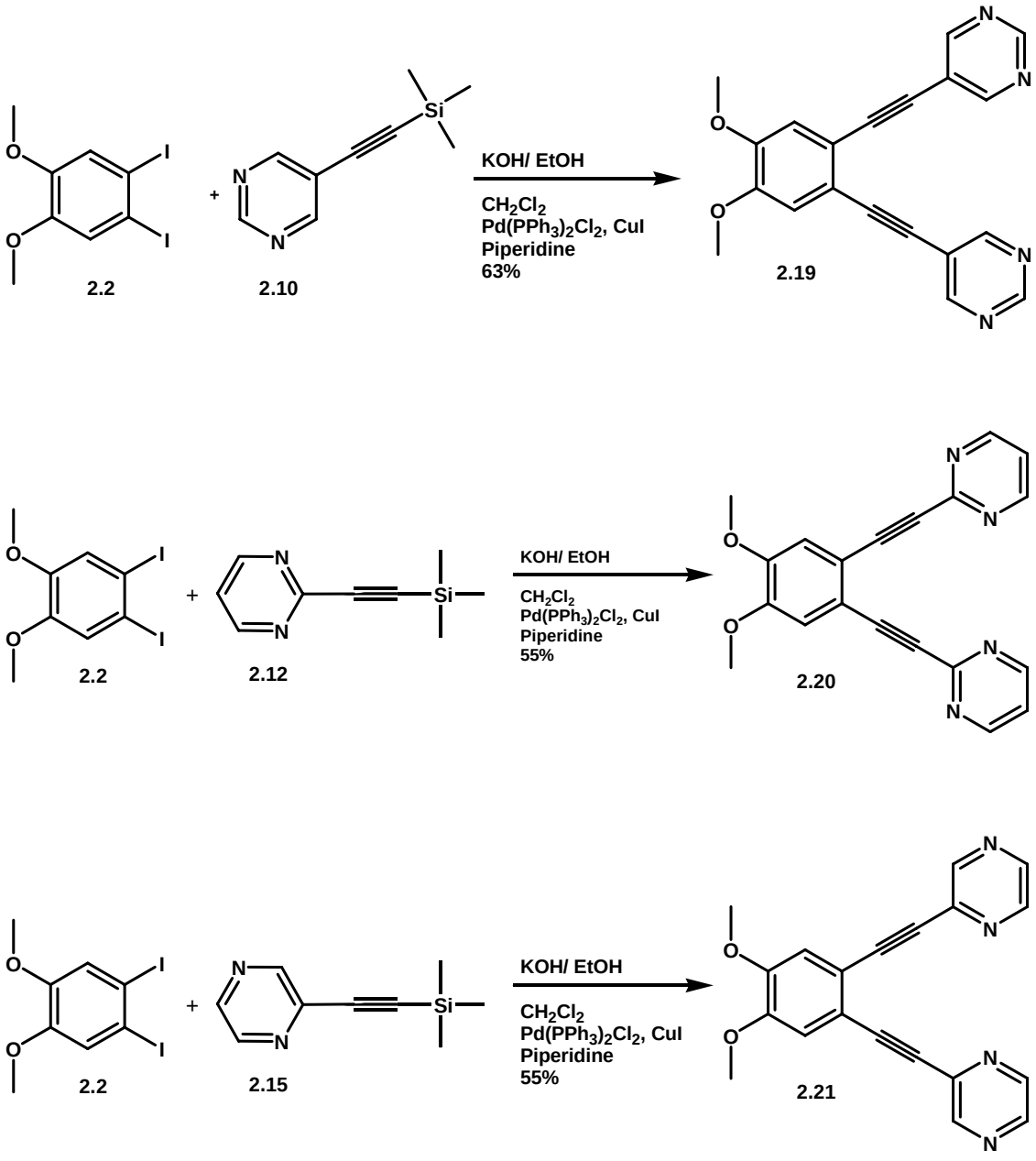

Scheme 2.4. Synthesis of trimeric ligands (cont.).

The crystal structures of three of these ligands, **2.16, 2.17,** and **2.18** can be seen in Figure 1.1. In **2.16**, the molecule is nearly planar, and the nitrogens of the pyridines are rotated away from each other. In the case of **2.17**, the pyridines are slightly twisted with

the nitrogens facing towards one another. The crystal structure of **2.18** reveals that one of the pyridine rings is twisted out of the plane.

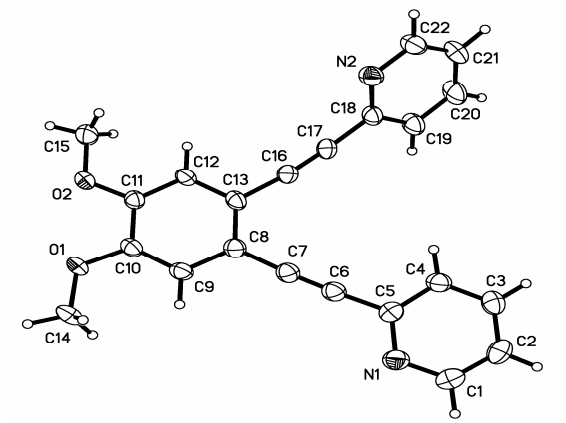

a).

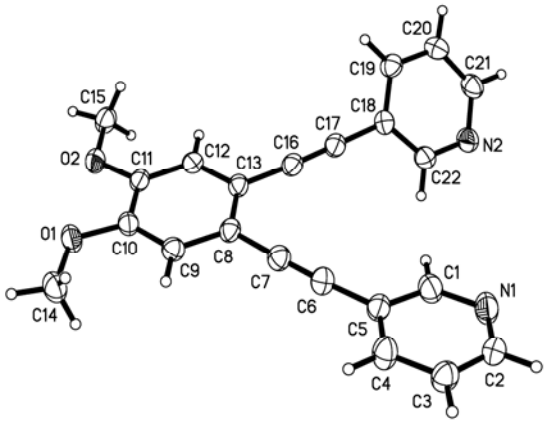

b).

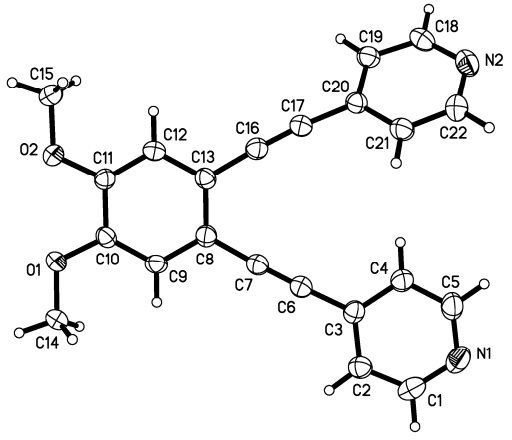

c)

Figure 2.1: Crystal structures of a) **2.16**, b)**2.17**, c)**2.18**.

The absorption spectra of the six trimers can be seen in Figure 2.2. The absorption spectra for **2.16** and **2.18** are more well defined where as **2.18** is more broad and less defined. This is probably due to the *ortho-meta* positioning in **2.16** and **2.18** of the nitrogen of the pyridines in relation to the alkyne arms of the molecule. All trimers except **2.21** demonstrate a maximum absorption around 260, 290, and 340 nm. A red shift from this wavelength to 280, 310, and 360 nm can be seen in the spectra of the pyrazine ligand **2.21**. Upon addition of trifluoroacetic acid a red shift and a broadening of the spectra is observed for all ligands except for **2.16** which sees a shift to 250, 300, and 335 (Figure 2.2).

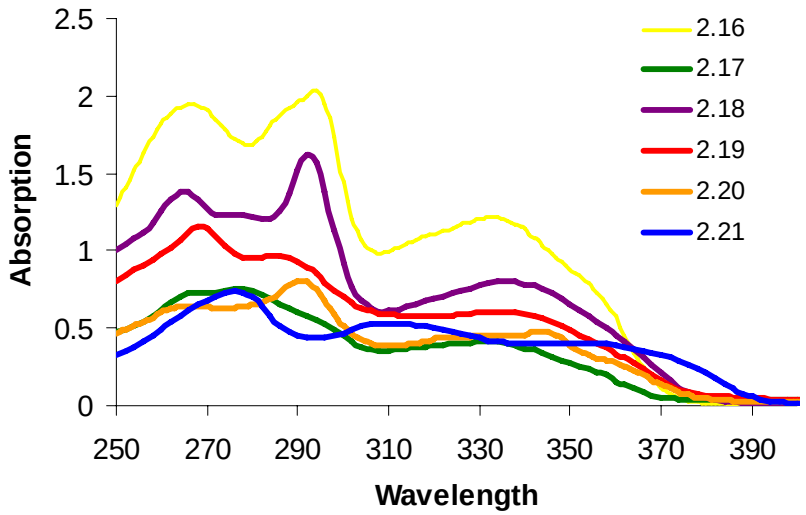

Figure 2.2: Absorption spectra of trimers in chloroform

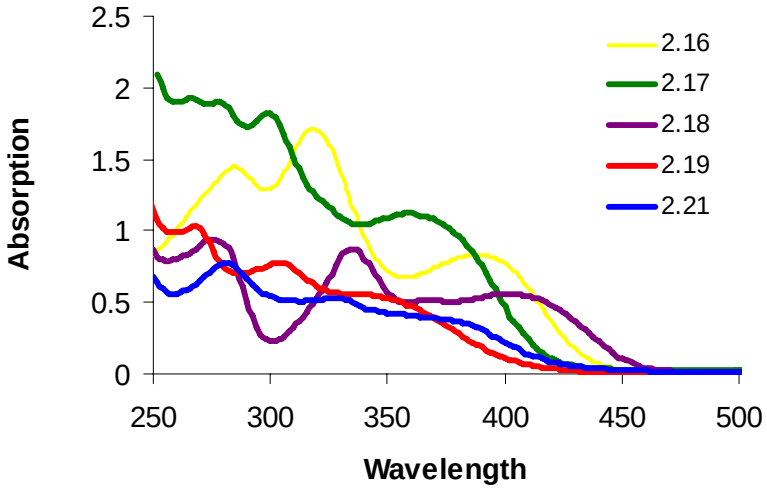

Figure 2.3: Absorption spectra of trimers in chloroform with the addition of trifluoroacetic acid

All six ligands are blue emissive in a solution of chloroform. In the solid state these ligands are yellow emissive. Once the ligands are protonated with trifluoroacetic acid, the fluorescence for all ligands is quenched due to the break in conjugation except for **2.16**. The reason for this shift in emission will be discussed further in Chapter 3.

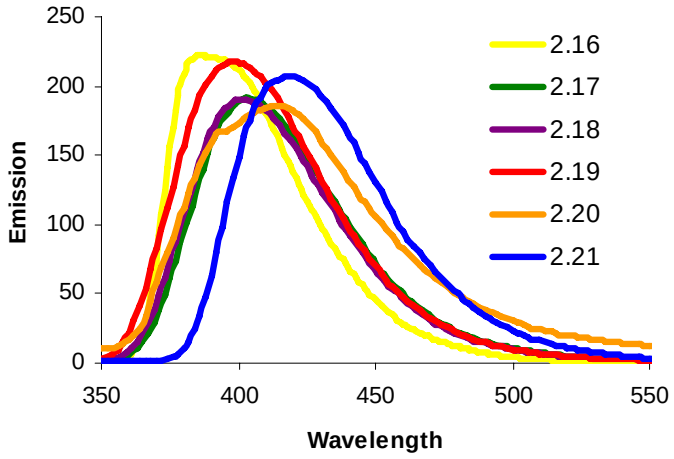

Figure 2.4: Emission spectra of trimer ligands in chloroform.

2.3 Conclusion

The synthesis, photophysical data and solid state structures for six *ortho*-phenyleneethynylene trimer compounds have been presented. These compounds are very interesting in that they are of similar shape and demonstrate different absorption and emission spectra by modifying the heterocyclic arms. In Chapter 3, **2.16** is presented again with its tetrameric, pentameric and heptameric forms. This trimer **2.16** will be seen again in coordination with various metals in Chapter 4.

2.4 Experimental

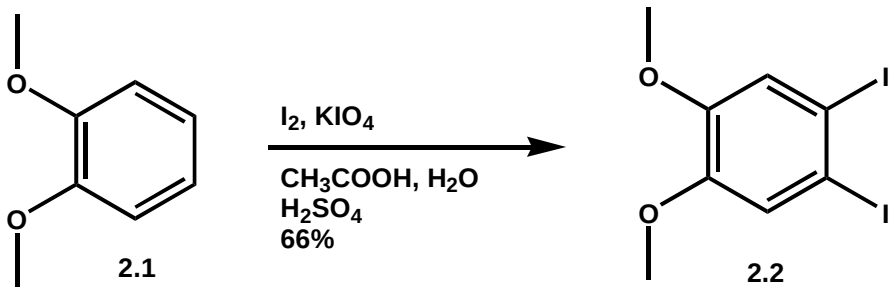

1,2-Diiodo-3,4-dimethoxybenzene (**2.2**)[9]. 1,2-dimethoxybenzene **2.1** (50g, 362mmol), I_2 (127.1g, 360 mmol), KIO_4 (82.8g, 360 mmol) were dissolved in 450ml (90%) acetic acid, 35 ml (7%) water and 15 ml (3%) H_2SO_4 in a 1000 ml three-necked round bottom flask equipped with a condenser. The flask is heated using an oil bath at 80°C for 48 h. The reaction mixture is washed with aqueous $NaSO_3$ and extracted with $CHCl_3$. The organic layer is neutralized with aqueous $NaHCO_3$. After removal of the solvent, *in vacuo* the product was pale yellow. Upon recrystallization from ethanol yields **2.2** as colorless crystals (94g, 66%). ^{1}H-NMR ($CDCl_3$, 300 MHz , 15 °C) δ 7.259 (s, 2H, aryl-H), 3.835 (s, 6H, OCH_3) ppm. ^{13}C-NMR ($CDCl_3$, 75 MHz, 20°C) 150.45, 121.32, 98.45, 52.67.

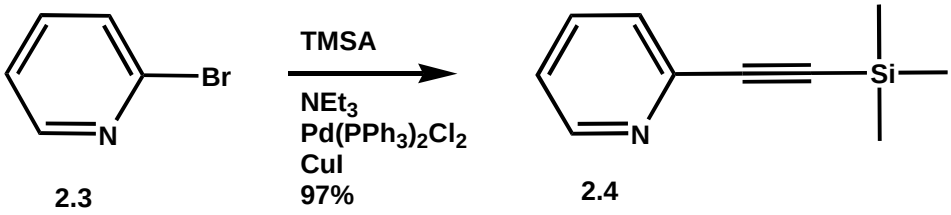

2-Trimethylsilylethynylpyridine (**2.4)** [11] 2-bromopyridine **2.3** (25g, 0.162 mol) is dissolved in NEt_3 (200 mL) in a Schlenk flask under N_2 atmosphere. Next, $Pd(PPh_3)_2Cl_2$ (0.57 g, .714 mmol.), CuI (0.308 g, 1.62 mmol) and PPh_3 (0.500 g) are added. The reaction is stirred for 16 h. at 60˚C. The resulting solution is washed with a 10% NH_4OH solution and extracted with hexanes (3x 200 mL). The organic layer is washed with water and extracted with hexanes (3x, 100 mL). The solvent is removed *in vaccuo.* The crude compound is purified by distillation to yield **2.4** as a colorless solid (27.5g, 0.157 mol) in a 97% yield. (^{1}H-NMR ($CHCl_3$, 300MHz) δ 8.43-8.40 (dt, 1H, pyridyl H), 7.48, 7.46,7.5 (t, 1H, pyridyl-H), 7.32-7.28 (dt, 1H, pyridyl-H), 7.09-7.05 (m, 1H, pyridyl-H), 0.01 (9H, Si-CH_3-H). ^{13}C-NMR ($CDCl_3$, 75 MHz, 20°C) 150.17, 143.29, 136.34, 127.51, 123.31, 104.03, 94.87, 0.07. Mp=29˚C.

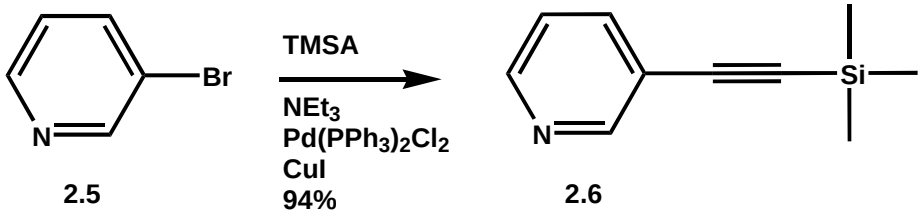

3-bromopyridine **2.5** (5 g, 32.5 mmol)[12] is dissolved in NEt_3 in a 50 mL Schlenk flask under nitrogen atmosphere. Next, $Pd(PPh_3)_2Cl_2$ (0.11 g, 0.143 mmol.), CuI (0.061 g, 0.324 mmol) and PPh_3 (0.100 g) are added. The reaction is stirred for 16 h. at 70˚C for 24 h. The solution is washed with 10% NH_4OH solution and extracted with hexanes. The

solvent is removed and the crude liquid is distilled to give **2.6** (5.34 g, 30.5 mmol) as a colorless oil in a 94% yield. ^{1}H-NMR ($CHCl_3$, 300MHz) δ 8.61 (m, 1H, pyridyl-H), 8.52 (m, 1H, pyridyl-H), 7.66-7.63 (dt, 1H, pyridyl-H), 7.41-7.38 (m, 1H, pyridyl-H) 0.21 (s, 9H, Si-CH_3-H) ^{13}C-NMR ($CDCl_3$, 75 MHz, 20°C) 152.54, 148.66, 138.59, 122.78, 120.21, 101.58, 98.89, -0.19.

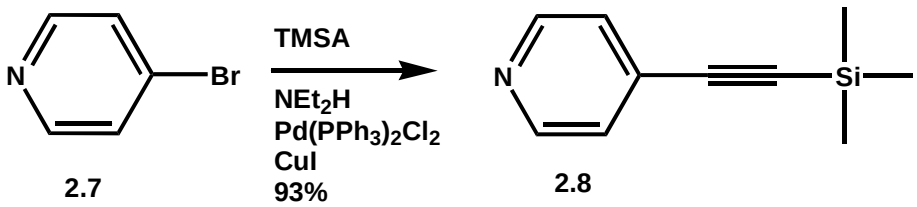

4-Trimethylsilylethynylpyridine (**2.8**)[11] In a 100 mL Schlenk flask under nitrogen atomsphere, 4-bromopyridine **2.7** (10g, 51.4 mmol) is dissolved in diethylamine (40 mL) in a 250 mL Schlenk flask under nitrogen atmosphere. Next, $Pd(PPh_3)_2Cl_2$ (0.359 g, 0.513 mmol.), CuI (0.098 g, 0.513 mmol) and PPh_3 (0.100 g) are added, and the reaction is capped. TMSA (15.29 mL, 102.8 mmol) is added to the reaction mixture via syringe. The reaction is stirred at 70 ˚C for 16 h. The solution is cooled to room temperature then washed with 10% NH_4OH solution and extracted with hexanes. The solvent is removed and the crude liquid is distilled under vacuum to furnish **2.8** (8.18g, 93%) as a colorless oil. ^{1}H-NMR ($CHCl_3$, 300MHz) δ 8.42, 8.41, 8.40 (t-pyridyl-H), 7.16, 7.15, 7.14 (t, pyridyl H), 0.12 (s, TMS-H) ^{13}C-NMR ($CDCl_3$, 75 MHz, 20°C) 149.41, 130.823, 101.73, 99.51, -0.60.

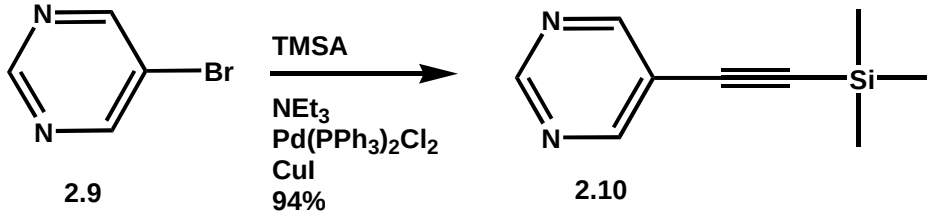

2.9 2.10

5-Trimethylsilylpyrimidine (2.10)[11] **2.9** is dissolved in a 250 mL Schlenk flask (5 g, 32.5 mmol) is dissolved in NEt_3 in a 50 mL Schlenk flask under nitrogen atmosphere. Next, $Pd(PPh_3)_2Cl_2$ (0.11 g, 0.143 mmol.), CuI (0.061 g, 0.324 mmol) and PPh_3 (0.100 g) are added. The reaction is stirred for 16 h. at 70˚C for 24 h. The solution is washed with 10% NH_4OH solution and extracted with hexanes. The solvent is removed and the crude liquid is distilled to give **2.10** (5.34 g, 30.5 mmol) as a colorless oil in a 94% yield. ^{1}H-NMR ($CHCl_3$, 300MHz) δ 9.04, 9.03, 9.02 (t, 1H, pyrimidyl-H), 8.82, 8.81 (d, 2H, pyrimidyl-H) 0.23 (s, 9H, $SiCH_3$-H) ^{13}C-NMR ($CDCl_3$, 75 MHz, 20°C) 160.32, 156.54, 118.34, 109.77, 94.23, 0.12.

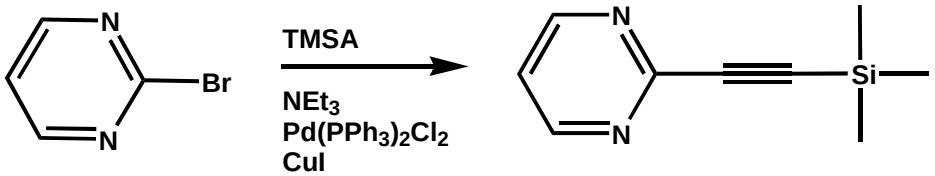

2.11 2.12

2-Trimethylsilylpyrimidine (2.12)[11] **2.9** is dissolved in a 250 mL Schlenk flask (2 g, 12.6 mmol) is dissolved in NEt_3 (15 mL) in a 50 mL Schlenk flask under nitrogen atmosphere. Next, $Pd(PPh_3)_2Cl_2$ (0.088 g, 0.126 mmol.), CuI (0.024 g, 0.126 mmol)

and PPh_3 (0.050 g) are added. The reaction is stirred for 16 h. at 70˚C for 24 h. The solution is washed with 10% NH_4OH solution and extracted with hexanes. The solvent is removed and the crude liquid is distilled to give **2.12** (2.13 g, 12.01 mmol) as a colorless solid in a 96% yield. ^{1}H-NMR ($CHCl_3$, 300MHz) δ 8.83, 8.82 (d, 2H, pyrimidyl-H) 7.19, 7.18, 7.16 (t, 1H, pyrimidyl-H), 0.28 (s, 9H, TMS-H) ^{13}C-NMR ($CDCl_3$, 75 MHz, 20°C) 158.42, 141.33, 102.43, 93.79, 0.11.

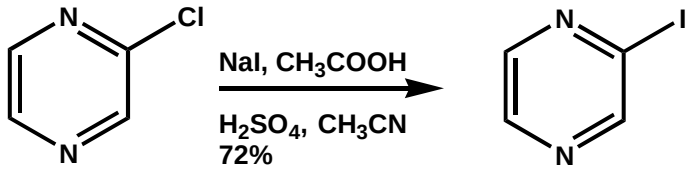

2.13 **2.14**

2-Iodopyrazine (**2.14**)[13] A 500 mL round bottom flask is equipped with a condenser, and a solution of acetonitrile (100mL), acetic acid (9.6mL) and NaI (30.0g, 0.200 mol) is added. 2-chloropyrazine **2.13** (9.63g, 84.0 mmol) is added last. The reaction is heated to reflux for 16 h. The reaction is cooled to RT, and the solvent is removed *in vaccuo.* Water (100 mL) and is added, and the solution is neutralized with $NaHCO_3$ and extracted with CH_2Cl_2. The CH_2Cl_2 solution is washed with a saturated solution of $Na_2S_2O_4$ and extracted with CH_2Cl_2. The solvent is removed *in vaccuo*. The product is distilled under vacuum to yield **2.14** (12.4 g, 60.3 mmol, 72%) as a colorless oil. ^{1}H-NMR ($CHCl_3$, 300MHz) δ 8.73 (q, 1H) 8.63-8.62 (dd, 1H), 8.16 (q, 1H). ^{13}C-NMR ($CDCl_3$, 75 MHz, 20°C)-153.08, 145.82, 142. 87, 118.49.

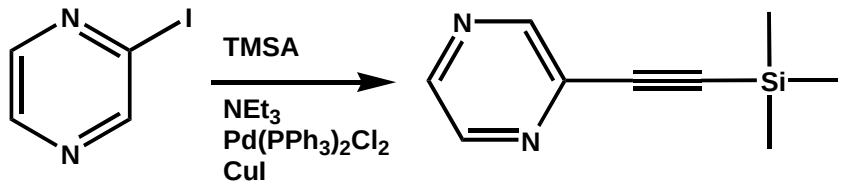

2.14 **2.15**

2-Trimethylsilylethynylpyrazine (**2.15**)[12] A Schlenk flask is flushed with nitrogen and **2.14** (4g, 19.5 mmol) is dissolved in NEt_3 (30 mL), $Pd(PPh_3)_2Cl_2$ (0.137g, 0.195 mmol), CuI (0.037g, 0.195 mmol) are added and the reaction is capped. TMSA (4.78g, 48.8 mmol) is added via syringe. The reaction is stirred for 16 h. at 70˚C for 24 h. The solution is washed with 10% NH_4OH solution and extracted with hexanes. The solvent is removed and the crude liquid is distilled to give **2.15** (3.36 g, 19.06 mmol) as a colorless solid in a 98% yield. ^{1}H-NMR ($CHCl_3$, 300MHz) δ 8.74 (m, 1H, pyrazyl-H), 8.63 (m, 1H, pyrazyl-H), 8.52 (m, 1H, pyrazyl-H), 0.31 (s, 9H, Si-CH_3-H). ^{13}C-NMR ($CDCl_3$, 75 MHz) 143.56, 142.84, 141.29, 104.34, 91.77, -0.28.

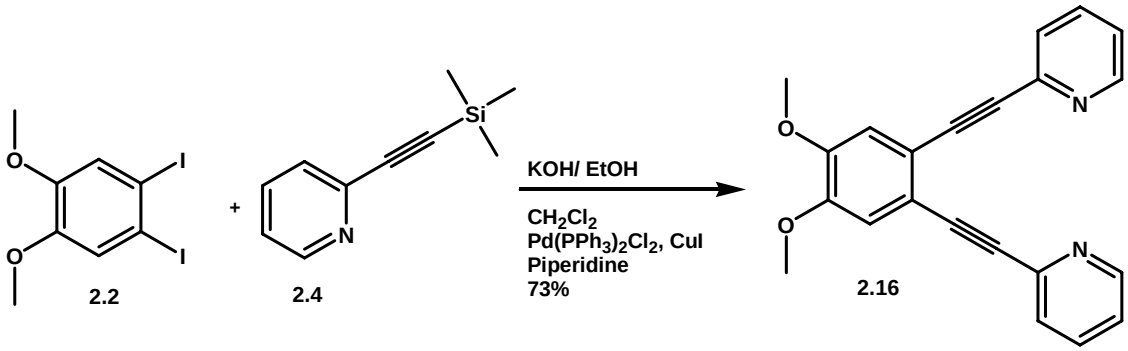

1,2-Dimethoxy-4,5-bis(2-pyridylethynyl)benzene (2.16) In a 50 mL flask under nitrogen atmosphere, 1,2-diiodo-dimethoxybenzene **2.2** (3.30 g, 9.70 mmol) and **2.14** (3.72 g, 2.12 mmol) are dissolved in CH_2Cl_2 (20 mL) and piperidine (2 mL). A 10 wt. % mixture of KOH in ethanol (3 mL) is added and stirred for 15 minutes. $Pd(PPh_3)_2Cl_2$ (0.059 g, .084 mmol) and CuI (0.0146 g..077 mmol) are added, and reaction is stirred for 12 h. at room temperature. The resulting mixture is poured into 150 mL CH_2Cl_2 and washed three times with 50 mL of water. The organic layer is washed with a 10% NH_4OH solution. The aqueous layer was washed three times with 100 mL CH_2Cl_2. Organic layers are combined and dried with $NaSO_4$. Purification was done by column chromatography on a deactivated (2% NEt_3/ 98% hexanes) column with eluent ethyl acetate/hexane (1:4). The resulting solid is recrystallized from ethyl acetate and hexanes (1:1) to yield a white crystalline solid (2.1 g, 73%). ^{1}H-NMR (acetonitrile, 300 MHz , 20°C) 3.90 (s, 6H, OCH_3), 7.24 (s, 2H, aryl-H), 7.38 (ddd, 2H, pyridyl-H), 7.77 (dt, 2H, pyridyl-H), 7.82 (td, 2H, pyridyl-H), 8.65 (d, 2H, pyridyl-H), ppm ^{13}C-NMR ($CDCl_3$, 75 MHz, 20°C) 150.28, 149.812, 143.83, 136.38, 127.54, 122.92, 118.65, 114.67, 91.94, 88. 33, 56.34 ppm MS-EI (70eV, 200°C): 340 (100%, M^+), 341 (25%, M^+), 342 (5%, M^+), 325 (M^+-CH_3, 15%,) 309 (M^+-OCH_3, 4%), 263 (97%, M^+-pyridine), 264 (22%, M^+-pyridine), 186 (68%, M^+- 2x pyridine), 187 (10%, M^+- 2x pyridine) m/z IR [KBr-pellet, cm^{-1}] 2200 (m), 1590 (w), 1570 (s), 1550 (w), 1510 (s), 1460 (m), 1450 (m), 1435 (w), 1425 (w) 1415 (w), 1360 (s), 1245 (s), 1210 (m), 1175 (w), 1095 (m), 1075 (w), 990 (m), 890 (w), 770 (m).

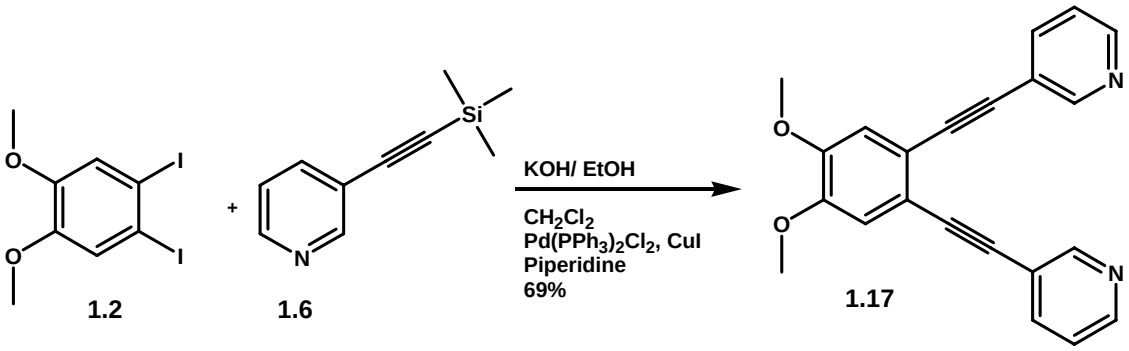

1,2-Dimethoxy-4,5-bis(3-pyridylethynyl)benzene (2.17) **2.2** (3.30 g, 8.46 mmol) and 3- trimethylsilylethynylpyridine **2.6** (3.72g, 21.25 mmol) are dissolved in 10 ml of CH_2Cl_2 and 2 ml of a 10 wt % solution of KOH/EtOH and stirred for 15 min in a nitrogen purged flask. Next, piperidine (1 mL), $Pd(PPh_3)_2Cl_2$ (0.06g, 0.08 mmol) and CuI (0.02 g, 0.09 mmol) are added. The reaction is stirred for 6 h. The resulting mixture is worked up with 10 % NH_4OH and extracted with CH_2Cl_2. The organic layer is dried over sodium sulfate, filtered and solvent is removed under pressure. Chromatography over silica gel with hexanes:EtOAc:NEt_3 (80:19:1) gives **2.17** (1.98g, 68.8%) as a white solid. ^{1}H-NMR- (300MHz, $CDCl_3$) δ 3.92 (s, 6H), 7.03 (s, 2H, aryl-H), 7.26, 7.27, 7.29 (m, 2H pyridyl- H), 7.76, 7.77, 7.79, 7.80 (dd, 2H) 8.53 (s, 2H), 8.76 (s, 2H). ^{13}C-NMR- (75 MHz, $CDCl_3$) δ 151.77,149.19, 148.36, 137.92, 122.92, 120.19, 117.94, 113.77, 91.19, 88.68, 55.81. IR- *ν* 2201, 1598, 1554, 1506, 1262, 1408, 1365, 1245, 1212, 1088, 1022, 990, 854, 800, 773, 697, 637 MP= 148 °C UV/Vis ($CHCl_3$) λ 276, 332. Emission λ ($CHCl_3$) 388.

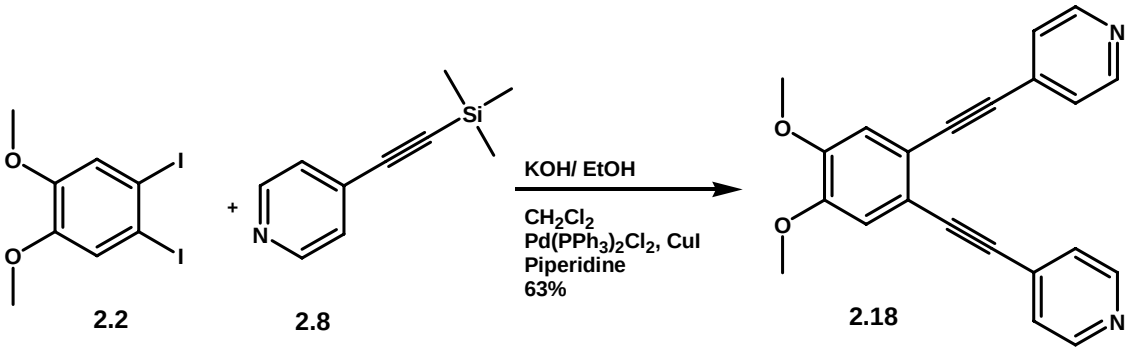

1,2-Dimethoxy-4,5-bis(3-pyridylethynyl)benzene 1.18. **2.2** (2.67 g, 6.85 mmol) and 4-trimethylsilylethynyl pyridine **2.8** (3.00 g, 17.10 mmol) are dissolved in 20 mL CH_2Cl_2 and 2 ml of a 10 wt % KOH/EtOH solution and stirred for 15 minutes in a nitrogen purged flask. Next, piperidine (1 mL), $Pd(PPh_3)_2Cl_2$ (0.050g, 0.070 mmol) and CuI (0.01g, 0.07 mmol) are added. The reaction is stirred for 6 h. at RT. The resulting mixture is washed with 10 % NH_4OH and extracted with CH_2Cl_2. The organic layer is dried with sodium sulfate, and the solvent is removed under pressure. The crude solid is purified by column chromatography over silica gel with eluent EtOAc:hexane (1:4) to give **2.18** (1.63 g, 62.5%) as a pale yellow solid. ^{1}H-NMR- ($CDCl_3$, 300MHz) δ 3.94 (s, 6H), 7.04 (s, 2H) 7.35, 7.36, 7.37, 7.37 (dd, 4H), 8.59, 8.61 (d, 4H) ^{13}C-NMR- (75 MHz, $CDCl_3$) δ 149.87, 149.80, 131.31, 125.24, 118.10, 114.17, 92.52, 89.75, 56.09.IR- *ν* 2198, 1719, 1588, 1552, 1407, 1363, 1254, 1218, 1080, 985, 862, 811, 695 MP=190 °C MS - 340, 325, 297, 268, 254, 170, 127, 100, 74 cm^{-1} UV/Vis ($CHCl_3$) λ 264, 292, 336. Emission ($CHCl_3$) λ 401.

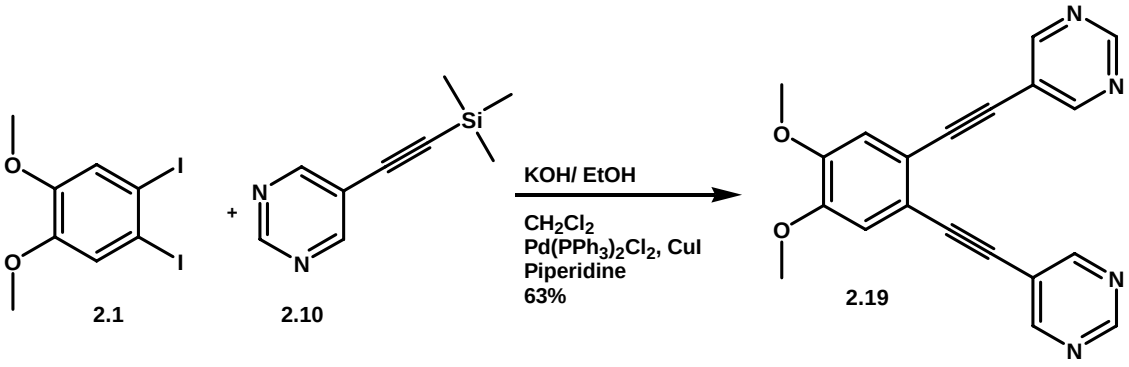

1,2-dimethoxy-4,5-bis(5-pyrimidylethynyl)benzene (**2.19)** In a nitrogen purged flask **2.2** (2.40 g 6.20 mmol) and **2.10** (2.70 g 15.30 mmol) are dissolved in 15 ml CH_2Cl_2 and 2 ml of a 10 wt % KOH/EtOH solution and stirred for 15 min. Next piperidine (2 mL), $Pd(PPh_3)_2Cl_2$ (0.04g, 0.06 mmol) and CuI (0.010g, 0.060 mmol) are added. The eaction is stirred for 6 h. The resulting mixture is washed with a 10 % NH_4OH solution and extracted with CH_2Cl_2. Crystallization from methanol gives **2.19** (1.2 g, 57%) as a colorless solid. (^{1}H-NMR- ($CDCl_3$, 300MHz) δ 3.94 (s, 6H,), 7.04 (s, 2H), 8.83 (s, 4H), 9.13 (s, 2H) ^{13}C-NMR- ($CDCl_3$, 75 MHz) δ 158.38, 156.81, 149.93, 119.75, 117.82, 114.18, 94.67, 85.35, 56.14. IR *v* 3019, 2932, 2205, 1588, 1537, 1508, 1450, 1421, 1370, 1254, 1217, 1130, 1072, 1036, 985, 862, 753, 716, 636.3. MP= 209 °C UV/Vis ($CHCl_3$) λ 268, 286, 334. Emission ($CHCl_3$) λ 400.

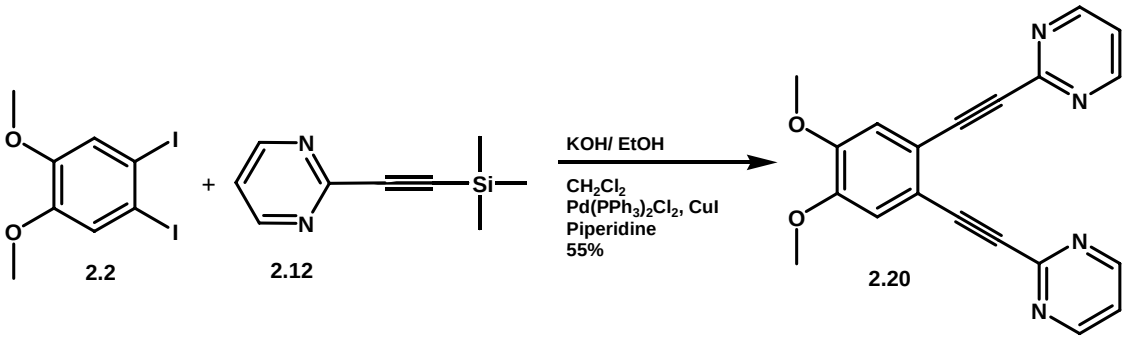

1,2-Dimethoxy-4,5-bis(2-pyrimidylethynyl)benzene (2.20). 2.2 (2.00 g, 5.89 mmol) and **2.12** (2.08 g, 118.2 mmol) are dissolved in piperidine (1 mL), CH_2Cl_2 (10 mL), and 2 ml of a 10 wt % KOH/EtOH solution in a Schlenk flask under nitrogen atmosphere for 15 min. $Pd(PPh_3)_2Cl_2$ (0.016 g, .02mmol), CuI (0.01g, .05 mmol), and PPh_3 (0.02 g, 0.07 mmol) are added, and the reaction is capped.and heated at 70° C for 12 h. The resulting mixture is washed with 10 % NH_4OH and extracted with CH_2Cl_2. After removing solvent under vacuum, the solid is crystallized from methanol to give **2.20** (1.13g, 55%) as a pale yellow solid. ^{1}H –NMR - ($CDCl_3$, 300MHz) δ 3.88 (s, 6H), 7.15 (s, 2H), 7.17-7.20 (t, 2H) 8.72-8.70 (d, 4H) ^{13}C-NMR- ($CDCl_3$, 75 MHz) δ 157.23 153.31, 149.99, 119.52, 117.84, 115.22, 90.99, 86.06, 56.13. UV/Vis ($CHCl_3$) λ 263, 289, 322, 342. Emission ($CHCl_3$) λ 416.

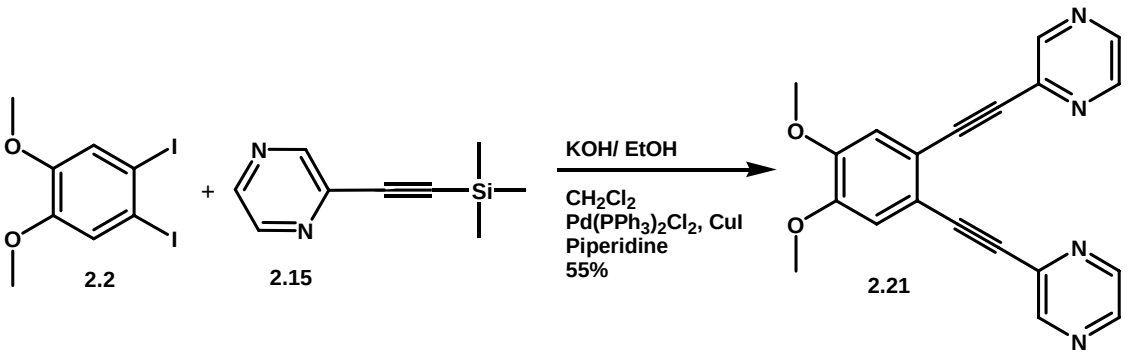

1,2-Dimethoxy-4,5-bis(2-pyrazylethynyl)benzene (2.21) **2.2** (1.00g, 2.56 mmol) and **2.15** (1.13g, 6.40 mmol) are dissolved in 10 ml CH_2Cl_2, 1 ml piperidine, and 2ml of a 10% KOH/EtOH solution and stirred for 15 minutes. $Pd(PPh_3)_2Cl_2$ (0.02g, 0.03mmol and CuI (.006 g, 0.03 mmol) are added. The reaction is stirred at room temperature for 6 h. The solution is washed with a 10 % NH_4OH and extracted with CH_2Cl_2 . The solvent is removed under pressure and the solid is recrystallized from methanol to yield **2.21** (0.55g, 53% yield.) ^{1}H-NMR- (300MHz, $CDCl_3$) δ 3.93 (s, 6H), 7.13 (s, 2H), 8.47, 8.48 (d, 2H), 8.58, 8.59, 8.59, 8.59 (m, 4H,). ^{13}C-NMR- (75 MHz, $CDCl_3$) δ150.08, 147.88, 144.52, 142.81, 140.31, 118.01, 114.34, 91.65, 89.32, 56.16. IR- v 2205, 1582, 1595, 1508, 1464, 1362, 1253, 1217, 1101, 1014, 948, 854, 651. Mp= 222 °C

2.5 References

1. Fiscus, J. E.; Shotwell, S.; Layland, R. C.; Smith, M. D.; zur Loye, H.-C.; Bunz, U. H. F., *Chem. Commun*. **2001**, 2674.
2. Shotwell, S.; Windscheif, P. M.; Smith, M. D.; Bunz, U. H. F., *Org. Lett*. **2004**, *6*, 4151.
3. S. Leininger, B. Olenyuk and P.J. Stang. *Chem. Rev.* **100** (2000), p. 853.
4. P.J. Stang and B. Olenyuk. *Acc. Chem. Res.* **30** (1997), p. 502.
5. D.M. Ciurtin, N.G. Pschirer, M.D. Smith, U.H.F. Bunz and H.-C. zur Loye. *Chem Mater.*
6. E. Bosch and C.L. Barnes. *Inorg. Chem.* **40** (2001), p. 3097.
7. Cassar, I. *J. Organomet. Chem.* **1975**, *93*, 253.
8. Sonogashira, K.; Tohda, Y.; Hagihara, N. *Tetrahedron Lett.* **1975**, *16*, 4467.
9. Kloppenburg, L., Jones, D. Bunz, U. H. F. *Macromolecules* **1999**, *32*, 4194.
10. Waybright, S. PhD thesis University of South Carolina, **2001.**
11. De la Rosa, Martha A.; Velarde, Esperanza; Guzman, Angel. Synthetic Communications (1990), 20(13), 2059-64.
12. De la Rosa, Martha A.; Velarde, Esperanza; Guzman, Angel. *Synthetic Communications* **1990**, 20(13), 2059-64.
13. Ple, Nelly; Turck, Alain; Heynderickx, Arnault; Queguiner, Guy Tetrahedron (1998), 54(33), 9701-9710.

CHAPTER 3

SYNTHESIS AND CHARACTERIZATION OF PYRIDINE CAPPED ORTHO-PHENYLENEETHYNYLENES

3.1 Introduction

Aryleneeethynylenes[1,2] (AE) constitute a general class of molecules in which arene units are connected by alkynyl linkers. In most of the aryleneethynylenes benzene rings are used as the arene of choice perhaps due to simplicity and commercial access to the starting materials. The first AEs reported were the cyclic trimers and hexamers[3-6] (Figure 3.1), and not linear oligomers. Linear oligomers of the *para* and *meta* type, were first synthesized[7-13] for their potential application in molecular electronics and to study solvent driven folding processes in conjugated oligomers.

The first linear *ortho*-oligo-PEs were synthesized by Grubbs and Kratz[14] (Figure 3.1), but despite their interesting thermal behavior and their unusual helical structures in the solid state, they have attracted much less attention than their *meta* or *para* counterparts. One investigation by Anderson[15] has utilized kinked PEs in which ortho-linkages were present as active materials for light emitting diodes.. Donor-acceptor *ortho*-PEs were investigated by Nicoud[16] et al. as NLO-type materials and showed interesting properties. Recently Tew et al.[17] have reported alkoxy substituted o-PE's (trimer to hexamer) and

have performed a theoretical study[18] of their helix formation. The "floppiness" of the *o*-PEs should give rise to a multitude of different conformations in solution and several conformations in the solid state. The compound and its parent[19,20,21] (without the methoxy groups)[22,23] has been found to be a suitable ligand for transition metals as it can coordinate in a trans-spanning fashion forming monomeric complexes, or be the bridging part of a metal organic coordination polymer. We wish to present the synthesis and the structural characterization of the pyridine end-capped *ortho*-PEs **2.2**, **3.1**, **3.2**, and **3.3**. These oligomers are attractive as active layers in light emitting diodes and as building blocks for larger metal organic solid state polymers.

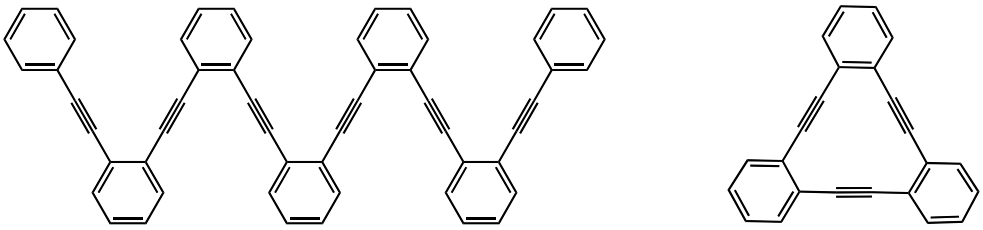

Figure 3.1: *Ortho*-phenyleneethynylene oligomers.

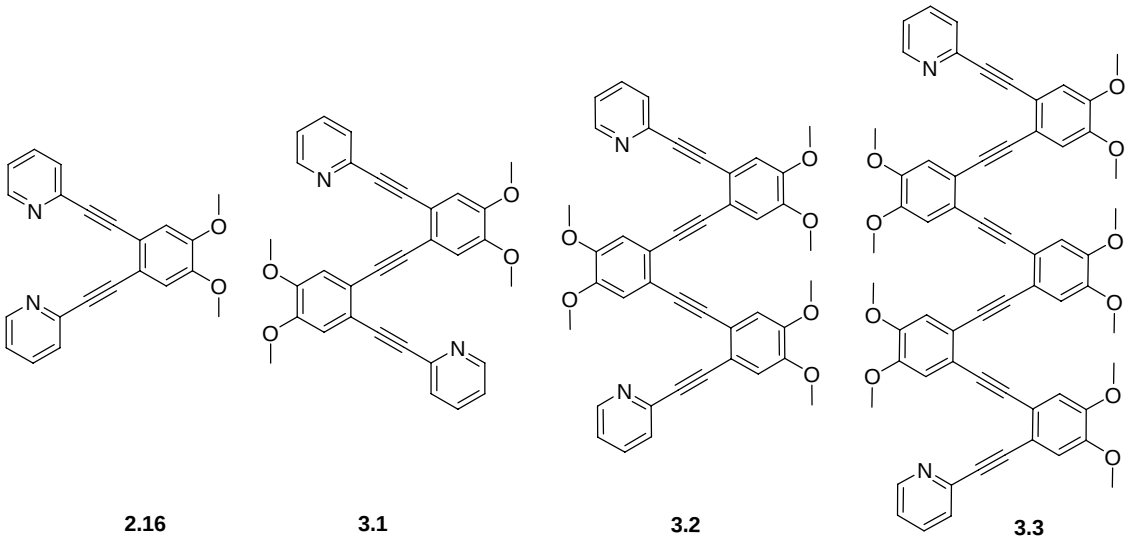

Figure: 3.2 Pyridine capped OPE's.

3.2 Results and Discussion

The synthesis of **1.16** (Figure 2.1) has been previously discussed in Chapter 1. Using the same reactants, but with an excess **1.2** with **1.4**, the mono coupled compound **2.4,** is produced in a 66 % yield. Upon alkynylation of **2.4** with trimethylsilylacetylene yields the unsymmetrical diyne, **2.5** which is a building block in the synthesis of longer oligomers, in a 97% yield. The longer tetramer is synthesized by treating **2.4** with acetylene gas under Sonogashira conditions to yield **2.1** in a 42% yield.

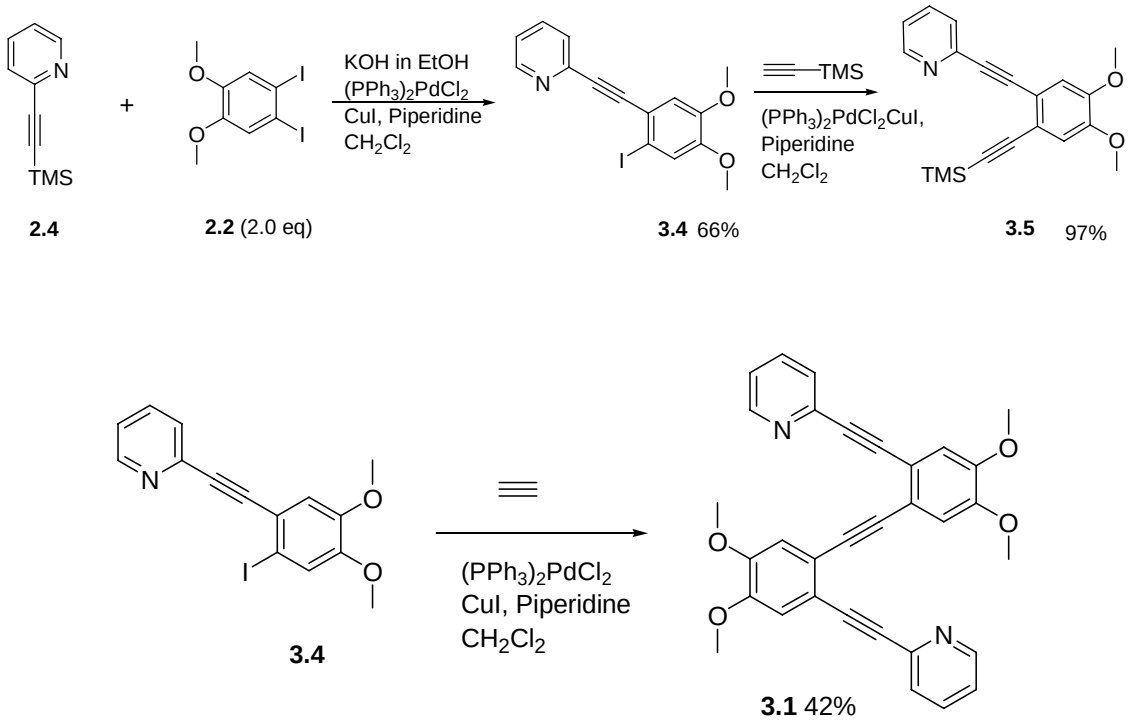

Scheme 3.1 Synthesis of tetramer **3.1.**

The synthesis of the other necessary building blocks for the creation of the pentamer and heptamer begins with the reaction of the **2.2** with 2.5 eq of TMS-acetylene to yield the dialkynylated compound **3.6** in an 88% yield. The dialkynylated compound **3.6** is treated with and excess of the diiodide **2.2**, to yield the diiodo trimer **3.7** in a 34 % yield.

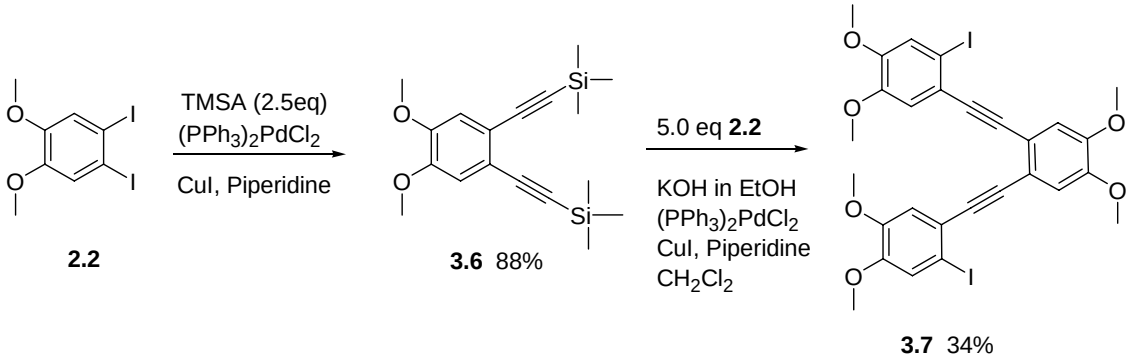

Scheme 3.2: Synthesis of *o*-diiodotrimer

The synthesis of the longer oligomers can be seen in Scheme 3.3**.** The dialkynyl compound **3.6** is deprotected and coupled in situ to the monosubstitued compound **3.4,** in a similar fashion as the previous compounds, in a 54% yield. The larger heptameric oligomer is created from the diiodo trimer **3.7** reacting with the asymmetrical alkyne **3.6** in a 34% yield.

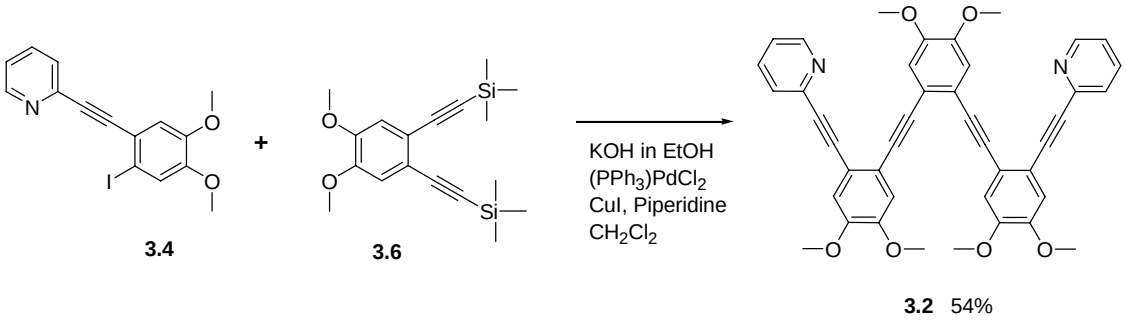

3.4 **3.6** **3.2** 54%

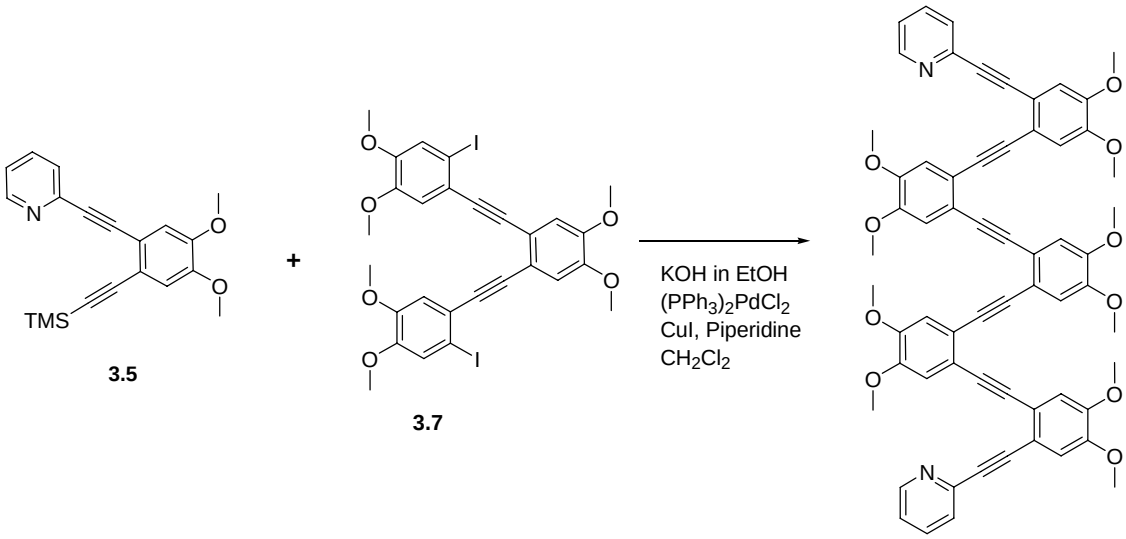

3.5 **3.7** **3.3** 34%

Scheme 3.3: Synthesis of **3.3**

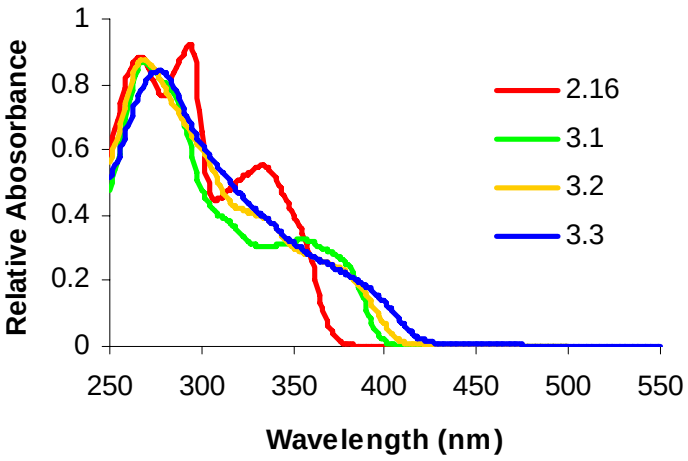

Figure 3.3: Absorption spectra in chloroform

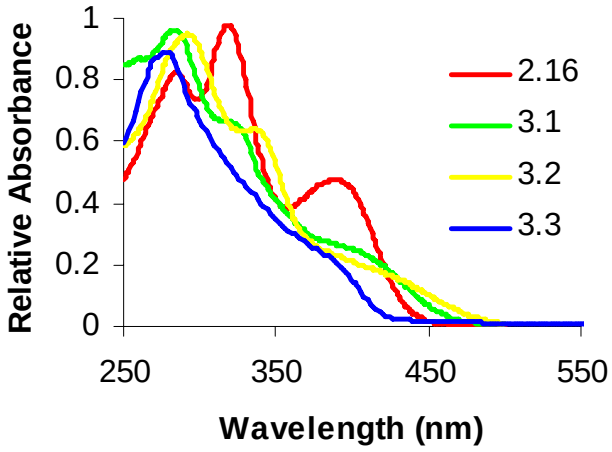

Figure 3.4: Absorption spectra in chloroform upon addition of TFA

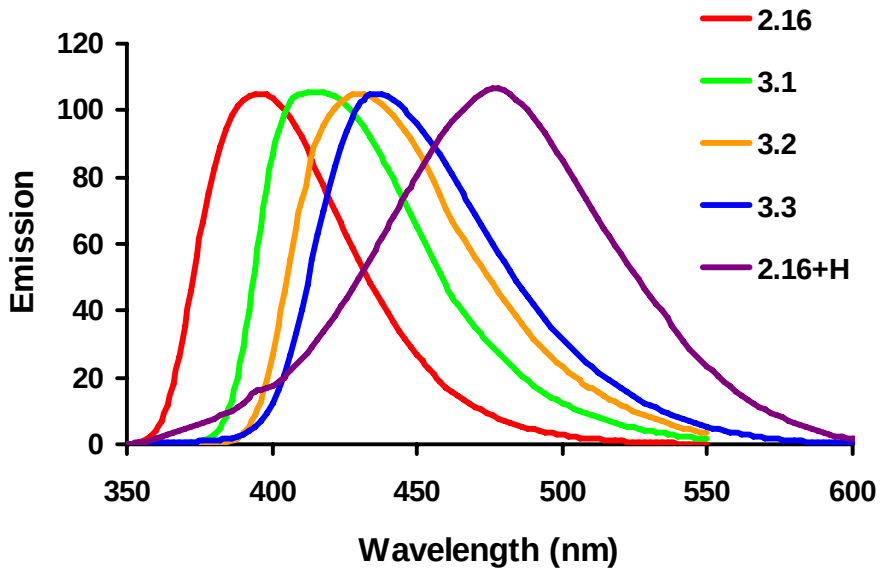

Figure 3.5: Emission spectra of ligands **2.16** and **3.1-3.3**.

The Uv-vis spectra of **2.16** and **3.1-3.3** in dilute solution are shown in Figure 3.3**.** With increasing length, λ_{max} is shifted from 324-408 nm. While the absorption of the trimer is well structured, the absorptions of the higher oligomers tend to become much broader, shoulder-like and less defined. We trace this behavior back to the conformational freedom of these floppy molecules. The larger the oligomer, the more conformation freedom the molecule has. As a consequence this increase in length leads to broadening of the absorption spectra. The presence of the pyridine end groups makes the Uv-vis spectra susceptible to the presence of acid, and addition of trifluoroacetic acid to dilute solutions of **2.16** and **3.1-3.3** lead to a significant bathochromic shift as seen in Figure 3.4. This shift is most distinct in the case of the trimer **2.16** and leads to further broadening of the Uv-vis features in **2.6** and **3.1-3.3** as shown in Figure 3.4 and Table 3.1.

Table 3.1. Optical and Photophysical Data of **2.16, 3.1-3.3**

	$\lambda_{max,abs}$ (nm)	$\lambda_{max,\ abs}$ + TFA (nm)	$\lambda_{max,em}$ (nm)	Φ_{sol} (%)
2.16	263, 294, 324	285, 318, 389	396, thin film: 508	36
3.1	268, 352	282, 322, 406	416, thin film: 538	28
3.2	265	291, 336	430, thin film: 542	28
3.3	272	276, 378	436, thin film: Nd	35

Table 3.1: Optical and Photophysical Data of **2.16**, **3.1**-**3.3**.

All of the oligomers are emissive, and contrary to the absorption spectra, the emission spectra do not broaden upon increasing from trimer **2.16** to heptamer **3.3**. A similar behavior is observed in the case of linear PEs[8], and it was explained by the planarization of the oligomers in the excited state. We can construe that planarization in the lowest excited state will drive the oligomers into a zig-zag type planar structure from which emission is observed.[8] The quantum yield of the emission for **2.16** and **3.1**-**3.4** is significant and in the range from 28-40%, but lower than that of the corresponding linear PEs

Upon addition of TFA the fluorescence of the oligomers is generally quenched, with the exception of the fluorescence of **2.16**, which shifts from 396 to 500 nm, i.e from purple to yellow. The emission for the tetramer through heptamer is quenched, while the emission of the trimer **2.16** demonstrates a red shift. A titration using trifluoroacetic acid was performed to determine at what equivalent of acid shifts the emission of **2.16**. As can be seen in Figure 3.6 and Figure 3.7, a shift can be seen beginning at 0.2 equivalents.

There is no further shift after 1.0 equivalent of acid. It can be concluded that in fact there is only one proton present.

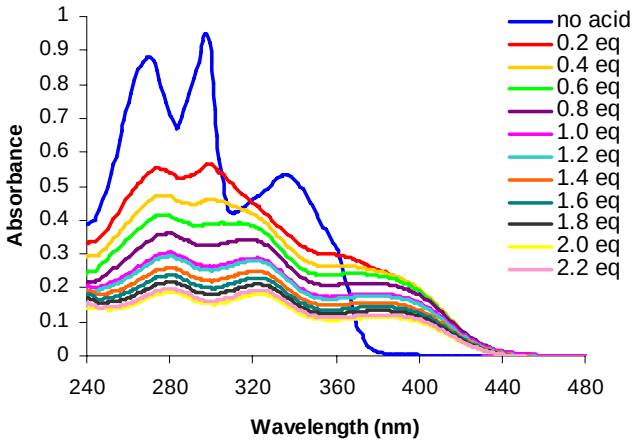

Figure 3.6: Absorption spectra of **2.16** with increasing amounts of TFA.

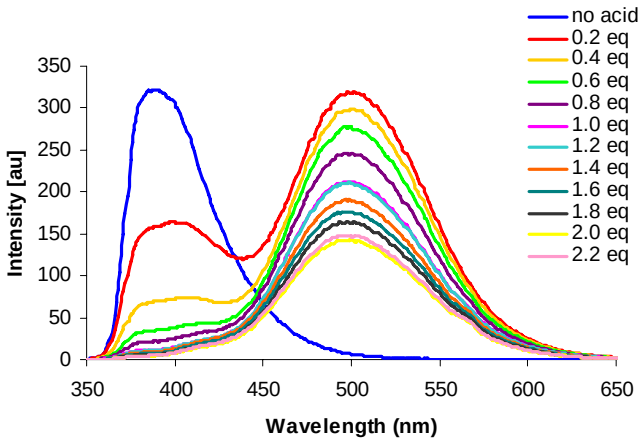

Figure 3.7: Emission spectra of **2.16** with increasing amounts of TFA.

A 631G** calculation was performed on **2.16** to determine difference between the band gap of the unprotonated form of the ligand with the protonated form. In this case the HOMO for the unprotonated form is -5.36 eV and the LUMO is -1.03 eV (Figure 3.7)

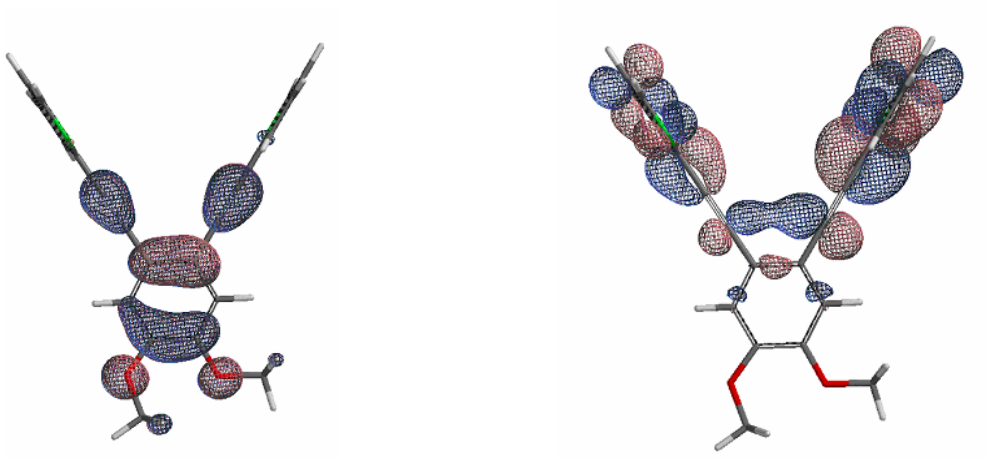

Figure 3.8: 6-31G** calculations of **2.16**. HOMO (left) LUMO (right).

The protonated form gives a HOMO estimate at -8.44 eV and a LUMO of -5.68 eV (Figure 3.7). This decrease in band gap indicates that the **2.16** will have a red shift. The protonated form of this compound also demonstrates a greater donor-acceptor character.

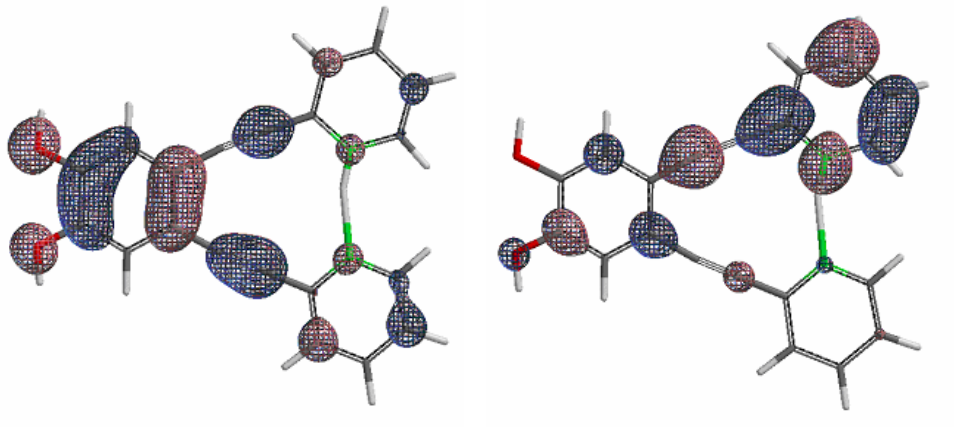

Figure 3.9: 6-31 G** calculation of **2.16** with a hydrogen between the nitrogens

In order to further study whether or not **2.16** was singly or doubly protonated, IR spectra were taken (Figure 3.9) of the base ligand and the protonated form. One clue to confirm the belief that ligand **2.16** is singly protonated between the nitrogens due to the disappearance of alkyne stretches at 2358 cm^{-1} and 2339 cm^{-1} (Figure 3.10) which is replaced by a single alkyne peak at 2200cm^{-1}. This shift can be attributed to a more symmetric molecule which can be traced to a singly protonated ligand which is planarizing.

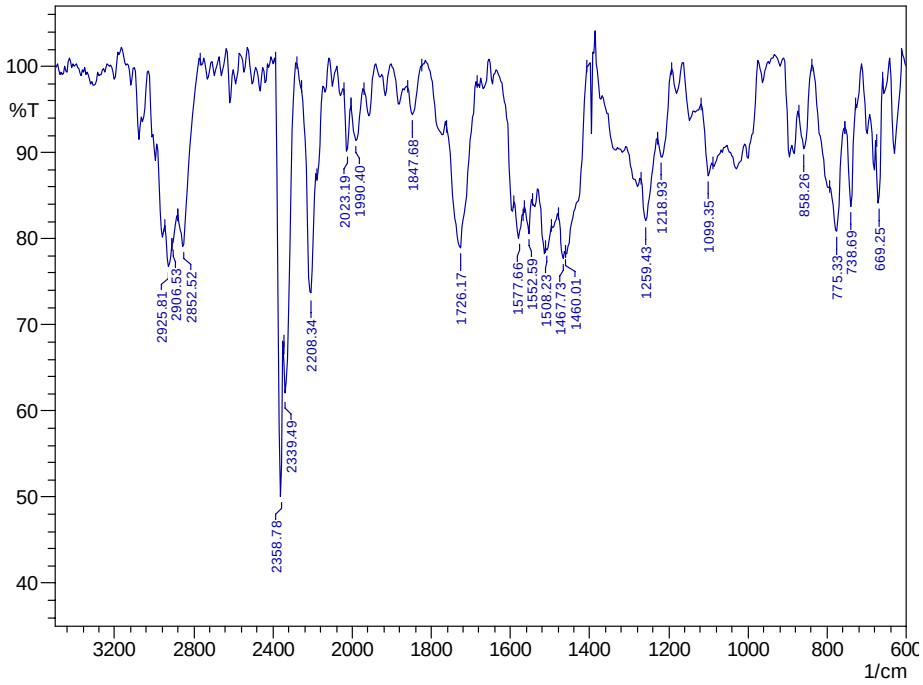

Figure 3.10: IR spectrumof **2.16**.

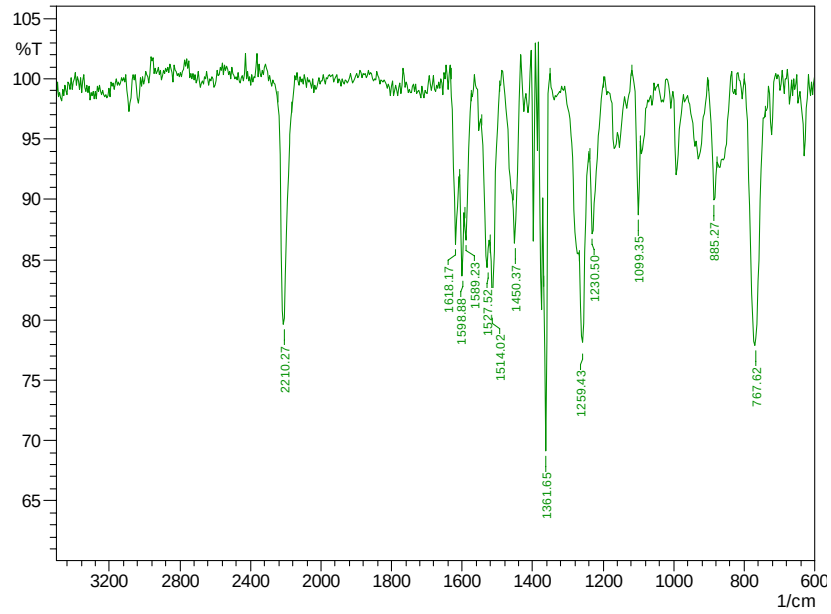

Figure 3.11: IR spectrum of **2.16** with HBr.

The oligomers **2.16** and **3.1-3.3** are flexible and could in principle attain any conformation ranging from completely planar to highly twisted and/or helical. While most of the conformations will be attained in solution, in the solid state one or several conformations should be preferred. The parent *ortho*-phenyleneethynylenes have been investigated by Grubbs and Kratz in 1993 [14], and the resulting solid state structures were highly helical. It was of interest in how far the presence of the methoxy groups and the pyridine units would make a difference in the solid-state organization of **2.16** and **3.1-3.3**.. Figure 3.10 shows the structures of **2.16, 3.1,** and **3.2** in the solid state. The oligomers **2.16** and **3.2** crystallized without solvent, while **3.1** co-crystalizes with one molecule of pyridine.

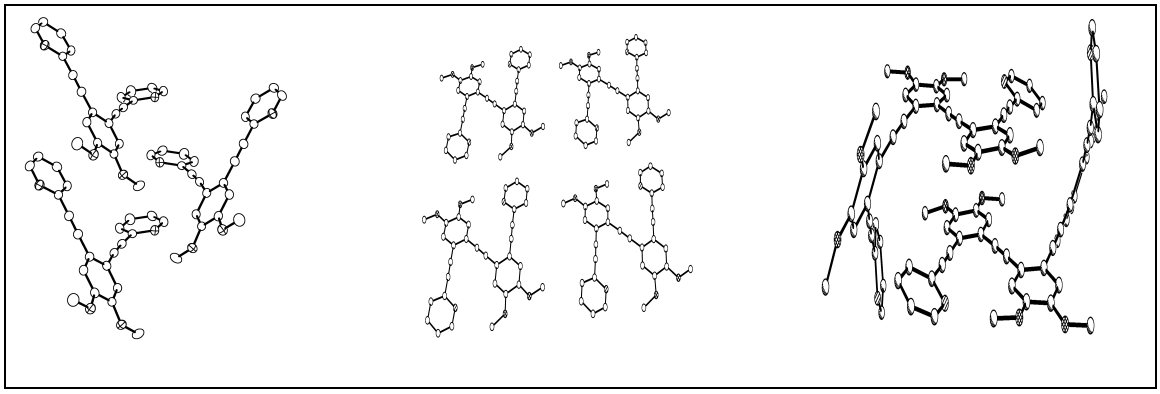

Figure 3.12: Solid State Structures of **2.16** and **3.1**-**3.3**

The bond lengths and bond angles are inconspicuous in all oligomers. The co-crystal of **3.1** the oligomer is virtually planar, with strong and sort π-π interactions between the arene units, while in the case of **2.16** and **3.2** the conjugated backbones are twisted out of the plane. While **3.1** is planar and **2.16** is twisted, the pentamer **3.2** forms a dimer in the solid state the looks almost like a collapsed box, with the 90-degree twisted pyridine units as its side walls. Our substituted oligomers seem to be more inclined towards either a planar or twisted conformation, but do not show a helical packing in the solid state.

2.3 Conclusion

In conclusion a series of pyridine-terminated *o*-aryleneethynylene oligomers (**2.16** and **3.1**-**3.3**) has been synthesized. We have examined their photophysics in solution and their structures in the solid state. The oligomers are emissive in solution and in the solid state, but only the **2.16** is fluorescent after addition of trifluoroacetic acid. The structures of **2.16, 3.1,** and **3.2** were determined by single-crystal X-ray diffraction. Contrary to the

hydrocarbon oligomers investigated by Grubbs and Kratz, **2.16**, **3.1** and **3.2** do not form helical structures; instead, either planar (**3.1**) or intermediate (**3.2**) arrangements are preferred in the solid state. At the moment, we are investigating the use of **2.16** and **3.1**-**3.3** as active layers in organic LEDs.

3.4 Experimental

General Coupling Procedure A

A Schlenk flask is flushed with nitrogen for approximately 30 min. The iodoarene, bis(triphenylphosphine)palladium(II) chloride ($(PPh_3)_2PdCl_2$) (1.0 mol %) and CuI (1 mol %) are dissolved in piperidine and solvent. The terminal alkyne is added via syringe. The reaction is stirred for 24 h at room temperature under nitrogen atmosphere.

General Coupling Procedure B

A Schlenk flask is flushed with nitrogen for approximately 30 min. The bromoarene, bis(triphenylphosphine)palladium(II) chloride $(PPh_3)_2PdCl_2$ (1.0 mol %), CuI (1 mol %), and PPh_3 are dissolved in triethylamine and CH_2Cl_2. After initial heating to 50° C, the reaction is stirred for 24 h.

General Coupling Procedure C

A Schlenk flask is flushed with nitrogen for approximately 30 min., and the iodoarene, piperidine, and catalysts are added as in **General Coupling Procedure A.** Acetylene gas is added. Reaction is agitated every ten minutes.

General Cleavage and Coupling Procedure D

A Schlenk flask is flushed with nitrogen for approximately 30 min. The iodoarene and TMS protected terminal alkyne are dissolved in CH_2Cl_2 and piperidine. A

concentrated solution of KOH/ethanol is added, and reaction is stirred for 5 min. $(PPh_3)_2PdCl_2$ (1 mol %) and CuI (1 mol %) are added last. Reaction was stirred for 24 h at room temperature.

General Cleavage and Coupling Procedure E

A Schlenk flask is flushed with nitrogen for approximately 30 min. The bromoarene and TMS protected terminal alkyne are dissolved in CH_2Cl_2 and triethylamine. A concentrated solution of KOH/ethanol is added, and reaction is stirred for 5 min. $(PPh_3)_2PdCl_2$ (1 mol %) and CuI (1 mol %) are added last. After initial heating to 50°C, the reaction is stirred for 24 h.

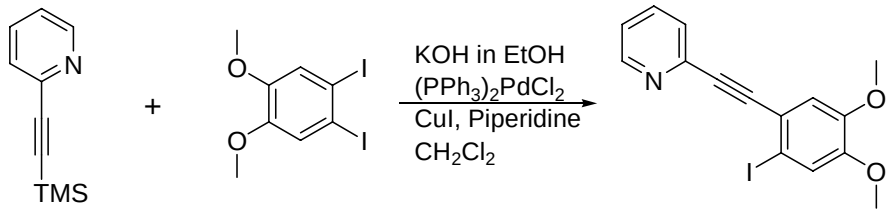

2.4 **2.2** (2.0 eq) **3.4** 66%

2-(2-Iodo-4,5-dimethoxy-phenylethynyl)-pyridine, 3.4, Using General Coupling procedure D, **2.2** (12.0 g, 30.7 mmol), $Pd(PPh_3)_2Cl_2$ (0.0870 g, 0.125 mmol) and CuI (0.0238 g, 0.125 mmol) was reacted with **2.2** (3.75 g, 10.3 mmol). The resulting mixture is washed with a 10% NH_4OH aqueous solution (100 mL), extracted with dichloromethane (100 mL) and dried with Na_2SO_4. The solvent is removed *in vacuo*. Purification was done by column chromatography on a deactivated column with eluent ethyl acetate:hexanes (1:4) to give **3.4** (1.64 g, 66 %), a colorless oil. ^{1}H-NMR ($CDCl_3$,

300 MHz , 15°C) δ 8.62 (dd, 1H, pyridyl-H), 7.74 (m, 1H, pyridyl-H), 7.63 (dd, 1H, pyridyl-H), 7.20 (m, $CDCl_3$, pyridyl-H, aryl-H), 7.11 (s, 1H, aryl-H), 3.88 (s, 3H, OCH_3), 3.85 (s, 3H, OCH_3) ^{13}C-NMR ($CDCl_3$, 75 MHz, 15°C) δ 150.37, 150.30, 149.00, 143.80, 136.37, 127.51, 123.03, 123.10, 121.21, 121.40, 115.55 (aryl/ pyridyl C's), 90.00, 91.00 (ethynyl C's), 56.45, 56.29 (O**C**H_3). IR (cm^{-1}):ν 3004.9, 2939.3, 2360.7, 2331.8, 2210.3, 1637.5, 1581.5, 1500.5, 1461.9, 1377.1, 1325.0, 1247.9, 1211.2, 1178.4, 1149.5, 1028.0, 995.2, 962.4, 854.4, 812.0, 773.4, 748.3, 667.3, 582.5.

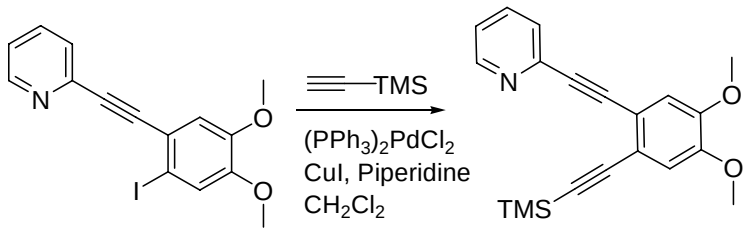

3.4 66% **3.5** 97%

(3.5) Using General Coupling Procedure A, **3.4** (1.10 g, 3.01 mmol), trimethylsilylacetylene (0.329 g, 3.36 mmol), $Pd(PPh_3)_2Cl_2$ (8.4 mg, 0.0120 mmol) and CuI (5.7 mg, 0.0301 mmol) are reacted. The reaction mixture is washed with a 10% NH_4OH aqueous solution (100 mL), extracted with dichloromethane (100 mL) and dried with Na_2SO_4. After column chromatography over silica gel with eluent, EtOAc:hexanes (1:4) furnishes **3.5** (0.970 g, 97 %) as a colorless solid. ^{1}H-NMR (300MHz, $CDCl_3$) δ 3.87, 3.89 (s 6H –OCH_3) 6.95, 7.07 (s 4H, aryl H) 7.19-7.20 (pyridyl H) 7.21-7.22 (m, pyridyl-H) 7.23 (m pyridyl H) 7.49 (m pyridyl H) 7.51 (m pyridyl H) 7.63-7.64(dd, pyridyl H) 7.65 (d, pyridyl H) 7.67 (d, pyridyl H) ^{13}C-NMR (75 MHz, $CDCl_3$) δ 149.79, 149.09, 148.85, 143.34, 135.72, 126.75, 122.33, 118.84, 117.83, 114.08, 113.98, 103.14,

96.92, 90.94, 87.92, 55.71, 55.68, -.19. IR (cm^{-1}): ν 3004.4, 2958.1, 2936.4, 2900.3, 2848.7, 2365.1, 2213.7, 2152.4, 1597.4, 1581.0, 1510.6, 1463.9, 1441.7, 1394.4, 1355.9, 1254.6, 1217.5, 1200.6, 1107.1, 1033.3, 999.5, 881.1, 844.8, 777.7, 759.9. Mp= 86˚C

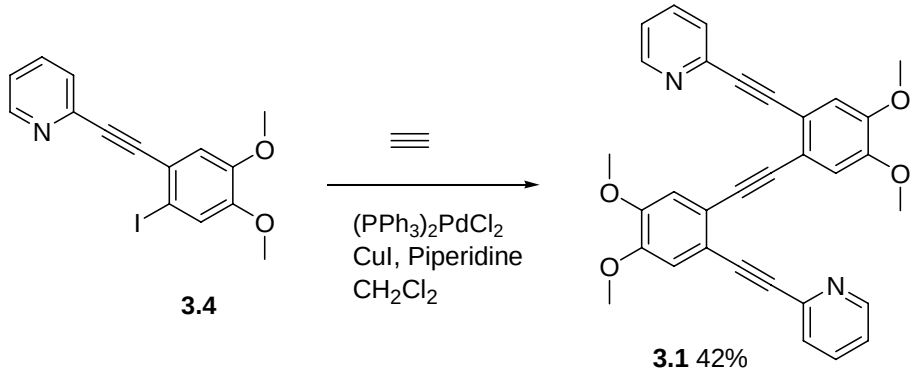

(3.1) Using General coupling procedure C, **3.4** (250 mg, 0.685 mmol), $Pd(PPh_3)_2Cl_2$ (1.9mg, 2.77 μmol) and CuI (1.3 mg, 6.85 μmol) were reacted with acetylene gas. The reaction mixture is washed with a 10% NH_4OH aqueous solution (100 mL), extracted with dichloromethane (100 mL) and dried with Na_2SO_4. Purification by column chromatography with eluent MeOH:CH_2Cl_2 (1:99) over alumina oxide basic affords **3.1** (144 mg, 42 %), as a colorless solid.. ^{1}H -NMR δ 3.88 (6H, OCH_3) 3.91 (6H, OCH3) 7.09 (d, pyridyl H) 7.11 (s, 2H, aryl H), 7.13 (d pyridyl H), 7.15 (s, 2H aryl H) 7.48 (d, pyridyl H) 7.5 (m pyridyl H) 7.54 (d pyridyl H) 7.56 (d pyridyl H) 8.46, 8.48 (dt pyridyl H). ^{13}C-NMR($CDCl_3$, 75MHz, 20°C) 150.02, 149.84, 149.31, 143.82, 136.15, 127.55, 122.67, 119.82, 117.77, 114.73, 114.36, 91.72, 91.36, 88.65, 56.32, 56.22. IR (cm^{-1}) ν 3008.7, 2941.2, 2908.5, 2362.6, 2331.8, 2208.3, 1706.9, 1647.1. 1585.4, 1569.9, 1512.1,

1461.9, 1367.4, 1263.3, 1234.4, 1118.6, 1001.0, 881.4, 858.3, 773.4, 746.4. MS 500 cm^{-1} UV/Vis ($CHCl_3$) λ 268, 352. Emission ($CHCl_3$) λ 416. mp= 248°C.

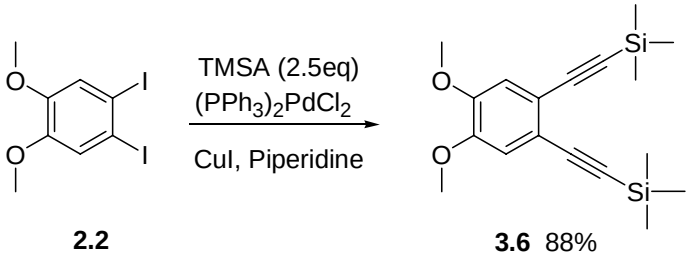

2.2 **3.6** 88%

(3.6) 1,2-Dimethoxy-4,5-bis-trimethylsilanylethynyl-benzene Using General Coupling Procedure A, 1,2-diiodo-3,4-dimethoxybenzene, **2.2**, (10.0 g, 25.6 mmol), $Pd(PPh_3)_2Cl_2$ (179 mg, 0.256 mmol) and CuI (48.6 mg, 0.256 mmol) were dissolved in CH_2Cl_2 (100 mL) and treated trimethylsilylacetylene (6.28 g, 64.1 mmol). The reaction mixture is washed with a 10% NH_4OH aqueous solution (100 mL), extracted with dichloromethane (100 mL). The CH_2Cl_2 layer is washed with a 25% aqueous solution of HCl (100 mL). The organic layer is dried with $MgSO_4$. After column chromatography over silica gel with eluent, EtOAc:hexanes (1:4). Compound **3.6** (7.41 g, 87.5 %), is recovered as a colorless solid. ^{1}H-NMR ($CDCl_3$, 300 MHz , 15 °C) δ 6.65 (s, 2H, aryl-H), 3.61 (s, 6H, OCH_3), 0.00 (s, 18H, $Si(CH_3)_3$ ^{13}C-NMR ($CDCl_3$, 75 MHz, 15°C) δ 149.19, 119.15, 114.50 103.62, 97.01. IR (cm^{-1}): ν 2958.6, 2360.7, 2331.8, 2150.5, 1647.1, 1589.9, 1554.5, 1508.2, 1450.4, 1394.4, 1346.2, 1249.8, 1211.2, 1001.0, 881.4, 8444.8, 758.0. Mp = 88°C.

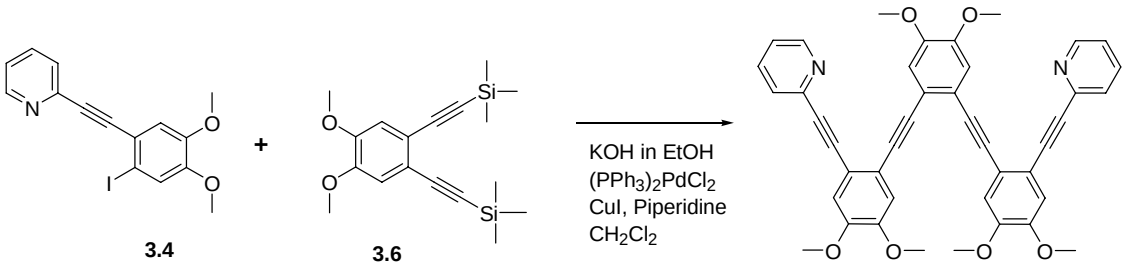

3.4 **3.6** **3.2** 54%

(3.2) Using General Coupling Procedure D, **3.6** (1.00 g, 3.02 mmol), $Pd(PPh_3)_2Cl_2$ (21.0 mg, 0.0300 mmol) and CuI (6.0 mg, 0.0300 mmol) was reacted with **3.4** (2.32 g, 6.32 mmol). The reaction mixture is washed with a 10% NH_4OH aqueous solution (100 mL), extracted with dichloromethane (100 mL) and dried with Na_2SO_4. After column chromatography over alumina oxide (basic) with eluent, CH_2Cl_2:MeOH (1:99) to yield **3.2** (210 mg, 54%) as a colorless solid. ^{1}H-NMR ($CDCl_3$, 300 MHz , 15°C) δ 3.79 (s, 6H, OCH_3), 3.85 (s, 6H, OCH_3) 3.87 (s, 6H, OCH_3), 6.98 (s, 2H, aryl), 7.04 (s, 2H, aryl) 7.11 (m, 2H, pyridyl H), 7.13 (s, 2H, aryl H) 7.54 (m 4H pyridyl H), 8.49, 8.51 (d 2H pyridyl H) ^{13}C-NMR ($CDCl_3$, 75 MHz) δ149.77, 149.39, 149.03, 148.83, 143.50, 135.87, 127.32, 122.42, 119.60, 118.67, 117.28, 114.17, 114.09, 91.441, 91.35, 90.86, 88.50, 5601, 55.91, 55.87. IR (cm^{-1}): ν 3008.7, 2939.3, 2837.1, 2360.7, 2331.8, 2208.3, 1589.2, 1512.1, 1461.9, 1371.3, 1228.6, 1128.3, 1002.9, 862.1, 669.3. UV/Vis ($CHCl_3$) λ 265. Emission ($CHCl_3$) λ 430. Mp= 195˚C

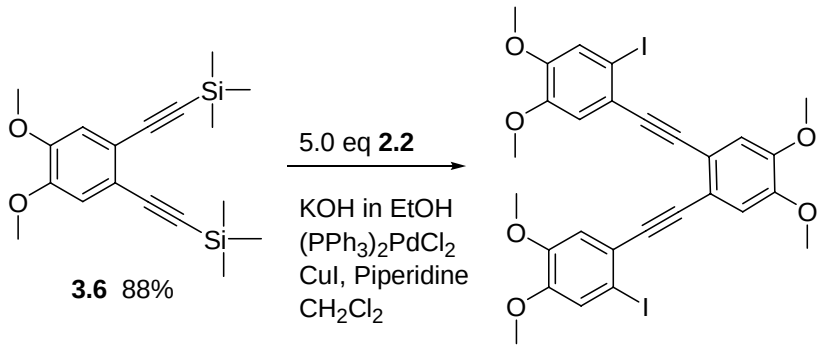

3.6 88%

3.7 34%

(3.7) 1,2-Bis-(2-iodo-3,4-dimethoxy-phenylethynyl)-4,5-dimethoxy-benzene Using General Coupling Procedure A, 1,2-diiodo-3,4-dimethoxybenzene, **2.2**, (2.13 g 5.50 mmol), $Pd(PPh_3)_2Cl_2$ (90.0 mg, 0.0100 mmol) and CuI (10.0 mg, 0.0600 mmol) is reacted with **3.7** (0.170 g, 0.910 mmol) in CH_2Cl_2 (100 mL). The reaction mixture is washed with a 10% NH_4OH aqueous solution (100 mL), extracted with dichloromethane (100 mL). The CH_2Cl_2 layer is washed with a 25% aqueous solution of HCl (100 mL). The organic layer is dried with $MgSO_4$. After column chromatography over silica gel with eluent, EtOAc:hexanes (1:4) gives **3.7** (220 mg, 34 %) as a colorless solid**.** ^{1}H-NMR δ 7.21, 7.06, 7.05 (6H, aryl-H) 3.92, 3.86, 3.71 (18H-OCH_3) ^{13}C-NMR ($CDCl_3$, 75 MHz, 15°C): 149.85, 149.39, 149.13 (aromatic C-OCH_3); 122.56, 121.107, 118.65, 115.41, 114.43; 94.34 (aromatic C-I); 90.70, 90.32 (C-ethynyl) ; 56.42, 56.29, 56.24 (O**C**H3). IR (cm^{-1}): ν 3003.0, 2937.4, 2360.7, 2331.8, 1633.6, 1593.1, 1506.3, 1458.1, 1394.4, 1319.2, 1230.5, 1168.8, 1093.6, 1012.6, 850.5, 750.3. Mp= 145°C.

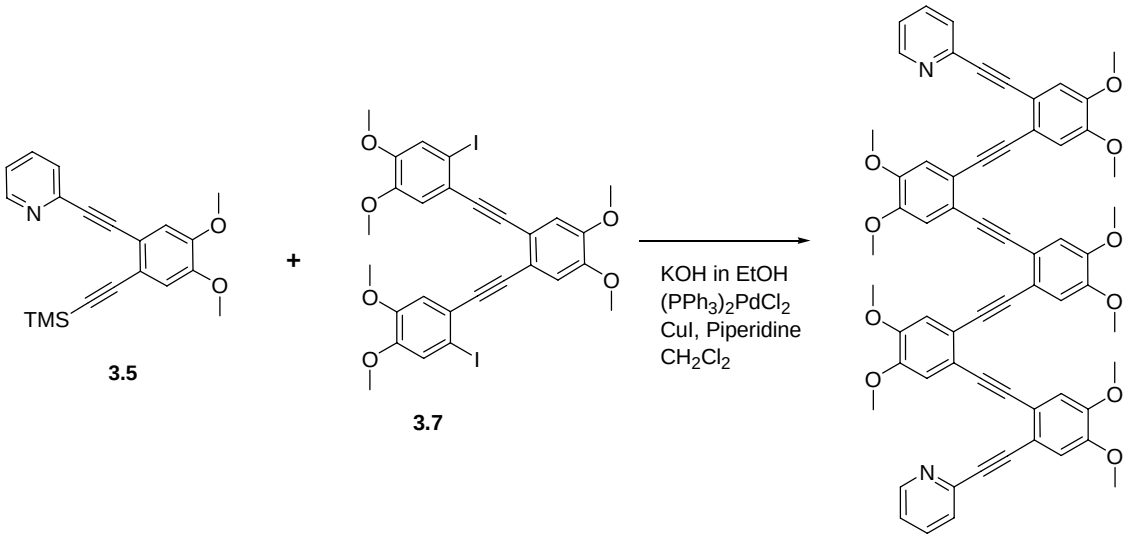

3.5 + **3.7** → **3.3** 34%

(**3.3)** Using Genereal Coupling Procedure D, **3.5** (300 mg, 0.895 mmol) **3.7** (252 mg, 0.355 mmol) $Pd(PPh_3)_2Cl_2$ (0.994 mg, 0.00142 mmol) and CuI (0.675, mg, 0.00355 mmol) are dissolved in dichloromethane (10 mL), piperidine (1 mL) and KOH 10 wt% in ethanol (1 mL). The reaction mixture is washed with a 10% NH_4OH aqueous solution (100 mL), extracted with dichloromethane (100 mL) and dried with Na_2SO_4. The solvent is removed *in vacuo.* The resulting solid is purified over alumina oxide with eluent methanol/CH_2Cl_2 (1:99) to yield **3.3** (120 mg, 34%) as a pale yellow solid. ^{1}H-NMR ($CDCl_3$, 300 MHz) 8.48 (d, 2H), 7.52 (d, 4H), 7.23 (t, 4H), 3.82-3.71 (30H –OCH_3) IR (cm^{-1}): ν 3008.7, 2939.3, 2837.1, 2360.7, 2331.8, 2208.3, 1589.2, 1512.1, 1461.9, 1371.3, 1228.6, 1128.3, 1002.9, 862.1, 669.3. IR (cm^{-1}): ν 3008.7, 2941.2, 2837.1, 2266.2, 1591.2, 1226.6, 1002.9, 864.1, 752.2, 671.2. UV/Vis ($CHCl_3$) λ 275. Emission ($CHCl_3$) λ 436.

3.5 References

1. Bunz, U. H. F.; *Chem. Rev.* **2000,** *100*, 1605-1644.
2. Bunz, U. H. F. *Acc. Chem. Res.* **2001**, *34*, 988-1010.
3. Haley, M. M.; Pak, J. J.; Brand, S. C. *Top. Curr. Chem.* **1999**, *201*, 81-130.
4. Youngs, W. J.; Tessier, C. A.; Brandshaw, J. D. *Chem. Rev.* **1999**, *99*, 3153-3180.
5. Staab, H. A.; Graf, F. Tetrahedron Lett. 1966, 751-754. (b)Staab, H. A.; Graf, F. *Chem. Ber.* **1970**, *103*, 1107.
6. Staab, H. A.; Graf. *Chem Ber*. **1970**. *103*, 1107-1108.
7. Schumm, J. S.; Pearson, D. L.; Tour J. M. *Angewente. Chem. Int. Ed. Engl. 1994,* 33, 1360-1363.
8. Sluch, M. L.; Godt, A.; Bunz, U. H. F.; Berg, M. A. *J. Am. Chem. Soc*, **2001**, *123*, 6447-6448.
9. Huang, L.; Tour, J.M. *J. Am. Chem. Soc.* **1999**, *121*, 4908-4909.
10. Nelson, J. C. ; Saven, J.G.; Moore, J. S.; Wolynes, P. G. *Science* **1997,** *277*, 1793-1796.
11. Matsuda, K.; Stone, M. T.; Moore, J. S. *J. Am. Chem. Soc.* **2002**. (c) Moore, J. S. *Acc. Chem. Res.* **1997**, 30, 402-413.
12. Moore, J. S. *Acc. Chem. Res*. **1997**, *30*, 402-413.
13. Hill, D. J.; Mio, M. J.; Prince, R. B.; Hughes, T. S.; Moore, J. S. *Chem. Rev*. **2001**, 101, 3893-4012.
14. Grubbs, R. H.; Kratz, D. *Chem. Ber. –Recl.* **1993**, 149-157.

15. Anderson, S. *Chemistry Eur. J.* **2001**, *7*, 4706-4714.

16. Wong, M. S.; Nicoud, J. F. *Tetrahedron Let.* **1994**, *35*, 6113-6116.

17. Blatchly, R. A.; Jones, J.V; Tew, G. N. *Org. Lett.* **2003,** *18,* 3297-3299.

18. Blatchly, R. A.; Tew, G. N. *J. Org. Chem.* **2003,** *68*, 8780-8785.

19. Fiscus, J.E.; Shotwell, S.; Layland, R.C.; Smith, M.D. zur Loye, H. C.; Bunz, U.H.F. *Chem. Comm.* **2001,** 2674-2675.

20. Shotwell, S.; Ricks, H. L.; Morton, J.; Laskoski, M.; Fiscus, J.; Smith, M. D.; Shimizu, K. D.; zur Loye, H, C.; Bunz ; zur Loye, H. C.; Bunz, U.H.F.; *J. Organomet. Chem.* **2003**, *671*, 43-51.

CHAPTER 4

COORDINATION COMPOUNDS OF 1,2-DIMETHOXY-4,5-BIS(2PYRIDYLETHYNYL)BENZENE

4.1 Introduction

Supramolecular chemistry has evolved rapidly during the last 20 years. A fascinating subfield of supramolecular chemistry is the metal-assisted synthesis of platonic solids, regular or truncated polyhedra, which form by self-assembly processes. Stang, Atwood, and Zaworotko have made great strides in the generation of a host of these beautiful topologies by clever metal–ligand combinations[1-5]. We have an interest in the metal-assisted supramolecular assembly of conjugated organic ligands toward novel photonic, electroactive, and structural materials[6-8].

Here we wish to demonstrate that one organic module 1,2-dimethoxy-4,5-bis(2-pyridylethynyl)benzene **2.16** (Figure 4.1) can form a supramolecular cycle, dimers and a polymer utilizing different inorganic connectors $Cu(OAc)_2$, $Cu(OTf)_2$, $(CH_3CN)_2PdCl_2$, $ZnBr_2$, ZnI_2, $CoCl_2$ and $[Rh(OAc)_2]_2$.

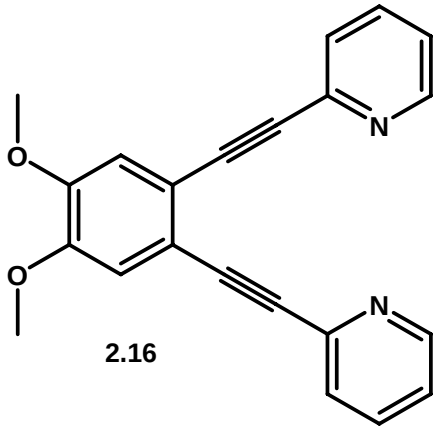

2.16

Figure 4.1: 1,2-dimethoxy-4,5-bis(2-pyridylethynyl)benzene **2.16**

Ueda[9,10], Bosch[11] and Thummel[12] have reported similar coordination compounds of the pincer ligand similar in shape to **2.16,** but lacking the methoxy groups**.**

4.2 Results and Discussion:

The first compounds to be presented are dimers composed of **2.16** with various metal salts of the formula $M(X_2)$ where M is the metal (Co, Hg, or Zn), and X is a halogen (Cl, Br or I). All dimeric compounds crystallized from slow diffusion reactions between solutions of ligand **2.16** and solutions of various metal(II) halide salts. Cobalt(II), zinc(II), and mercury(II) are all divalent cations that have the tendency to adopt a tetrahedral coordination environment. In each of the seven dimers presented here, every divalent metal cation binds two halogen ligands for charge balance and two nitrogen donor atoms from two different ligands of **2.16** to complete the tetrahedral coordination

environment (Figures 3.2 and 3.3). Ligand **2.16** in its planar configuration would be unable to complete the tetrahedral coordination geometry of the metal due to its rather fixed geometry (V-shape). However, 2-pyridyl rings are free to rotate out of the plane of the ligand and coordinate to the neutral metal-halide unit in a tetrahedral fashion. Although polymer formation is possible given the specific coordination environment of the metal and the availability of the second nitrogen donor atom of the ligand, two identical tetrahedrally coordinated metal atoms come together to form dimers instead. All atoms of the dimers rest on general crystallographic position and the dimers themselves are located about inversion centers such that the asymmetric units contain only one metal cation, one **2.16** ligand, and two halogen ligands. Six of the seven dimeric compounds are isostructural, whereas, the dimer formed with HgI_2 has similar features but crystallizes in a different space group.

Compound **4.1** contains Co^{2+}, which is found in typical tetrahedral coordination.[3]This tetrahedral preference, apparently, cannot be conveniently satisfied through a ring closure that would require a rotation of the pyridyl rings away from the 180° angle found in the copper complex. The result of such a rotation would be an elongated Co–N bond. Instead, the pyridyl rings rotate away from each other by 128° and bind to separate cobalt atoms with bond lengths of 2.03 Å, which is typical for Co–N bonds. The tetrahedral coordination in each case is completed by two chlorine atoms. The overall structure (Fig.3.2) consists of two molecules of **2.16** bridging two cobalt atoms. An inversion center is located in the middle of the dimer.

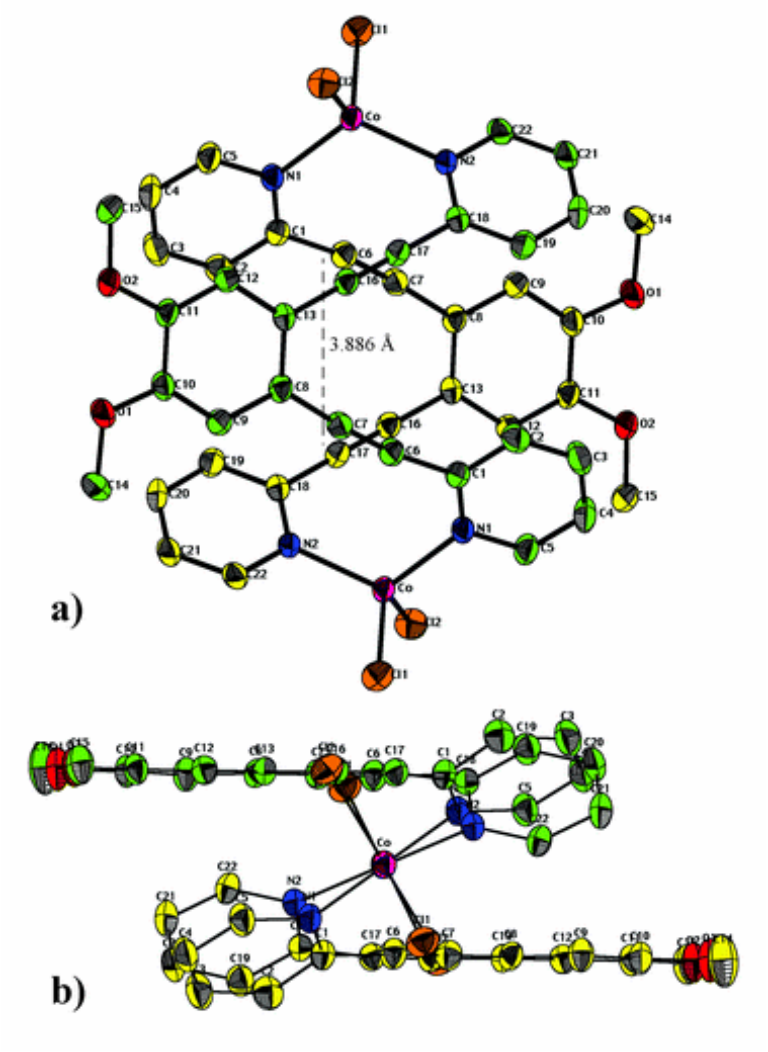

Figure 4.2: Dimer **4.1** of ligand **2.16** with $CoCl_2$. Hydrogen atoms have been omitted for clarity. (a) a view of **4.1** from above showing the tetrahedral coordination of cobalt; (b) a view of **3** from the side showing the opposing orientations of **2.16** and the rotation of the pyridyl rings.

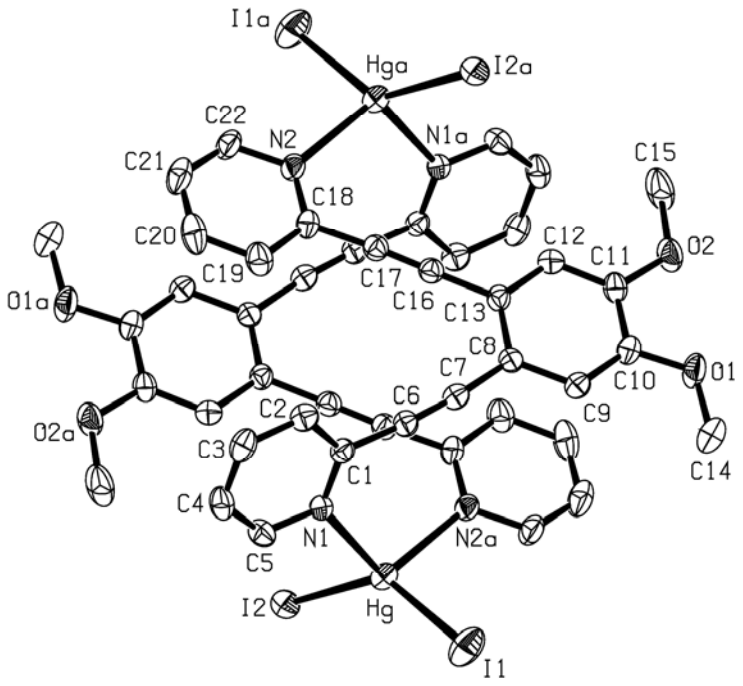

Figure 4.3: Dimer, **4.2** of **2.16** with HgI_2 Thermal ellipsoid plot of the $[HgI_2(\mathbf{1.16})]_2$ **3.2** dimer. Displacement ellipsoids are drawn at the 30% probability level

When the isostructural compounds **4.1**-**4.6** are viewed along the [001] direction, the dimers are observed to exist in a layered arrangement in which the dimers are tilted oppositely in alternating layers (Figure 4.4). These dimers are further organized into rows running parallel to the crystallographic c-axis. For compound **4.2**, rows of the coordination dimers run along the [100] direction. As in compounds **4.1**-**4.6**, the dimers

in **4.2** also exist in a layered arrangement. However, the dimers in **4.7** all tilt in the same direction (Figure 4.5).

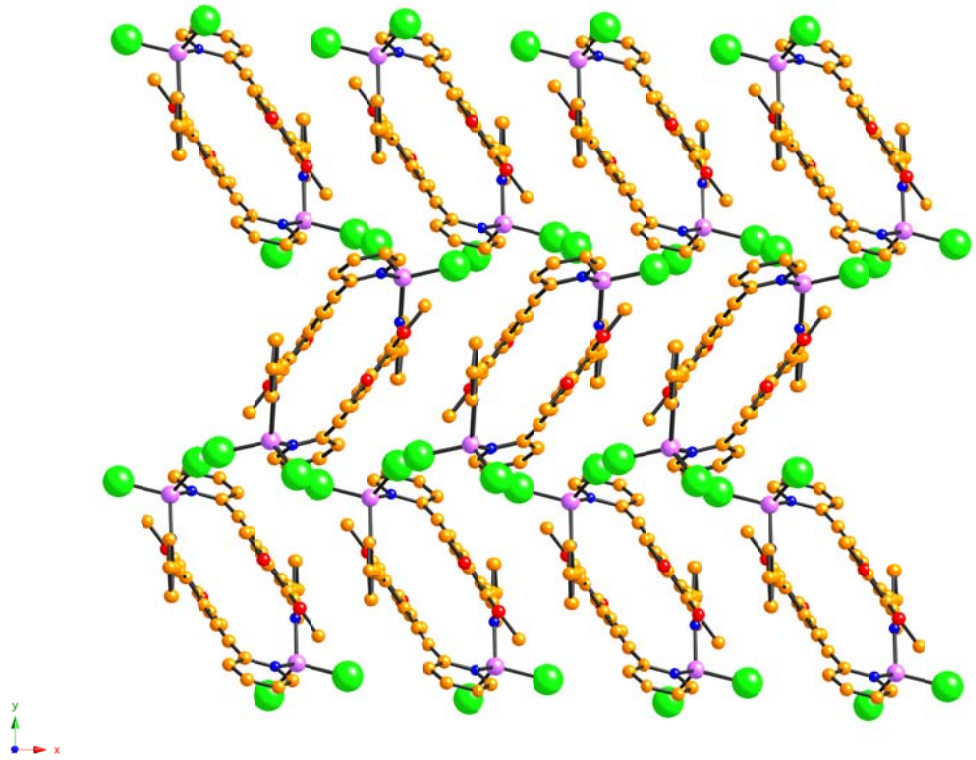

Figure 4.4: Crystal packing in $[HgCl_2(\mathbf{2.16})]_2$ representing isostructural compounds **4.1-4.6**. Hg atoms shown as pink spheres; Cl, green; C, yellow; N, blue; O, red. H atoms are not shown.

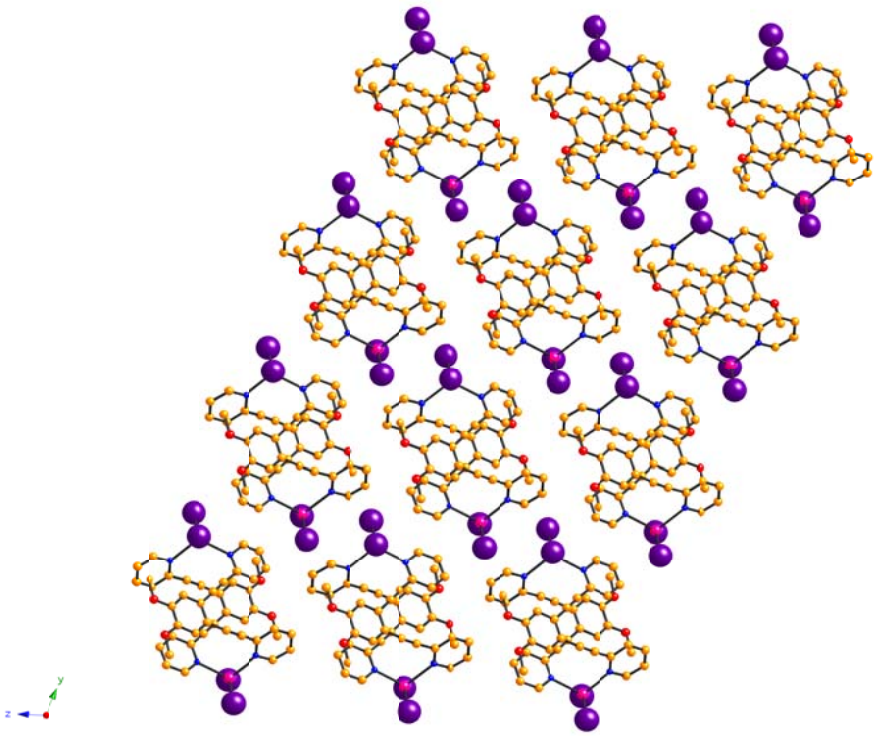

Figure 4.5: Crystal packing in $[HgI_2(\mathbf{1.16})]_2$ (**4.7**). Hg atoms shown as pink spheres; I, purple; C, yellow; N, blue; O, red. H atoms are not shown.

The coordination preference of the metal center or the location of open coordination sites on the metal center seem to be the primary factors contributing to the

structure and dimensionality of the products. Both of these factors are somewhat dependent on the nature of the counterions used for charge balance (anion charge, anion coordination ability, and steric bulk of the anion). Additionally, the rotational flexibility of the 2-pyridyl rings about the C-C single bonds joining them to the rest of the ligand contributes to the versatility of this ligand in forming different structures with different metal salts. Thus, while it is not possible to predict absolutely the structure and dimensionality of products formed with **2.16**, the fundamental aspects of the coordination chemistry, i.e., the coordination preference of the metal or the identity of the counterions, may be used to rationalize the structure formed. In fact, all the divalent metal halides studied thus far have resulted in the formation of dimers when reacted with the **2.16**; and we may thus predict that dimers are likely to result from the reaction of other divalent metal halides with the **2.16**.

$CoCl_2$[1,2-dimethoxy-4,5-bis(2-pyridylethynyl)benzene] **(4.1)**

The tetrahedral coordination environment around the metal is distorted from the ideal 109.5° angles, with both the nitrogen atoms and the chlorine atoms pushed away from each other and towards the other pair (∠N-Co-N = 117.53(9)°, ∠Cl-Co-Cl = 112.81(3)°). The averaged Co-N and Co-Cl bond lengths of 2.028 Å and 2.236 Å are well within normal bonding distances. The pyridyl groups of the ligand are rotated approximately 128° out of the plane of the central benzene ring, with the two central benzene rings in each dimer being parallel. The perpendicular distance between the ligands is about 3.5 Å, and the Co…Co separation is about 9.2 Å.

$ZnCl_2$[1,2-dimethoxy-4,5-bis(2-pyridylethynyl)benzene] **(4.2)**

In **4.2** (Figure 3.6), the angles around zinc range from 116.39(7)° to 105.11(5)° (∠N-Zn-N = 116.39(7)°, ∠Cl-Zn-Cl = 113.72(2)°). The Zn-N and Zn-Cl average bond lengths of 2.0410 Å and 2.2387 Å are well within the normal bonding distances. The pyridyl groups of the ligand are rotated approximately 140° out of the plane of the central benzene in **4.2**, and the two central benzene rings of each dimer are parallel. The perpendicular distance between the ligands is approximately 3.4 Å while the Zn…Zn separation is about 9.3 Å.

$ZnBr_2$[1,2-dimethoxy-4,5-bis(2-pyridylethynyl)benzene] **(4.3)**

In **4.3**, the angles around zinc range from 117.03(9)° to 105.05(7)° (∠N-Zn-N = 117.03(9)°, ∠Br-Zn-Br = 114.131(17)°). The Zn-N and Zn-Br average bond lengths of 2.041 Å and 2.3673 Å are well within the normal bonding distances. The pyridyl groups are rotated about 140° out of the plane of the central benzene, with the two central benzene rings of each dimer being parallel. The perpendicular distance between the ligands is approximately 3.4 Å while the Zn…Zn separation is about 9.3 Å.

ZnI_2[1,2-dimethoxy-4,5-bis(2-pyridylethynyl)benzene] **(4.4)**

In **4.4**, the angles around zinc range from 104.50(7)° to 116.79(9)° (∠N-Zn-N = 116.79(9)°, ∠I-Zn-I = 113.923(14)°). The average Zn-N and Zn-I bond lengths of 2.037 Å and 2.5647 Å are well within the normal bonding distances. The pyridyl groups are rotated approximately 141° out of the plane of the central benzene, with the two central

benzene rings of each dimer being parallel. The perpendicular distance between the ligands is about 3.3 Å while the Zn…Zn separation is approximately 9.4 Å.

$HgCl_2$[1,2-dimethoxy-4,5-bis(2-pyridylethynyl)benzene] **(4.5)**

In **4.5**, the angles around mercury range from 118.99(9)° to 98.98(7)° (∠N-Hg-N = 118.99(9)°, ∠Cl-Hg-Cl = 116.57(3)°). The average Hg-N and Hg-Cl bond lengths of 2.271 Å and 2.4519 Å are well within the normal bonding distances. The pyridyl groups are rotated about 141° out of the plane of the central benzene, with the two central benzene rings of each dimer being parallel. The perpendicular distance between the ligands is about 3.5 Å while the Hg…Hg distance is approximately 9.4 Å.

$HgBr_2$[1,2-dimethoxy-4,5-bis(2-pyridylethynyl)benzene] **(4.6)**

In **4.6**, the angles around mercury range from 120.43(3)° to 100.55(13)° (∠N-Hg-N = 117.04(17)°, ∠Br-Hg-Br = 120.43(3)°). The average Hg-N and Hg-Br bond lengths of 2.305 Å and 2.5341 Å are well within the normal bonding distances. The pyridyl groups are rotated about 143° out of the plane of the central benzene, with the two central benzene rings of each dimer being parallel. The perpendicular distance between the ligands is approximately 3.5 Å while the Hg…Hg separation is about 9.6 Å.

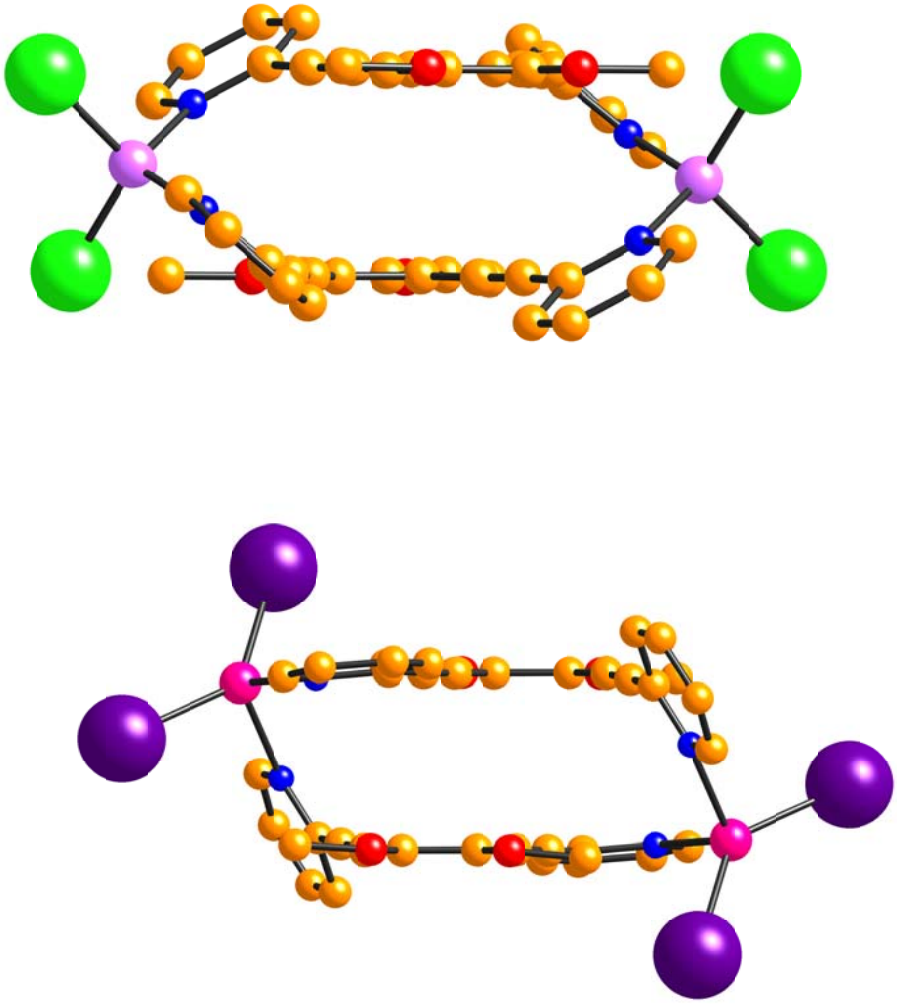

Figure 4.6. Side-on views of $[ZnCl_2(dmpeb)]_2$ (**4.2**, top) and $[HgI_2(dmpeb)]_2$ (**4.4**, bottom) illustrating the difference in the orientation of the ligated pyridyl rings. Zn atoms shown as pale purple spheres; Hg, pink; Cl, green; I, purple; C, yellow; N, blue; O, red. H atoms are not shown.

HgI_2[1,2-dimethoxy-4,5-bis(2-pyridylethynyl)benzene] **(4.7)**

Like compounds **4.1**-**4.6**, each metal cation in compound **4.7** is bonded to two halide ligands and two ligands of **2.16** in a distorted tetrahedral environment; and each dmpeb ligand bridges two cations in order to form dimers which rest on inversion centers (Figure 3). However, in **4.7**, only one pyridyl group rotates out of the plane of the central benzene ring (112.6°) while the other pyridyl group remains essentially planar (174.7°; Figure 6). In **4.7**, the bond angles about Hg^{2+} range from 136.56(2)° to 99.14(12)° (∠N-Hg-N = 110.45(16)°, ∠I-Hg-I = 136.56°), and the Hg-N (average Hg-N: 2.432 Å) and Hg-I (average Hg-I: 2.6625 Å) distances are typical. The central benzene rings in **4.7** lie in parallel planes and the perpendicular distance between ligands is approximately 3.3 Å. The Hg…Hg separation in **4.7** is approximately 9.6 Å.

The second type of coordination geometry presented here two complexes which form an 11-membered ring which is formed by coordination of a metal, $Cu(OAc)_2$ and $(CH_3CN)_2PdCl_2$.

Single crystals suitable for X-ray diffraction of Cu(**1**)$(OAc)_2{\cdot}CH_3OH$ **4.8** were obtained by layering a methanol solution (1 mL) of $Cu(OAc)_2{\cdot}H_2O$ (2.0 mg, 0.01 mmol) over a dichloromethane solution (1 mL) of **2.16** (6.7 mg, 0.02 mmol), with a layer of pure methanol separating them (20% yield). Compound **4.8** demonstrates the preference of Cu^{2+} for square planar coordination with copper positioned snugly between the two pyridyl rings. The resulting N–Cu–N (Cu–N 2.01 Å, N–Cu–N 172.98°) bonds close an eleven membered, triangular ring (**4.7**), which is nearly identical to the structures

reported by Bosch and Barnes for 1,2-bis(2-pyridylethynyl)benzene. The square planar coordination of copper is completed by two *trans* oxygen atoms from separate acetate groups.

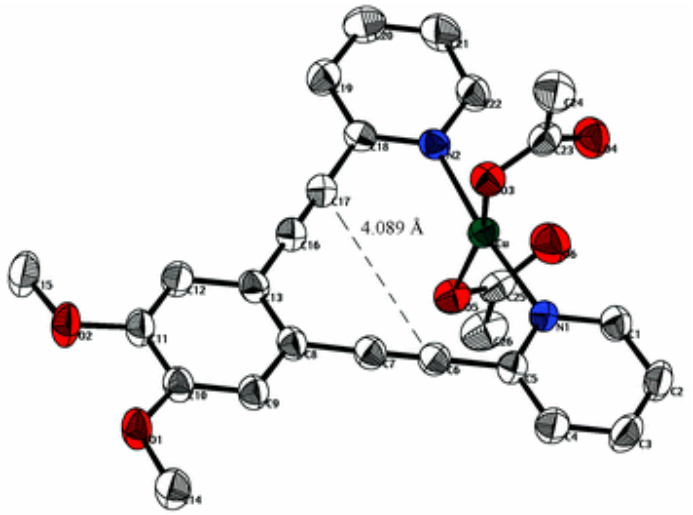

Figure 4.7: A single molecule of **4.8** with $Cu(OAc)_2$. The hydrogen atoms and methanol group have been omitted for clarity.

We obtained **2.16**·$PdCl_2$, i.e. **4.9**, by layering a solution of $(CH_3CN)_2PdCl_2$ in acetonitrile over a solution of **2.16** in dichloromethane. Overnight block-shaped crystals formed in a 65% yield at the interface of the two solvents. Attempts to grow crystals of **4.9** by mixing of **2.16** and $(CH_3CN)_2PdCl_2$ in a suitable solvent did not work. Figure 3.9 shows the ^{1}H-NMR spectra of the ligand **2.16** (bottom) and that of the complex **4.9** (top). The downfield shift of the signals of the pyridine ligand upon complexation is considerable and is due to the electron withdrawing effect of the $PdCl_2$ moiety. It is clear

from the simple and clean spectrum that the crystallization experiment produces only one compound under these conditions. The isolated specimens were of good quality, and a single crystal structure analysis of **4.9** was undertaken. The ORTEP of **4.9** is displayed in Figure 4.8.

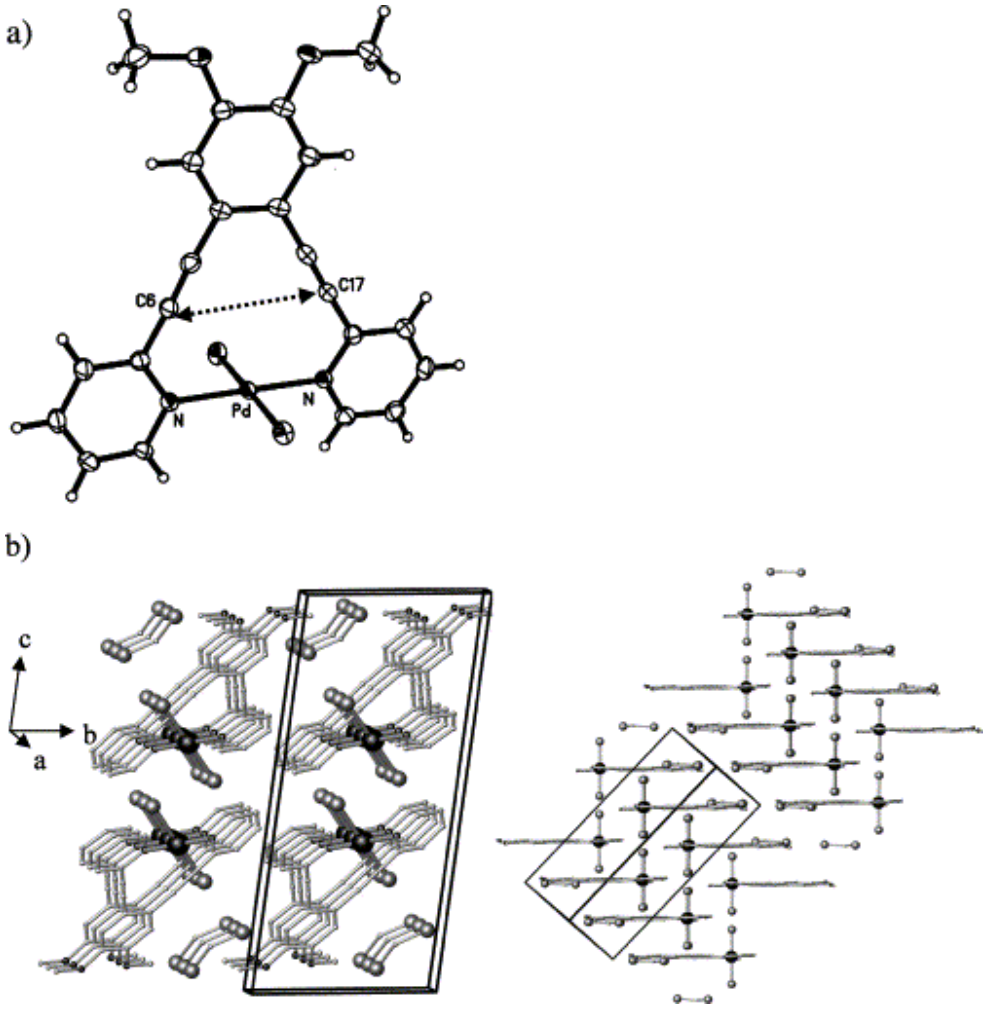

Fig. 4.8: (a) Molecular structure (ORTEP, 50% probability level) of **4.9**. The dotted arrow marks the diyne distance that is relevant for a Bergman cyclization (3.96 Å). The Pd---N distances are 2.01 Å and identical to those reported by Bosch and Barnes for a similar complex. (b) Packing of **4.9** in the solid state. The packing is influenced by the proximity of the halogens in adjacent $PdCl_2$-units and the intercalated solvent molecules (CH_2Cl_2).

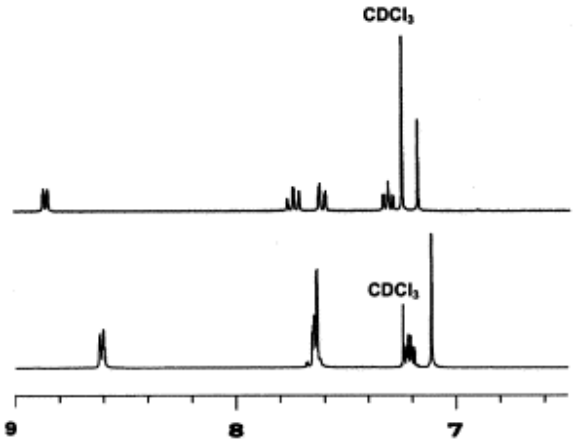

Figure 4.9: Top: ^{1}H-NMR spectrum of **4.9**. Bottom: ^{1}H-NMR spectrum of **2.16**.

The next type of *trans*-spanning coordinating complexes is a dimer formed by $Cu(OTf)_2$ with **2.16**. In this case, two ligands of **2.16** are bound around one metal.

In the first experiment a solution of copper(II)triflate in methanol was layered over a solution of **2.16** in dichloromethane. After several days, well-developed blue-green needles were harvested by filtration (30%). These needles are very sensitive to solvent loss when removed from the mother liquor. Attempts to obtain an ^{1}H-NMR spectrum of this compound was unsuccessful due to the paramagnetic nature of this d^9 Cu(II) complex. The harvested specimens were of good quality and a single crystal X-ray structure determination of **4.10** was possible.

Figure 4.10 shows the molecular structure of **4.10** and its packing in the solid state. Remarkable is the intramolecular shortening of the alkyne–alkyne distance upon co-ordination of the Cu^{2+} salt. This distance (arrow) decreases from 4.25 Å in the

uncomplexed *cis*-form of **2.16** (as calculated by 6-31G**) to 3.98 Å in the enediyne system of **4.10**.

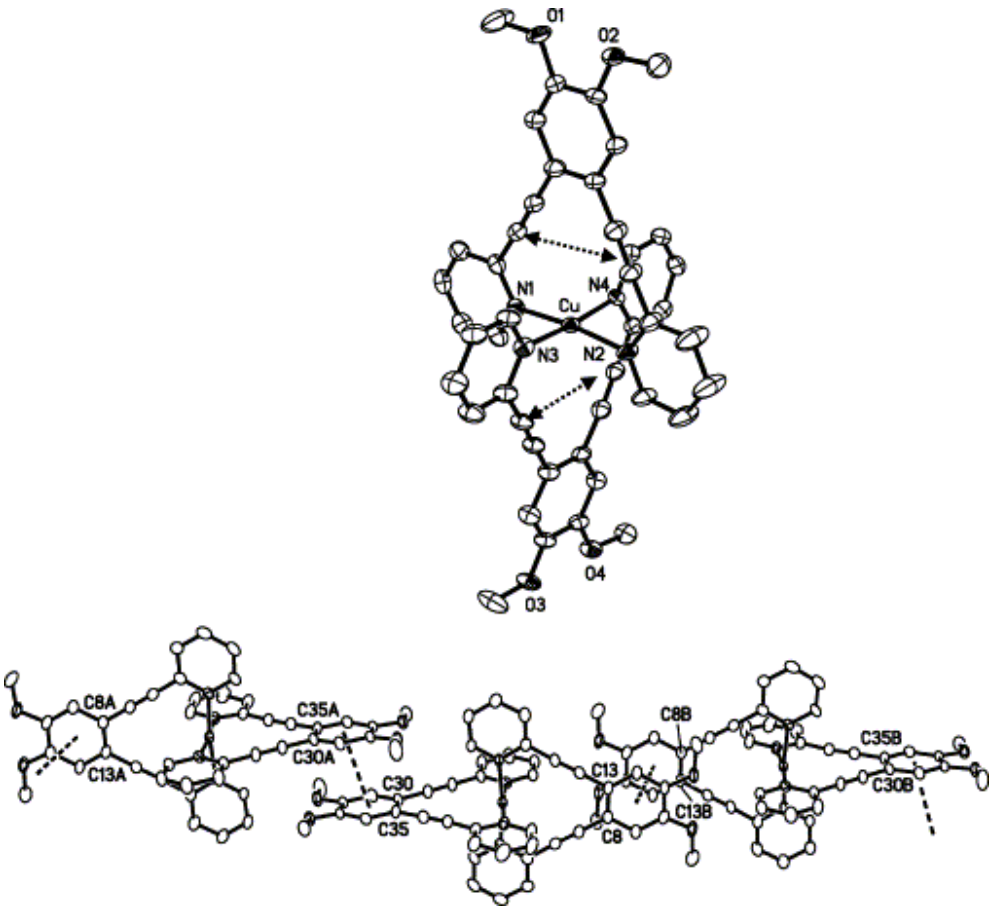

Figure 4.10: ORTEP(40% probability level) of **4.10**. The dotted arrows mark the diyne distances that are relevant for a Bergman cyclization (3.96 and 3.99 Å). Bottom: linear chains of molecules of **1.16**are held together by π–π stacking interactions. The centroid–centroid distances shown by the dotted lines are 3.47 and 3.51 Å, respectively.

The octahedral molecules of **4.10** arrange in a linear chain in the solid state. This chain is formed by the π–π stacking of dimethoxybenzene rings on top of each other. In this packing pattern the electron-rich methoxy groups of one ring are placed over the

electron-deficient carbon atoms (C30A and C35A) of a second dimethoxybenzene unit. The tight interaction (3.48 Å, dotted line) of these benzene rings is probably due to an electrostatic/charge effect.

A cursory examination of the differential scanning calorimetry data of **4.9** and **4.10** shows that these materials undergo Bergman type reactions at elevated temperatures and The ligand **2.16** melts at 168 °C and shows an exothermic reaction at 276 °C (62 kcal mol^{-1}). Upon complexation **4.9** does not melt, but instead a structural change is witnessed (319 °C, −4.6 kcal mol^{-1}, **4.9**) that is followed by a strong exotherm (344 °C, −22 kcal mol^{-1}, **4.9**). The second, larger exotherm is due to a Bergman-type rearrangement in the solid state. The coordination of $PdCl_2$ increases the temperature for this rearrangement significantly perhaps because the $PdCl_2$ acts as a 'stopper' between the enediyne termini. The complex **4.10** was too sensitive (loss of solvent) to perform meaningful DSC measurements.

The final type of complex formed is metal containing *ortho*-phenyleneethynylene polymer formed from $[Rh(OAc)_2]_2$. Crystals of *catena*-poly{$[Rh(OAc)_2]_2$**2.16**·CH_2Cl_2} **4.11** were prepared by layering except that $[Rh(OAc)_2]_2$ (maintaining the ligand to metal ratio) and ethanol was substituted for methanol (40% yield).

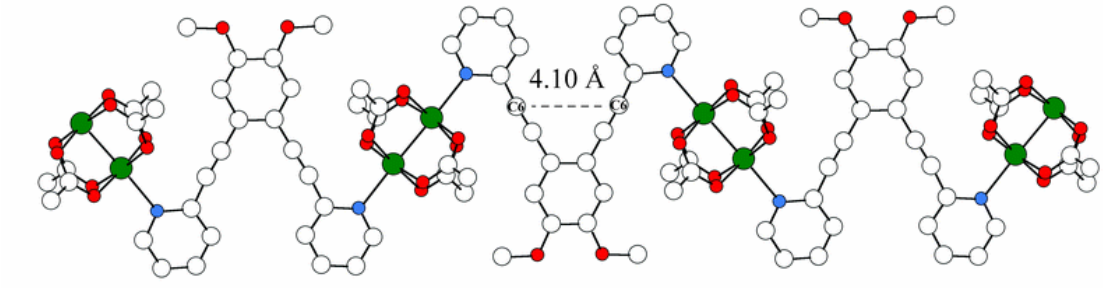

Figure 4.11: A view of **4.11** showing the connectivity of **2.16** and the rhodium dimer. Hydrogens have been omitted for clarity.

Tetrakis(carboxylato)rhodium compounds were first discovered in 1960, but it was not until 1981 that the first polymeric species containing such a rhodium dimer was synthesized.[5] A survey of the CSD indicates that **2.16** is the largest ligand yet used in such a polymeric species. The polymeric structure is charge balanced, eliminating the need for counterions competing for binding sites. This leads to higher site symmetry and makes such rhodium dimers attractive building blocks for coordination polymers.[6] Because of its length, the dirhodium moiety cannot fit between the pyridyl rings and achieve ring closure, as in **4.8** and **4.9**, despite the favorable linear arrangement of the binding sites. Consequently, the pyridyl rings rotate outward by 180° to form a polymer chain with the rhodium dimer bridging adjacent ligands in a zig-zag fashion. This polymer is a supramolecular analogue of the hitherto unknown *ortho*-PPE and as such is a fascinating structure. The Rh–N distance within the polymer is 2.25 Å, typical for Rh–N bonds in such systems.

4.3 Conclusion:

These metal-ligand systems each form a distinctly different structure and between them, demonstrate the importance of the free rotation of the pyridyl rings around the carbon–carbon bonds for facilitating the formation of the three structure types. These structures demonstrate the diversity, which can be achieved using **2.16** that is made possible by the ability of the ligand to distort itself to the preferred coordination environment of the metal center. While one may expect a slight bending of the pyridylethynyl legs either towards or away from each other, these three structures show that rotation of the pyridyl ring around the ethynyl linkage seems more favorable.

4.4. Experimental

Compound **2.16** was synthesized using literature procedures. All other reagents were of commercial grade and used as obtained. ^{1}H- and ^{13}C-NMR spectra were recorded in $CDCl_3$ on a Bruker AM 300 or a Varian Mercury 400 spectrometer. The mass spectra were measured on a VG 70SQ. IR spectra were obtained using a Shimadzu FTIR-8400 with KBr pellets. X-ray crystal structure analyses were performed at 293 K using a Bruker SMART APEX CCD-based diffractometer system Mo–K_α, (λ=0,71073Å).

(**4.9**) Compound **2.16** (93.6 mg, 0.274 mmol) was dissolved in dichloromethane (3 ml) and placed in a vial. A solution of $(CH_3CN)_2PdCl_2$ (87.9 mg, 0.339 mmol) dissolved in 8 ml of acetonitrile was carefully layered on top of the dichloromethane solution. The vial was capped and placed in the dark for 12 h, after which brownish block-like crystals of **4.9** (93.0 mg, 65%) were collected by vacuum filtration, washed with warm acetonitrile, and dried. IR (cm^{-1}): ν2950, 2212, 1591, 1531, 1371, 1256, 991, 768. ^{1}H-NMR (300 MHz, $CDCl_3$): δ8.85 (dd, 2H, $^{3}J_{H,H}$=6.6 Hz, $^{4}J_{H,H}$=0.83 Hz, pyr-H), 7.73 (ddd, 2H, $^{3}J_{H,H}$=9.3 Hz, $^{4}J_{H,H}$=1.7 Hz, pyr-H), 7.60 (dd, 2H, $^{3}J_{H,H}$=8.8 Hz, $^{4}J_{H,H}$=0.83 Hz, pyr-H), 7.30 (dtd, 2H, $^{3}J_{H,H}$=9.1 Hz, $^{4}J_{H,H}$=1.7 Hz, pyr-H), 7.17 (s, 2H, arom.-H), 3.98 (s, 6H, OCH_3). MS (EI) *m/z* Calc. for M^+ ($C_{22}H_{16}Cl_2N_2O_2Pd$) 516.0, decomposition before could be M^+ determined.

(**4.10**) A solution of $Cu(OTf)_2$ (3.6 mg, 10 μmol) in ethanol (1 ml) was layered over a solution of (**2.16**) (6.8 mg, 20 μmol) in chlorobenzene (1 ml) with a layer of ethanol

separating them. Upon diffusion of the layers, blue–green crystals formed of **4.10** (3.1 mg, 30%). One needle was coated in inert oil and mounted on a thin glass fiber for single crystal structure determination.

(4.1) A solution of $CoCl_2 \cdot 6H_2O$ in ethanol (0.01 mmol, 1 mL) was layered over a solution of the ligand in dichloromethane (0.02 mmol, 1 mL) with a layer of neat ethanol (1mL) separating them. Blue-green needles formed upon diffusion of the two solutions into one another, and the crystals were isolated in 29% yield based on Co. One needle was coated in an inert oil and mounted on the end of a thin glass fiber for single crystal structure determination.

(4.2) A solution of $ZnCl_2$ in methanol (0.01 mmol, 1 mL) was layered over a solution of the ligand in dichloromethane (0.02 mmol, 1 mL) with a layer of neat methanol (1mL) separating them. Yellow prismatic crystals formed upon diffusion of the two solutions into one another, and the crystals were isolated in 48% yield based on Zn. One crystal was mounted onto the end of a thin glass fiber using inert oil for single crystal structure determination.

(4.3) A solution of $ZnBr_2$ in methanol (0.01 mmol, 1 mL) was layered over a solution of the ligand in dichloromethane (0.02 mmol, 1 mL) with a layer of neat methanol separating them. Yellow bars formed upon diffusion of the two solutions into one

another, and the crystals were isolated in 42% yield based on Zn. One bar was epoxied onto the end of a thin glass fiber for single crystal structure determination.

(4.4) A solution of ZnI_2 in methanol (0.01 mmol, 1 mL) was layered over a solution of the ligand in dichloromethane (0.02 mmol, 1 mL) with a layer of neat methanol (1mL) separating them. Yellow crystals formed upon diffusion of the two solutions into one another, and the crystals were isolated in 19% yield based on Zn. An irregular fragment sectioned from a larger crystal was mounted onto the end of a thin glass fiber using an inert oil for structure determination.

(4.5) A solution of $HgCl_2$ in methanol (0.01 mmol, 1 mL) was layered over a solution of the ligand in dichloromethane (0.02 mmol, 1 mL) with a layer of neat methanol (1mL) separating them. Yellow-orange crystals formed upon diffusion of the two solutions into one another, and crystals were isolated in 37% yield based on Hg. An irregular crystal was cut from a larger aggregation and epoxied onto the end of a thin glass fiber for single crystal structure determination.

(4.6) A solution of $HgBr_2$ in ethanol (0.01 mmol, 1 mL) was layered over a solution of the ligand in chloroform (0.02 mmol, 1 mL) with a layer of neat ethanol (1mL) separating them. Yellow plate crystals formed upon diffusion of the two solutions into one another, and the crystals were isolated in 19% yield based on Hg. A plate was epoxied onto the end of a thin glass fiber for single crystal structure determination.

(4.7) A solution of HgI_2 in methanol (0.01 mmol, 1 mL) was layered over a solution of the ligand in dichloromethane (0.02 mmol, 1 mL) with a layer of neat methanol (1mL) separating them. Yellow bars formed upon diffusion of the two solutions into one another, and the crystals were isolated in 25% yield based on Hg. A bar was cut to size and epoxied onto the end of a thin glass fiber for single crystal structure determination.

4.5 References

1. S. Leininger, B. Olenyuk and P.J. Stang. *Chem. Rev.* **100** (2000), p. 853.
2. P.J. Stang and B. Olenyuk. *Acc. Chem. Res.* **30** (1997), p. 502.
3. P.J. Stang. *Chem. Eur. J.* **4** (1998), p. 19.
4. B. Olenyuk, J.A. Whiteford, A. Fechenkötter and P.J. Stang. *Nature* **398** (1999), p. 796.
5. B. Olenyuk, A. Fechenkötter and P.J. Stang. *J. Chem. Soc. Dalton* (1998), p. 1707.
6. Kitamura, H.; Ozawa, T.; Jitsukawa, K.; Masuda, H.; Aoyama, Y.; Einaga, H., *Inorg. Chem*. **2000**, *39*, 3294.
7. Fiscus, J. E.; Shotwell, S.; Layland, R. C.; Smith, M. D.; zur Loye, H.-C.; Bunz, U. H. F., *Chem. Commun*. **2001**, 2674.
8. Roh, S.-G.; Nah, M.-K.; Oh, J. B.; Baek, N. S.; Park, K.-M.; Kim, H. K., *Polyhedron* **2005**, *24*, 137.
9. Schlutheiss, N.; Ellsworth, J. M.; Bosch, E.; Barnes, C. L., *Eur. J. Inorg. Chem*. **2005**, 45.
10. Cotton, F. A.; Dikarev, E. V.; Petrukhina, M. A., *J. Organomet. Chem*. **2000**, *596*, 130.
11. Crawford, C. A.; Day, E. F.; Streib, W. E.; Huffman, J. C.; Christou, G., *Polyhedron* **1994**, *13*, 2933.
12. Cotton, F. A.; Lin, C.; Murillo, C. A., *Acc. Chem. Res*. **2001**, *34*, 759.

13. Miyasaka, H.; Clerac, R.; Campos-Fernandez, C. S.; Dunbar, K. R., *J. Chem. Soc., Dalton Trans.* **2001**, 858.

14. Batten, S. R.; Hoskins, B. F.; Moubaraki, B.; Murray, K. S.; Robson, R., *Chem. Commun*. **2000**, 1095.

15. Campos-Fernandez, C. S.; Thomson, L. M.; Galan-Mascaros, J. R.; Ouyang, X.; Dunbar, K. R., *Inorg. Chem*. **2002**, *41*, 1523.

16. Su, C.-Y.; Goforth, A. M.; Smith, M. D.; zur Loye, H.-C., *Inorg. Chem*. **2003**, *42*, 5685.

17. Su, C.-Y.; Cai, Y.-P.; Chen, C.-L.; Smith, M. D.; Kaim, W.; zur Loye, H.-C., *J. Am. Chem. Soc*. **2003**, *125*, 8595.

18. Do, L.; Halper, S. R.; Cohen, S. M., *Chem. Commun*. **2004**, 2662.

19. Reger, D. L.; Watson, R. P.; Gardinier, J. R.; Smith, M. D., *Inorg. Chem*. **2004**, *43*, 6609.

20. Abourahma, H.; Moulton, B.; Kravtsov, V.; Zaworotko, M. J., *J. Am. Chem. Soc*. **2002**, *124*, 9990.

21. Lozano, E.; Nieuwenhuyzen, M.; James, S. L., *Chem. -Eur. J.* **2001**, *8*, 735.

22. Shotwell, S.; Windscheif, P. M.; Smith, M. D.; Bunz, U. H. F., *Org. Lett*. **2004**, *6*, 4151.

CHAPTER 5

TETRA-PYRIDYL LIGANDS WITH A THIOPHENE CORE

5.1: Introduction

Tetraethynylthiophenes were first synthesized by Whitesides[1] for their future use in the formation, by oxidative polymerization, of highly cross-linked organic solids. These solids demonstrate a high degree of hardness and thermal stability. Later, tetraethynyl thiophenes such as the ones seen in Figure 4.1 were investigated for the uses as discotic liquid crystals[2-4].

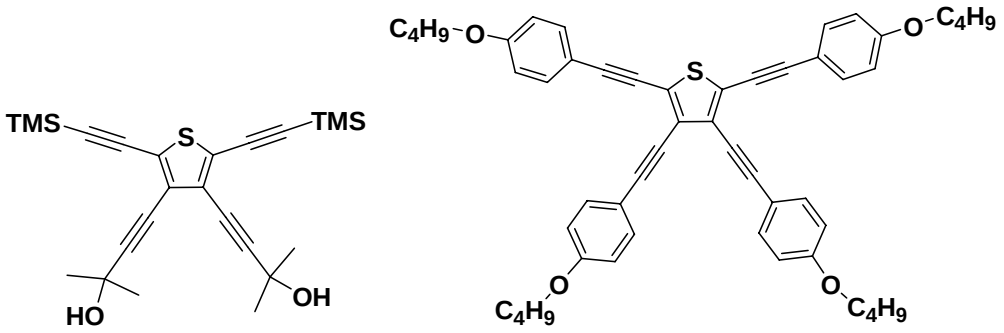

Figure 5.1: Examples of previously synthesized tetraethynylthiophenes.

Here two additional tetraethynyl thiophene compounds are presented. These compounds have alkynyl groups with pyridines as end-caps. These compounds are green emissive in solution and yellow emissive in the solid state. Their absorption and

emission spectra can be modified by the addition of various metals which would allow these compounds to be valuable in metal sensing applications. The pyridine in the *para* position offers conjugation whereas in the *meta* system conjugation is broken. It was of interest to determine the effect of similar compounds varying by the presence of a conjugated system.

5.2 Results and Discussion

We have prepared two ligands containing thiophene as the core and alkynylpyridines as the arms. The first synthetic method is seen in Scheme 4.1. The core of the ligand is synthesized by the iodination of thiophene using literature procedures[3] to obtain **5.2**. In this method the alkynes were attached by utilizing TMSA forming **5.3**. During the deprotection step with KOH/EtOH, a dark red precipitate formed, and an insoluble solid was obtained which was not the desired deprotected tetraalkyne according to ^{1}H-NMR and ^{13}C-NMR. It was necessary to select a different method for synthesizing the ligands.

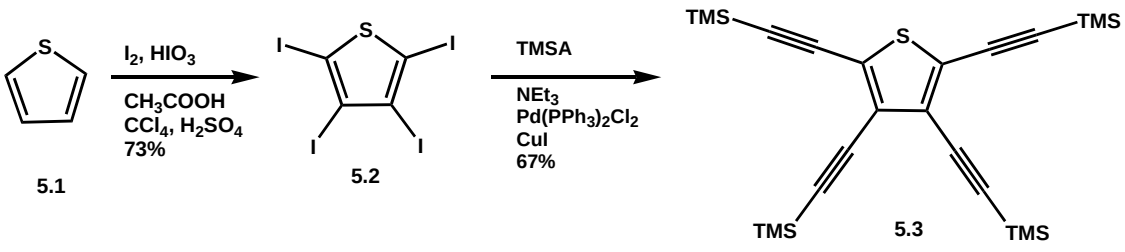

Scheme 5.1: Synthesis of tetraethynylthiophene

A new method was to use alkynyl pyridines and couple them to **5.2**. As seen in previous syntheses presented, the *in situ* coupling and deprotection reaction using KOH was a valuable method in obtaining the target compound. This method was initially utilized for the synthesis of these ligands, however, no coupling of the alkyne occurred. This problem could be remedied by deprotecting the alkyne, isolating it, and using coupling it to the thiophene core with absence of KOH. As seen in Scheme 5.2, deprotection of the TMS group in **2.6** with KOH/EtOH furnishes the free alkyne **5.4**. The ligand **5.5** is assembled using HCSH reaction conditions coupling the free alkyne **5.4** to tetraiodothiophene **5.2**.

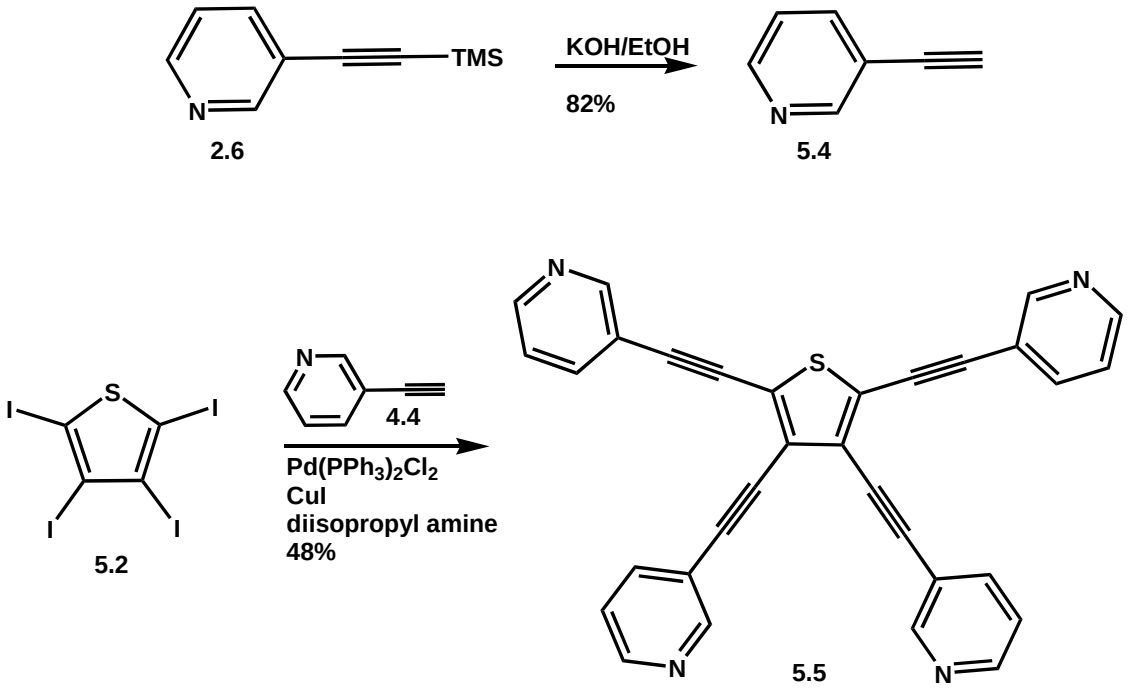

Scheme 5.2. Synthesis of the thiophene ligand **5.5**

This thiophene ligand **5.5** displays shifts in absorption and emission spectra upon exposure to different metals. The greatest shifts can be seen by utilizing $Hg(OTf)_2$ in Figure 5.2 and AgOTf in Figure 5.3. In this experiment, increasing equivalents (0-6eq) were employed. In the case of the emission spectra, there is a slight shift and decrease in emission until it is quenched at four equivalents of the metal salt.

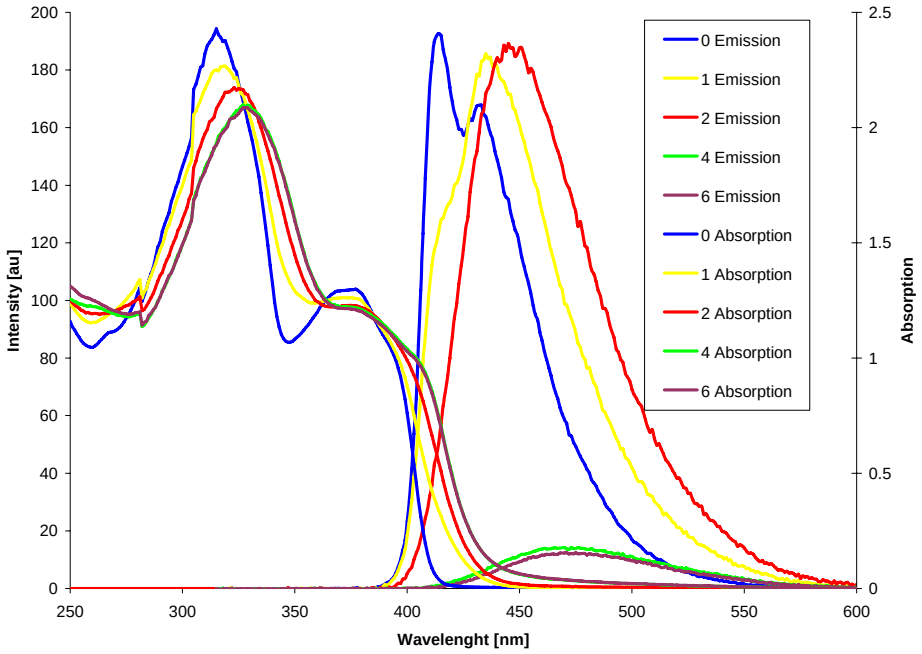

Figure 5.2: Absorption and Emission of **5.5** with $Hg(OTf)_2$

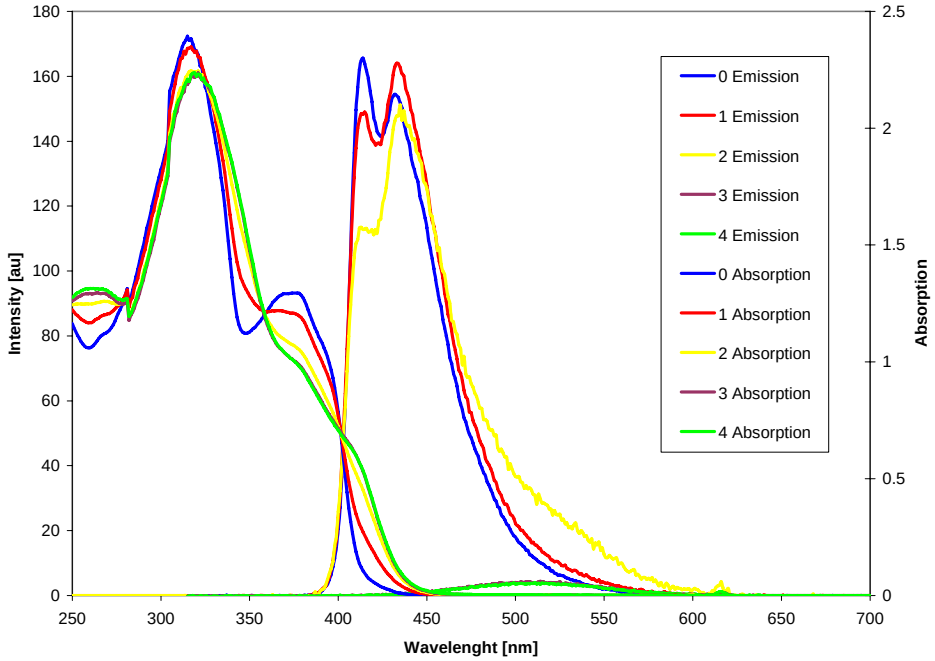

Figure 5.3: Absorption and Emission of **5.5** with AgOTf

The synthesis of a second thiophene ligand can be seen in Scheme 4.2 using similar synthetic techniques seen in Scheme 5.1.

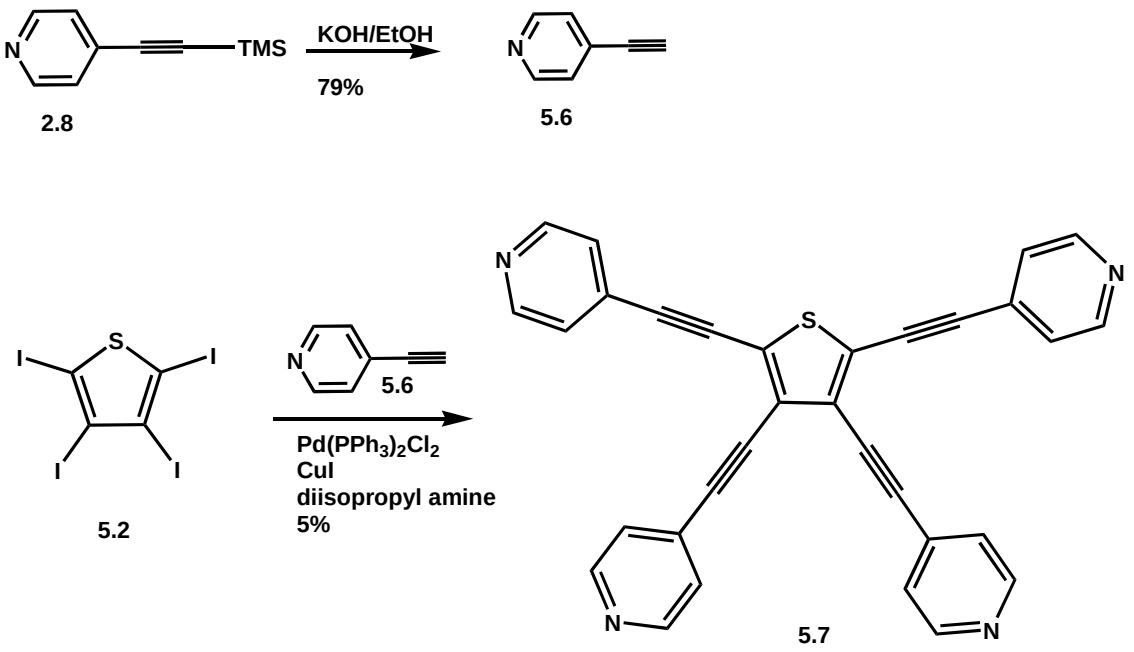

Scheme 5.3: Synthesis of the thiophene ligand **5.7.**

As can be seen in Figure 5.4 and 5.5, this ligand also demonstrates shifts in absorption and emission spectra. In this case, more metals were tested. Upon addition of NaCl, $Ca(NO_3)_2$ and KOTf, there is not a significant shift in absorption and no quenching of emission occurs. However, noticeable red shifts in absorption and decrease in emission can be seen upon addition of an excess of $Zn(OTf)_2$ and $Mg(OTf)_2$.

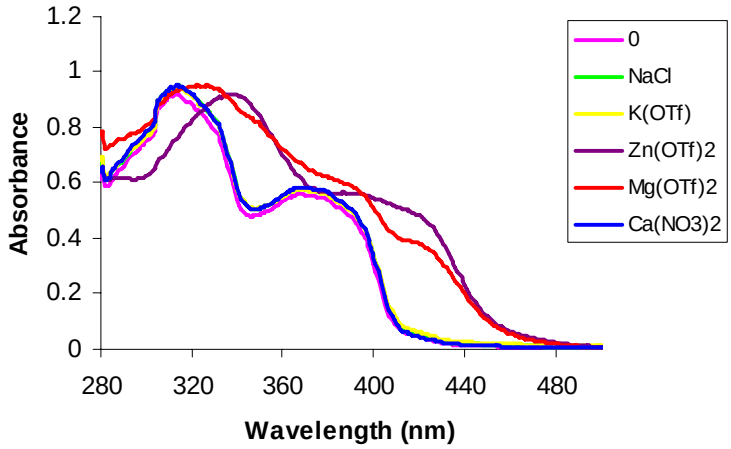

Figure 5.4: Absorption of **5.7** in chloroform with various metal salts

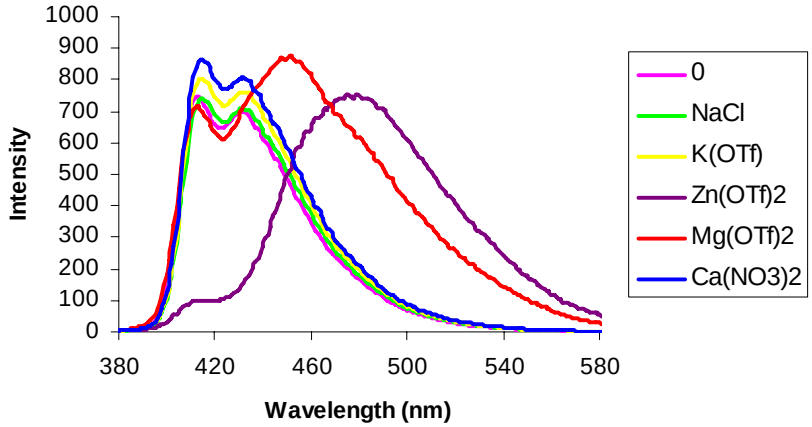

Figure 5.5. Emission spectra of **5.7** in chloroform with various metal salts

5.3 Conclusion

Two new thiophene and pyridine containing ligands have been synthesized, and their optical and metal sensing properties have been tested. The compounds show promise in future applications in the field of determining specific metals due to their ability to display varying absorption and emission spectra upon exposure to various metals.

5.4 Experimental

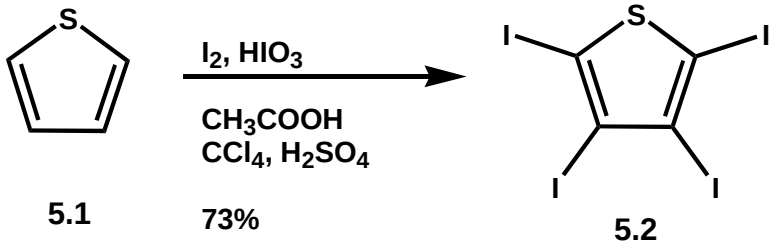

5.1 5.2

2,3,4,5-Tetraiodothiophene (5.2). A solution of acetic acid (170 mL), H_2O (78 mL), and CCl_4 (64 mL) is prepared and added to a 1000 mL three-necked flask which is equipped with a condenser. I_2 (84.9 g, 0.352 mol), HIO_3 (31 g, 0.716 mol), and thiophene **5.1** (16.8 g, 0.2 mol) is added next. H_2SO_4 (4.5 mL) is added last. The reaction is refluxed for 1 week. CCl_4 (100 mL) and H_2O were added, and the reaction was heated to reflux and then cooled to room temperature. The solid is filtered and washed with a 5% $Na_2S_2O_3$ solution followed H_2O. The solid is recrystallized twice from dioxane which yielded a pale yellow solid (84.9 g, 73%) ^{13}C-NMR ($CDCl_3$, 75 MHz, 20°C) 83.52, 93.41.

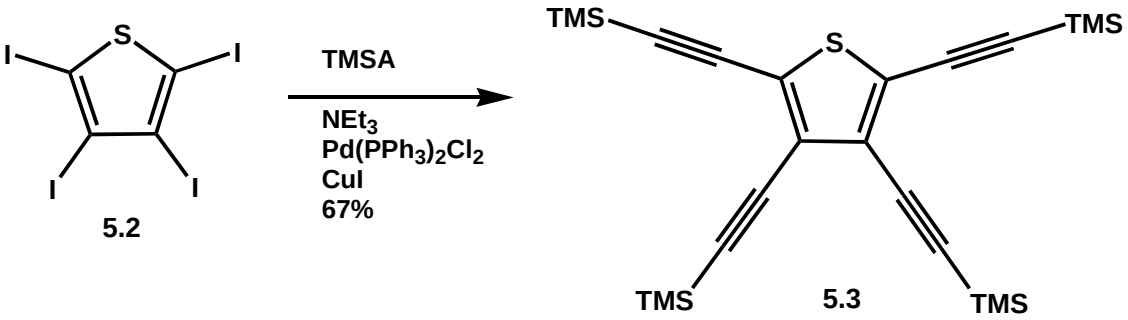

5.2 5.3

2,3,4,5-Tetrakis-trimethylsilanylethynyl-thiophene (5.3) **5.2** (5.00 g, 8.49 mmol) is added to NEt_3 (15 mL) in a 38 mL pressure tube under nitrogen atmosphere. The catalysts, $Pd(PPh_3)_2Cl_2$ (0.59g, 0.085 mmol) and CuI (0.16g, 0.085 mmol) are added next. TMSA (4.16g, 42.4 mmol) is added via syringe. The reaction is capped and stirred for 24 h. at 65˚C. The reaction is then allowed to cool to room temperature. The crude mixture is washed with an aqueous solution of 10% NH_4OH and extracted with heaxane (3x 100 mL). The hexane layer is washed with water and extracted with hexanes (3x 100 mL). The solvent is removed invaccuo to yield a light brown compound which is then purified by column chromatography over silica gel with eluent hexanes to yield **5.3** as a pale yellow solid. H-NMR ($CDCl_3$) δ 0.253. ^{13}C-NMR ($CDCl_3$) 121.15, 119.491, 105.59, 95.02, 0.249.

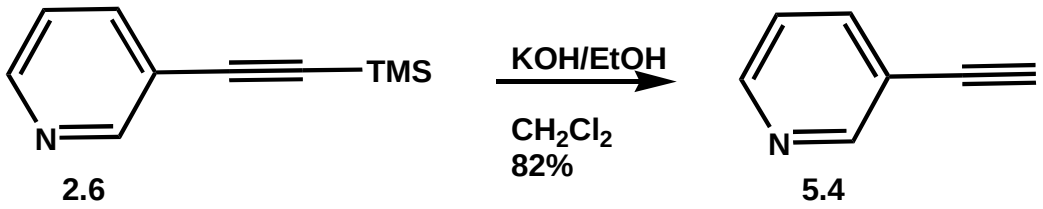

2.6 **5.4**

3-Ethynyl-pyridine (5.4) **1.6** (3 g, 17.1 mmol) is dissolved in CH_2Cl_2. A solution of 10% KOH/EtOH (3 mL) is added. The reaction is stirred at room temperature for 1 h. The solvent is removed in vacuuo without heat. The crude product is sublimed under vacuum to yield **5.4** (1.44g, 82%)) as a colorless solid. ^{1}H-NMR δ 8.68 (m, 1H, pyridyl-H), 8.58-8.56 (m, 1H, pyridyl-H), 7.69 (m, 1H, pyridyl-H), 7.26-7.23 (m, 1H, pyridyl-H), 3.28 (s, 1H, ethynyl-H). ^{13}C-NMR 150.63, 147.52, 138.31, 123.47, 82.43, 81.35.

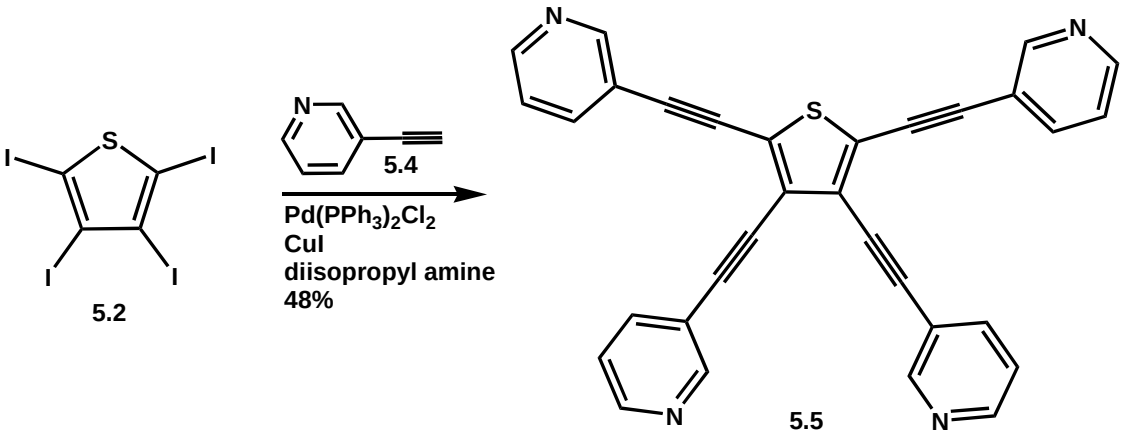

2,3,4,5-tetrakis-(3-pyridylethynyl)-thiophene (5.5) A 50 mL pressure tube is flushed with nitrogen, **5.2** (1 g, 1.70 mmol), THF (10 mL), toluene (5 mL) and diisopropyl amine (3 mL). $Pd(PPh_3)_2Cl_2$ (0.012g, 0.017 mmol) and CuI (0.0032 g, 0.017 mmol) are added. **5.4** (0.875 g, 8.50 mmol) is dissolved in THF (1 mL) and added to the reaction. The reaction is capped and stirred for 24 h at 65˚C. The solvent is removed under vacuum. The crude product is dissolved in CH_2Cl_2 (5 mL), and hexane (50 mL) is added, and a pale yellow solid is formed. The solid is filtered and precipitated again in the same manner as above. The solid is filtered again to yield **5.5** (0.399g, 48%) as a pale yellow solid. ^{1}H-NMR δ 8.78 (s, 4H, pyridyl-H), 8.57 (s, 4H, pyridyl-H), 7.84, 7.83, 7.82, 7.81, 7.80, 7.79 (dt, 4H, pyridyl-H), 7.32-7.28 (m, 4H, pyridyl-H). ^{13}C-NMR ($CDCl_3$) δ 152.09, 151.97, 138.34, 138.32, 127.74, 125.66, 123.14, 119.58, 119.19, 95.78, 92.94, 85.23, 84.04. Mp=177-179˚C.

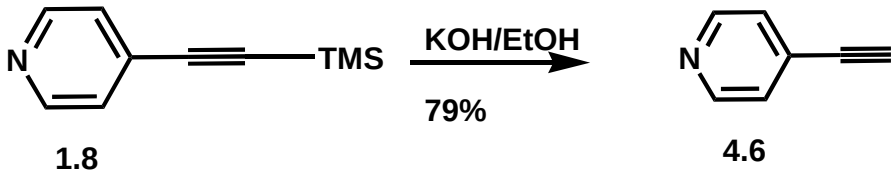

1.8 4.6

4-ethynyl-pyridine (**5.6**) **2.8** (1g, 5.71 mmol) is dissolved in CH_2Cl_2. A solution of 10% KOH/EtOH (2 mL) is added, and the reaction is stirred for 1 h. The solvent is removed under vacuum. Purification by vacuum sublimation yields **5.6** (0.466g, 79%) as a colorless solid. ^{1}H-NMR δ 8.51, 8.50, 8.49, 8.48 (dd, 2H, pyridyl-H), 7.26, 7.25, 7.24, 7.24 (dd, 2H, pyridyl-H) 3.25 (s, 1H, ethynyl-H) ^{13}C-NMR 149.46, 130.07, 125.85, 81.87, 80.75.

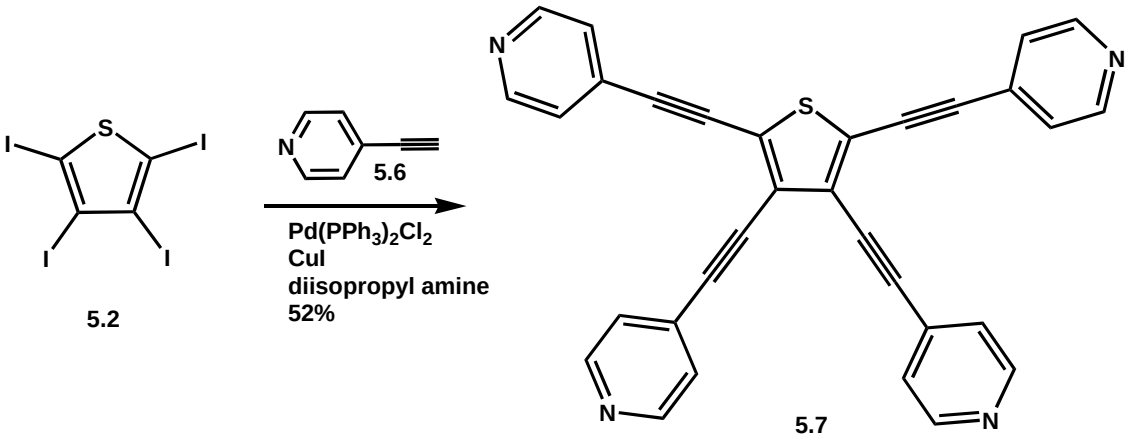

2,3,4,5-tetrakis-(4-pyridylethynyl)thiophene (5.7) A 50 mL pressure tube is flushed with nitrogen, **5.2** (0.462 g, 0.784 mmol), THF (5 mL), toluene (3 mL) and diisopropyl amine (2 mL). $Pd(PPh_3)_2Cl_2$ (54.0 mg, 0.0784 mmol) and CuI (15.0 mg, 0.0784 mmol) are added. **4.6** (0.350 g, 3.53 mmol) is dissolved in THF (1 mL) and added to the reaction. The reaction is capped and stirred for 24 h at 65˚C. The solvent is removed

under vacuum. The crude product is dissolved in CH_2Cl_2 (5 mL), and hexane (50 mL) is added, and a pale yellow solid is formed. The solid is filtered and precipitated again in the same manner as above. The solid is filtered again to yield **5.7** (0.123 g, 32%) as a pale yellow solid. ^{1}H-NMR ($CDCl_3$) δ 8.64 (dd, 8H, pyridyl-H), 7.42 (dd, 8H, pyridyl-H). ^{13}C-NMR ($CDCl_3$) 150.34, 148.65, 130.67, 130.126, 125.72, 125.51, 97.14, 94.27, 86.23, 84.99.

5.5 References

1. Neenan, T. and Whitesides, G. M. *J. Org Chem*. 1988, 53, 2489-2486.
2. Chen et al. Chem. Mater. 2004, 15, 2379-2385.
3. Youngs, W. et al. *Chem. Mater*. 1999, 11, 3050-3057.
4. a) Kishikawa. K; Harris, M. C.; Swager, T. M. *Chem. Mater.* **1999**, *11,* 867. b) Paraskos, A. J.; Swager, T. M. *Chem Mater* **2002**, *14*, 4543. c) Eichhorn. S. H.

CHAPTER 6

DIPHENYLAMINE POLYMERS CONTAINING ARYLENEETHYNYLENES

6.1. Introduction:

Poly(aryleneethynylene)s (PAE)s are polymers of fascinating structure and properties, spanning a wide spectrum.[1a-e] Some of their representatives, particularly the highly fluorescent poly(*para*phenyleneethynylene)s (PPEs) are important materials with applications in sensors,[2] light emitting diodes,[3] sheet polarizers,[4] and in the field of molecular electronics.[5] In this chapter, diphenyl (DPA) polymers with various comonomers are presented. Previously, triphenyl amine (TPA) has been mainly used as a hole transporting layer in organic LED's.[6-8] The first case of TPA polymers containing ethynyl and aromatic monomers such as anthracene and biphenyl were synthesized by Kim *et al.*[9] These polymers are structurally rigid due to aromatic and acetylene units and demonstrate high thermal stability. These polymers, however, demonstrate poor solubility due to lack of solubilizing groups on the monomers.

In this chapter, rather than using three phenyl groups as substituents on the amine we chose to substitute on of the phenyl groups with a dodecyl group which allows for better solubility. Also the DPA monomers were polymerized with various monomers such as

alkyl and alkoxy benzes, alkyl fluorenes, and fluorenone. It was of interest to see how the variation of monomers changed the absorption and emission spectra of the polymers.

6.2 Results and Discussion :

In order to improve the solubility of the DPA polymers, the addition of a long alkyl chain was implemented. This solubilizing group is added using 1-iodo-dodecane to create the alkyl substituted amine **6.2**.[10] (Scheme 5.1) In order to perform the HCSH reaction, it was necessary to add a halogen to both phenyl groups on the amine. Reacting BTEACl with ICl forms a salt, $BTEAICl_2$, **6.3**. This salt **6.3** is used with $CaCO_3$ to iodinate **6.2** in the phenyl position para to the amine **6.4.** in an excellent yield.[11] This monomer can be coupled with various diacetylenes to form polymers, which is seen later, or it can be reacted with TMSA to form **6.5** as seen in Scheme 6.1. Subsequent deprotection of the TMS group yields the dialkynyl compound **6.6**, which is then used with dihalo compounds in order to form DPA polymers.

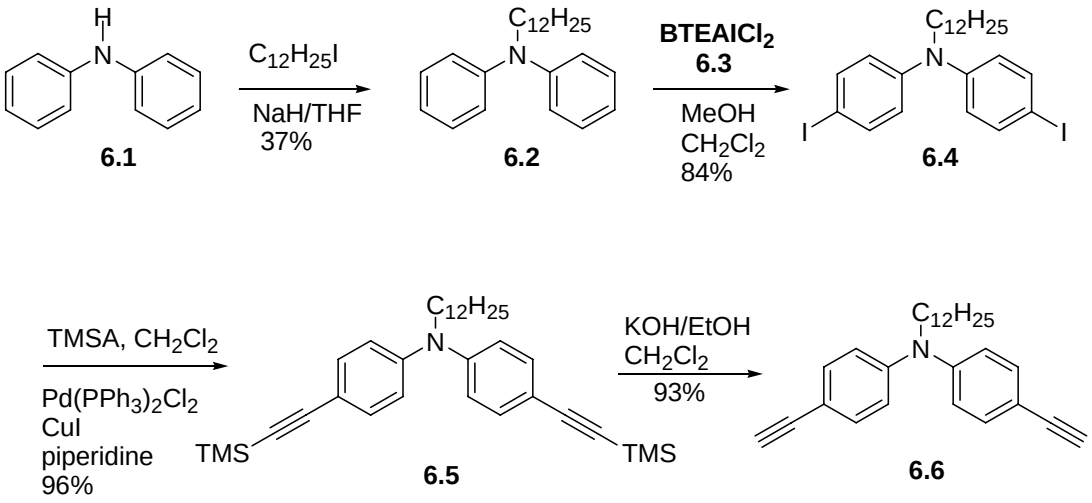

Scheme 6.1: Synthesis of DPA monomers

The monomers **6.7** and **6.9** are prepared according to literature procedures.[12] The Pd catalyzed reaction of **6.7** and **6.9** with the diiodo amine **6.4** gives polymers **6.8** and **6.10** as seen in Scheme 6.2. These polymers demonstrate that it is feasible to put diphenylamine and related monomers into the PPE backbone.

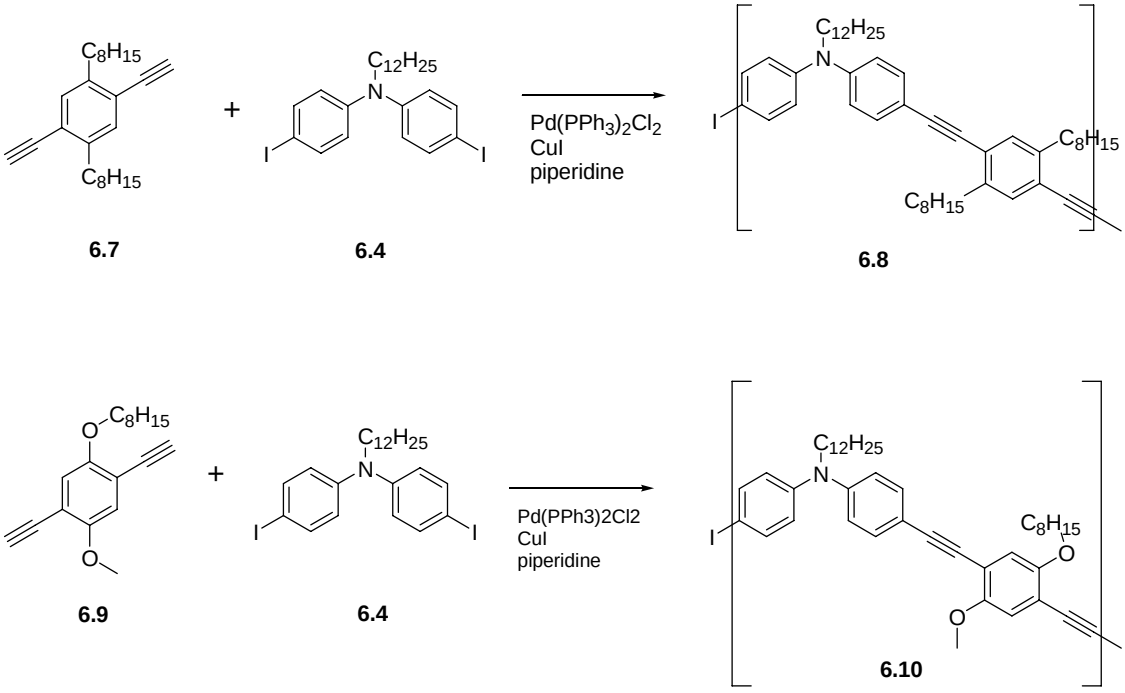

Scheme 6.2: Synthesis two DPA polymers: **6.8** and **6.10**

The absorbance spectra of **6.8** and **6.10** in solution and the solid state can be seen in Figure 6.1. There is a red shift in absorbance from the alkoxy PPE **6.10** (390 nm) from the alkyl PPE **6.8** (422 nm) in a choloroform solution. The absorption for **6.8** is blue-shifted in solution and the solid state from a typical alkoxy PPE.[10] It is found that usually when a comonomer is used that does not contain alkoxy units, then a blue shift in λ_{max} occurs. There is a slight shift in absorption from the solution to the solid state in There is a slight shift in absorption from the solution to the solid state in both **6.8** and **6.10**.

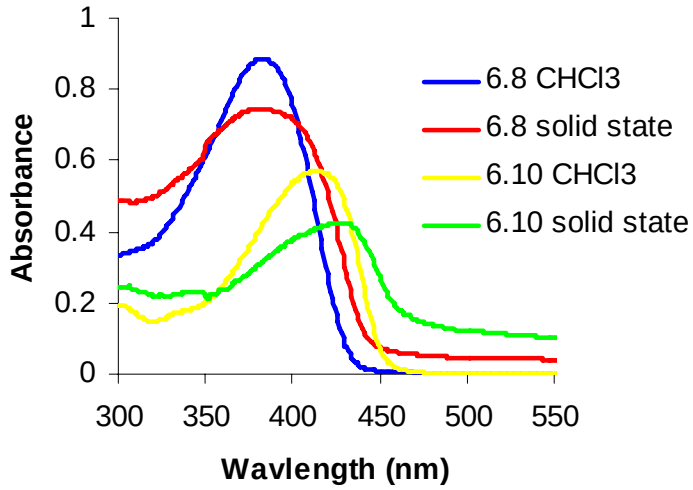

Figure 6.1: Absorbance of polymers **6.8** and **6.10** in chloroform and solid state.

The emission spectra of **6.8** and **6.10** show a red shift in emission in a chloroform solution, which is typical between standard alkyl PPEs and alkoxy PPEs. In the solid state, a red shift from solution is observed in both **6.8** and **6.10**.

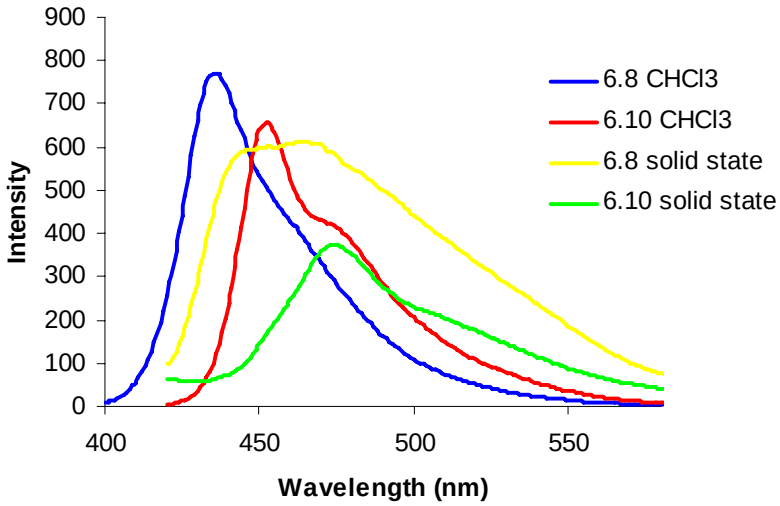

Figure 6.2: Emission of **6.8** and **6.10**.

Another DPA polymer is created from the reaction of diiodoTIPS monomer **6.11**, which was provided by Dr. Brian Englert, with **6.6** using HCSH conditions. This polymer is yellow in the solid state and is green-yellow emissive in the solid state and in a chloroform solution. A red shift in emission can be seen. The polymer shows promise in future use in reaction with azides to form polymers with triazole side groups or reaction with dendrons to form PAE's with dendrimeric side chains.

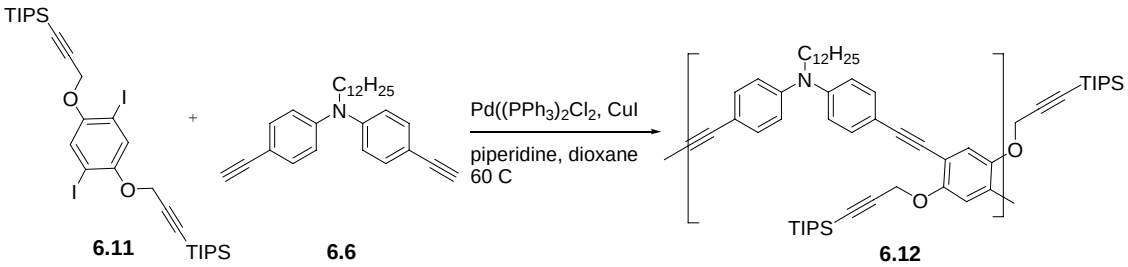

Scheme 6.3: Synthesis DPA polymer with alkynyl side groups

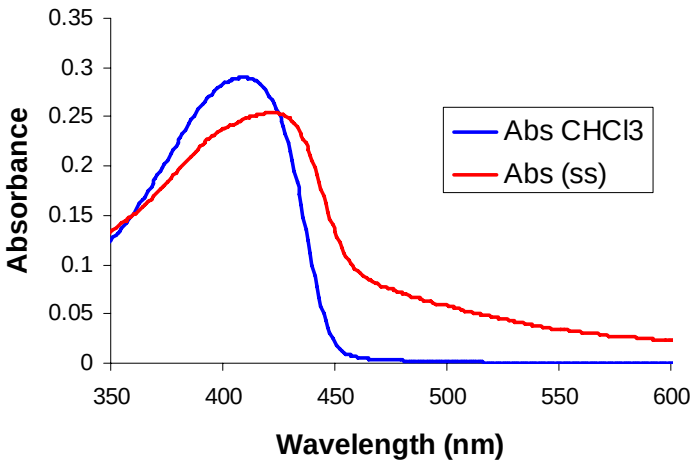

Figure 6.3 Absorption of polymer **6.12**

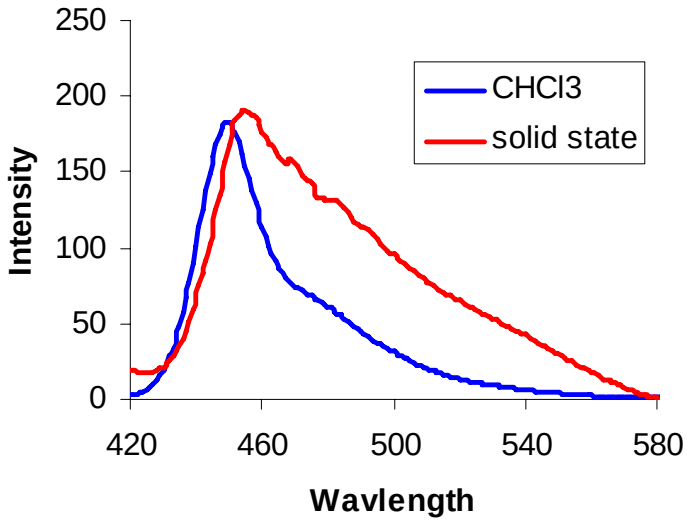

Figure 6.4 Emission spectra of polymer **6.12** in chloroform solution and the solid state.

It was of interest to investigate the effect of using a different type of monomer such as fluorene into the backbone of the polymer rather than using a benzene containing monomer. The synthesis of a fluorene containing DPA polymer, **6.16,** is shown in Scheme 5.4. The TMS protected monomer **6.14** is formed using the previously synthesized brominated fluorene **6.13** under HCSH conditions. Subsequent deprotection using KOH/EtOH forms the diethynyl substituted fluorene **6.15**. This monomer **6.15** undergoes polymerization with **6.14** to yield the polymer **6.16** as a yellow solid.

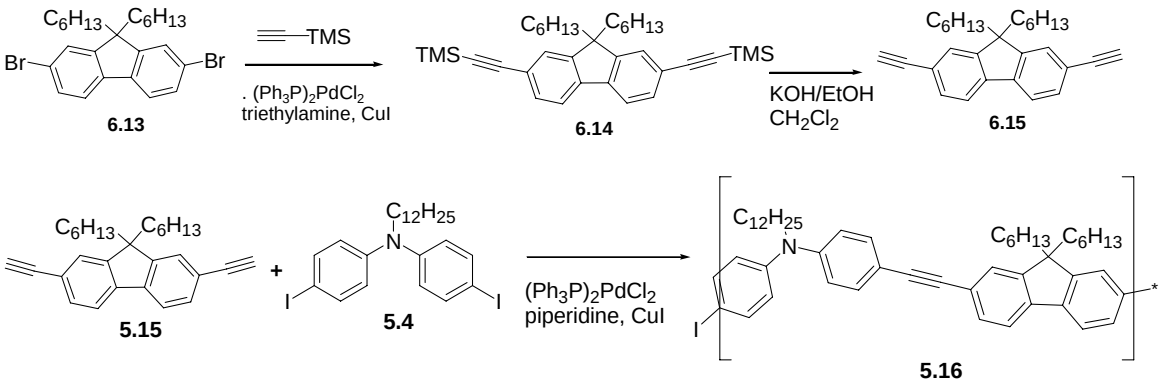

Scheme 6.4: Synthesis of a fluorene-DPA polymer

The absorption and emission spectra of **6.16** are shown in Figure 5.5. The polymer is fluorescent in chloroform solution but the fluorescenece is quenched upon addition of trifluoroacetic acid.

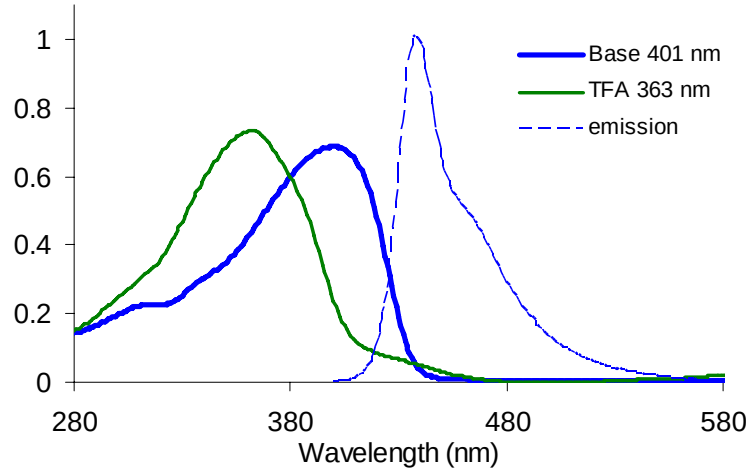

Figure 6.5: Absorption and emission of **6.16**

The synthesis of a fluorenone-DPA polymer can be seen in Scheme 6.5. The fluorenone has been chosen in order to yield energy transfer to low bandgap segments. This allows for a red shift in absorption and emission. This synthesis begins with the iodination of fluorene **6.7** followed by the oxidation to the fluorenone to form 2.7-diiodofluorenone **6.18.** Monomers **6.6** and **6.19** are reacted under HCSH conditions to produce polymer **6.20.**

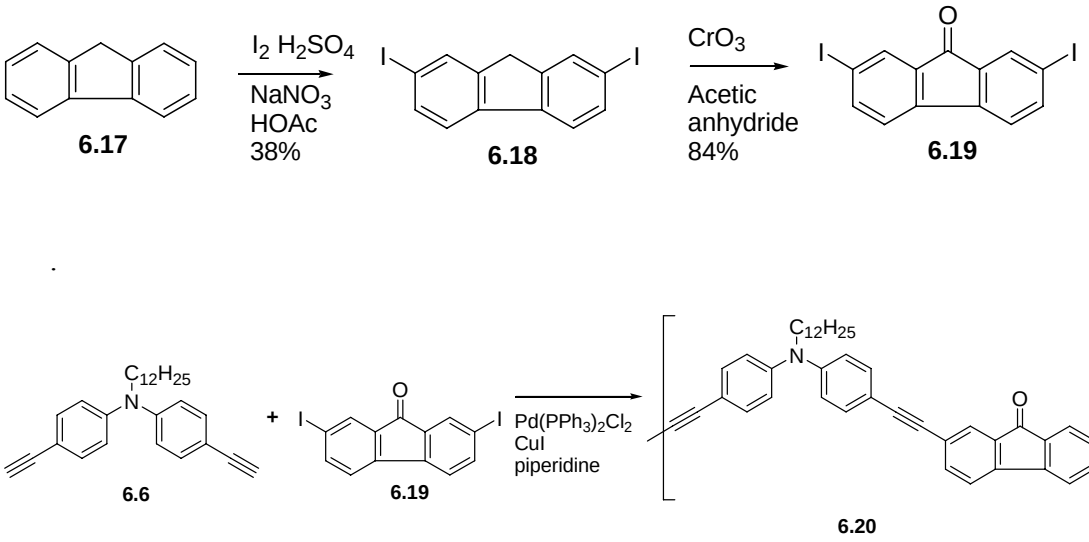

Scheme 6.5: Synthesis of a fluorenone-DPA polymer **6.20**

The absorption and emission spectra for **6.20** can be seen in Figure 6.6 This polymer is orange fluorescent in a thin film but is not fluorescent in a solution of chloroform. However, in a solution of THF the polymer is weakly yellow emissive. When it is dissolved in dioxane, the polymer is moderately emissive, but not as emissive as standard PPE's or the other DPA polymers presented here.

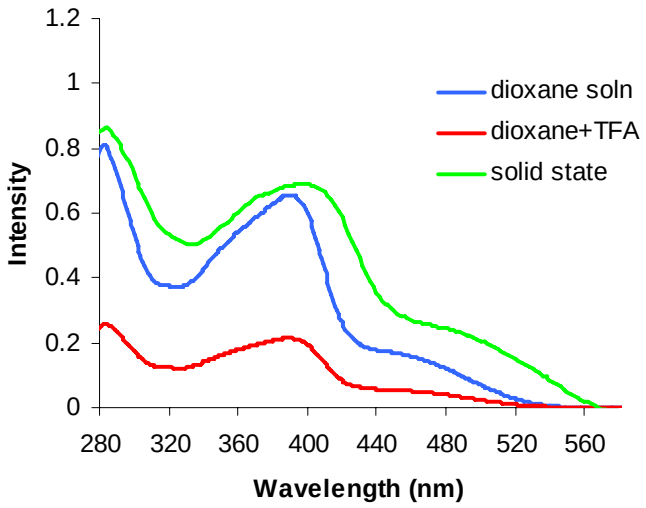

Figure 6.6: Absorption of **6.20.**

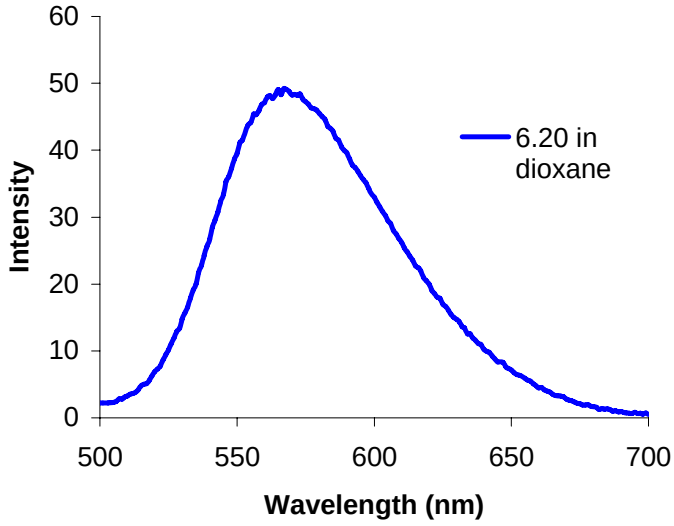

Figure 6.7. Emission of **6.20.**

The synthesis of the dihydroxy-DPA polymer is important in further synthesis of a redox-active quinone containing polymer. As seen in Scheme 6.6, the DPA **6.6** is reacted under Pd-catalyzed conditions with a protected hydroquinone **6.21** to form polymer **6.22.** Subsequent deprotection gives polymer **6.23** in a reasonable yield. The absorption and emission spectra of **6.22** can be seen in Figure 6.8.

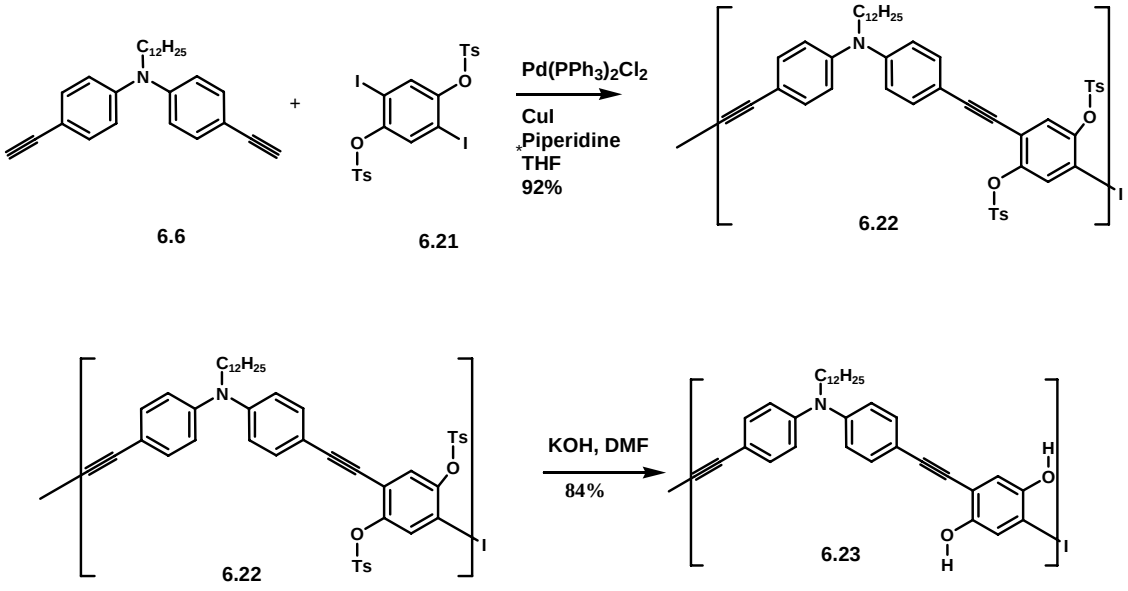

Scheme 6.6: Synthesis of hydroquinone polymer **6.22** and **6.23**

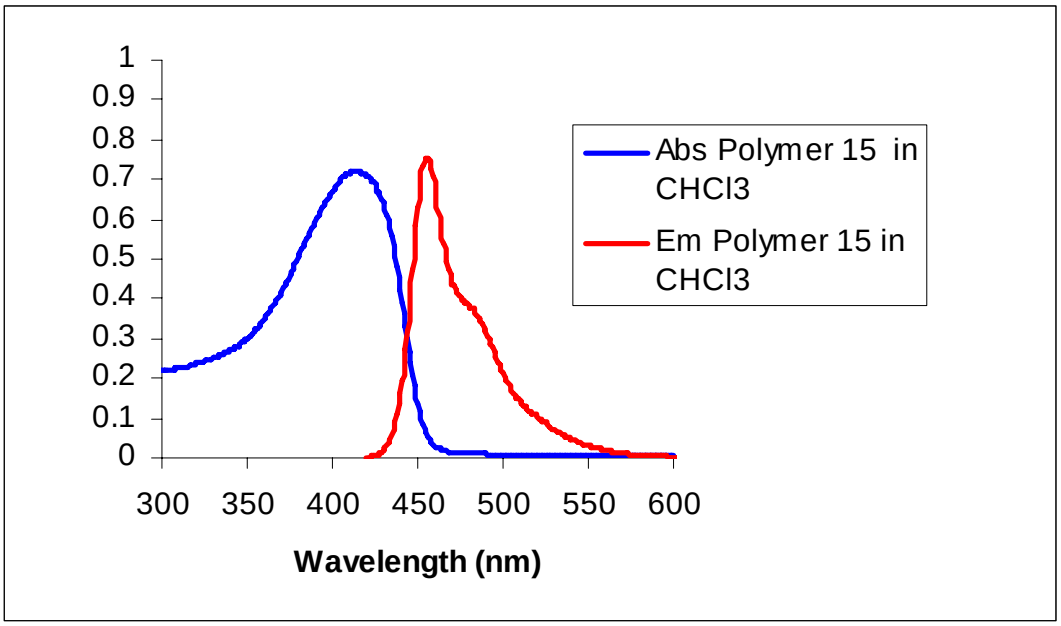

Figure 6.8: Absorption and emission of **6.22.**

6.3 Conclusion

These polymers are the first of this type of DPA polymers to be synthesized. It can bee seen that DPA can be incoorperated into a PAE backbone rather easily. These polymers demonstrate interesting properties in absorption and emission especially with respect to the change of comonomer. The absorption and emission are valuable due to their sensitivity towards change in pH. One future goal for this project would be to examine the influence of metals on these polymers.

5.4. Experimental

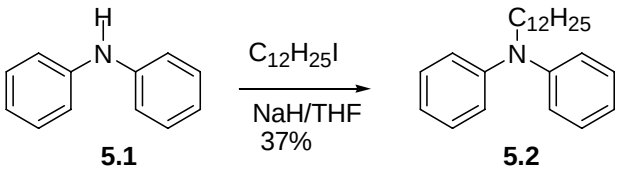

5.1 **5.2**

Didodecyl-diphenyl-amine (5.2) Diphenylamine **5.1** (15.0 g, 88.75 mmol) is dissolved in dry THF in an oven dried Schlenk flask equipped with a condenser under nitrogen atmosphere. NaH (2.23 g, 92.9 mmol) is added and the reaction is heated at 65˚C for 1 h. 1-iodododecane (80 mL, 399.37 mmol) is added and the reaction is refluxed for 18 h. The reaction is cooled to room temperature and quenched with ice. The solution is extracted with ether and dried over sodium sulfate. The solvent is removed in vaccuo. The resulting liquid is purified by column chromatography over silica with eluent hexane to yield **5.2** (11.08 g, 37%) as a colorless oil. ^{1}H-NMR ($CDCl_3$) δ 7.38-7.32 (m, 4H, aryl-H), 7.11-7.08 (m, 4H, aryl-H), 3.81, 3.78, 3.76 (t, 2H, alkyl-H), 1.79, 1.77, 1.75 (t, alky.H), 1.40, 1.38, 1.37 (alkyl-H), 1.01, 0.99, 0.97 (alkyl-H). ^{13}C-NMR ($CDCl_3$) δ 147.93, 129.98, 120.88, 52.35, 31.87, 29.8, 29.37, 27.49, 27.15, 22.72, 14.19.

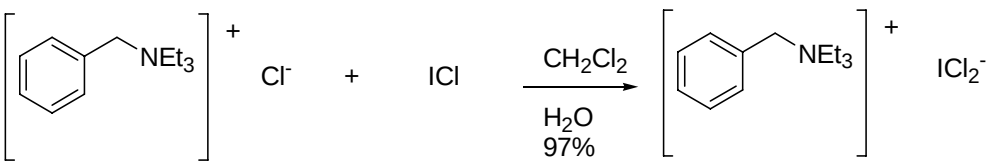

5.3

$BTEAICl_2$ (5.3) BTEACl (45.6g, 0.20mol) is dissolved in 200 mL of water, and ICl (32.5 g, 0.20 mol) is dissolved in 400 mL CH_2Cl_2. The H_2O solution is slowly added dropwise to the ICl solution. The solution is initially brown, then becomes yellow. CH_2Cl_2 is added, and the organic is separated. The solvent is removed, and the crude product is crystallized twice from 3:1 CH_2Cl_2:ether. The product **5.3** is isolated as a yellow solid (75.7 g, 97%).

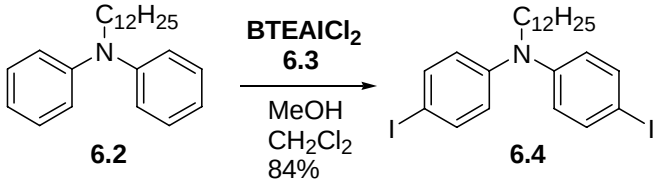

Dodecyl-bis-(4-iodo-phenyl)-amine (**6.4)** Dodecyl-diphenyl-amine **6.2** (11.14 g, 0.0330mol) is dissolved in 100 mL CH_2Cl_2. $BTEAICl_2$ (27.04 g, 0.0693 mol) is dissolved in 100 mL of methanol and added to the CH_2Cl_2 solution. $CaCO_3$ (10.0 g) is added last, and the reaction is stirred for 14 h. The mixture is filtered to remove the excess $CaCO_3$. The solvent is removed in vaccuo and the crude product is dissolved in ether and washed with a 5% $NaHSO_3$ aqueous solution. The ether fraction is washed three times with water, and the solvent is removed in vaccuo to yield **6.4** (16.41g, 84%) as a colorless oil. ^{1}H-NMR ($CDCl_3$) δ 7.54, 7.52 (d, 4H, aryl H), 6.77, 6.74 (D, 4H, aryl H), 3.65, 3.63, 3.60 (t, 2H, alkyl H), 1.63 (alkyl H), 1.28 (alkyl H). ^{13}C-NMR ($CDCl_3$) δ 146.96, 137.96, 83.85, 52.22, 31.93, 29.65, 29.61, 29.59, 29.40, 29.37, 27.22, 27.02,

22.74, 14.24. IR cm^{-1} (KBr) 2951.85, 2922.92, 2851.56, 1589.23, 1574.77, 1486.05, 1466.76, 1359.72, 1309.58, 1277.75, 1244.97, 1187.10, 1057.88, 1005.81, 810.05, 743.51, 718.43.

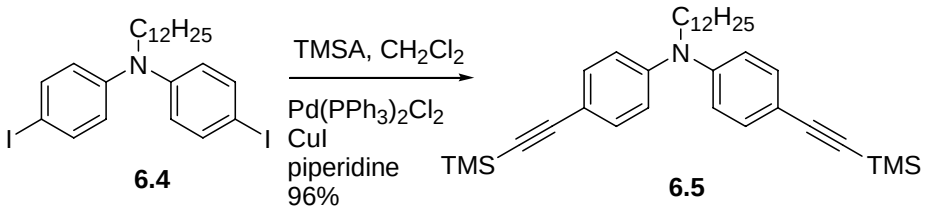

Dodecyl-bis-(4-trimethylsilanylethynyl-phenyl)-amine (6.5). In a nitrogen purged 100 mL Schlenk flask, **6.4** (3.39 g, 5.75 mmol)) is dissolved in CH_2Cl_2 (20 mL) and piperidine (1 mL). $Pd(PPh_3)_2Cl_2$ (0.052 g, 0.073 mmol) and CuI (0.014 g, 0.073 mmol) are added next, and the reaction is capped. TMSA (2.14 mL, 14.3 mmol) is added via syringe. The reaction is stirred for 12 h. The resulting solution is washed with a 10% NH_4OH solution and extracted with hexane. The hexane is washed with water and extracted with hexane. The organic fraction is dried over sodium sulfate. The organic fraction is filtered over alumina oxide neutral to yield **6.5** (2.84 g, 93%) as a colorless oil. ^{1}H-NMR ($CDCl_3$) δ 7.59 (s, 4H, aryl-H)), 7.19 (s, 4H, aryl-H), 2.61, 2.57, 2.54 (t, 2H, alkyl-H) 1.72, 1.70,1.69 (t, 2H, alkyl-H), 1.28-.1.20 (m, alkyl-H), 0.28-0.80 (m, alkyl-H), 0.231 (s, 9H, Si-CH_3 H). ^{13}C-NMR ($CDCl_3$) δ 147.32, 133.01, 120.34, 115.49, 105.35, 92.89, 52.15, 31.98, 29.69, 29.63, 29.41, 27.44, 27.06, 22.78, 14.23, 0.21.

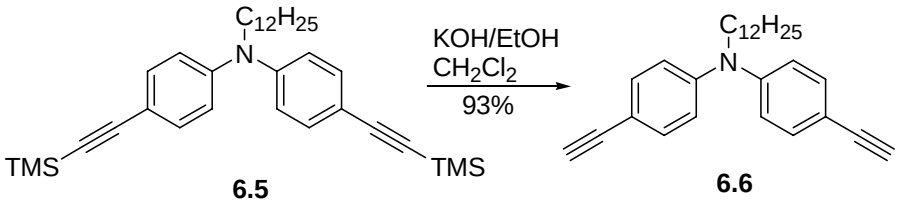

6.5 6.6

Dodecyl-bis-(4-ethynyl-phenyl)-amine (6.6). In a 100 mL round bottomed flask, **6.5** (900 mg, 1.7 mmol) is dissolved in CH_2Cl_2. A 10% wt KOH/EtOH solution (1 mL) is added and the reaction is stirred for 30 min. The solvent from the solution is removed. The crude mixture is washed with water and extracted with hexane. The solvent is remove to yield **5.6** (0.654 g, 99%) as a colorless oil ^{1}H-NMR ($CDCl_3$) δ 7.42 (d, 4H, aryl-H), 6.97, 6.94 (d, 4H, aryl-H), 3.72, 3.69, 3.67 (t, 2H, alkyl-H), 3.033 (s, 2H, ethynyl-H), 1.65, 1.29, 0.93, 0.92, 0.89 (alkyl-H). ^{13}C-NMR ($CDCl_3$) δ 147.40, 133.10, 114.5, 83.76, 76.21, 52.14, 31.34, 29.66, 29.60, 29.38, 27.36, 27.02, 22.74, 14.19.

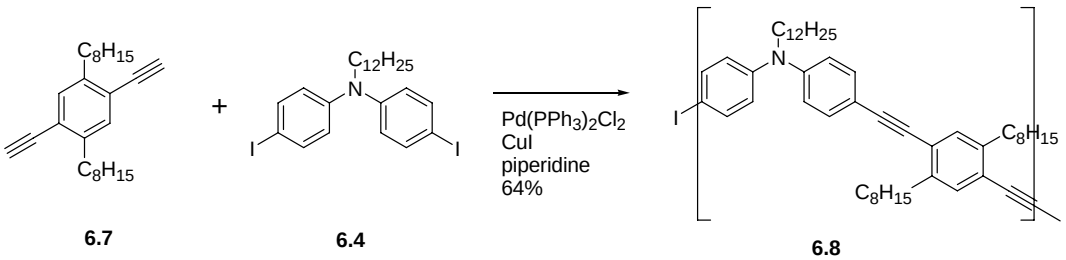

6.7 6.4 6.8

Polymer (6.8). In a nitrogen flushed 25 mL tubular Schlenk flask under nitrogen atmosphere, **6.4 (**200 mg, 0.519 mmol) and **6.7** (287 mg, 0.519 mmol) are dissolved in

piperidine (3 mL) and THF (1 mL) under nitrogen stream. The catalysts $Pd(PPh_3)_2Cl_2$ (0.0182g, 0.00259 mmol) and CuI (0.0049g, 0.00259 mmol) are added and the reaction is capped and heated at 60˚C for 48 h. The reaction mixture is added dropwise to MeOH (500 mL), and a yellow precipitate forms. The mixture is filtered to obtain **5.8** (210 mg, 64%) as a yellow solid. ^{1}H-NMR ($CDCl_3$) δ 7.60, 7.58, 7.33, 7.02, 6.928,6.91, 6.87, 6.84, 3.69, 2.76, 1.82, 1.67, 1.29, 0.91. ^{13}C-NMR δ 147.25, 147.08, 146.89, 132.46,132.42, 124.37, 122.64, 120.52, 118.02, 115.93, 115.07, 94.05,88.17, 87.96, 84.99, 52.29, 40.28, 38.60, 32.59, 32.24, 31.98, 29.70, 29.46, 29.41, 28.99, 28.76, 27.50, 27.38, 27.08, 25.65, 23.22, 22.78, 14.25, 10.91. MW=7400.

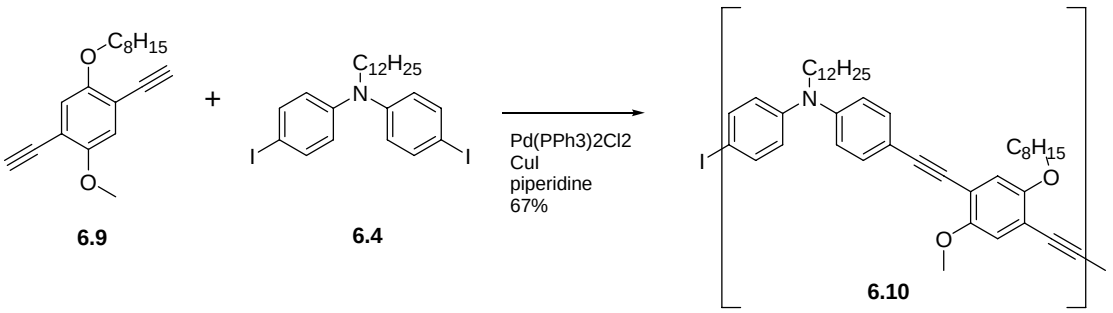

Polymer (6.10). In a nitrogen flushed 25 mL tubular Schlenk flask under nitrogen atmosphere, **6.4** (2.08g, 3.54 mmol) and **6.9** (1 g, 3.54 mmol) are dissolved in piperidine (3 mL) and THF (1 mL) under nitrogen stream. The catalysts $Pd(PPh_3)_2Cl_2$ (0.0247 g, 0.0354 mmol) and CuI (0.006g, 0.0354 mmol) are added and the reaction is capped and heated at 60˚C for 48 h. The reaction mixture is added dropwise to MeOH (500 mL), and a yellow precipitate forms. The mixture is filtered to obtain **6.10** (2.62g, 67%) as a yellow solid. ^{1}H-NMR ($CDCl_3$) δ 7.43, 7.26, 6.98, 4.82, 3.73, 1.67, 1.26, 1.06, 0.89.

^{13}C-NMR ($CDCl_3$) 152.35, 147.20, 132.59, 120.43, 118.91, 115.71, 114.34, 101.79, 95.47, 89.86, 84.80, 58.42, 52.27, 31.98, 29.68, 29.49, 29.41, 27.56, 27.14, 22.77, 18.64, 14.22, 11.23. IR 2953.78, 2923.66, 1594.06, 1519.80, 1464.83, 1368.40, 1260.39, 1216.03, 1182.28, 1034.74, 818.73, 802.33, 760.87, 668.29. MW=8801.

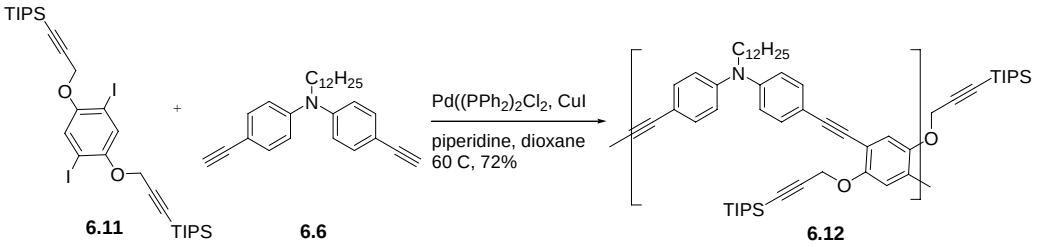

(6.12) In a nitrogen flushed 25 mL tubular Schlenk flask under nitrogen atmosphere, **6.11** (2.00, 2.67 mmol) and **6.6** (1.03 g, 2.67 mmol) are dissolved in piperidine (3 mL) and THF (1 mL) under nitrogen stream. The catalysts $Pd(PPh_3)_2Cl_2$ (0.0187, 0.0267 mmol) and CuI (0.0051g, 0.0267) are added and the reaction is capped and heated at 60˚C for 48 h. . The reaction mixture is added dropwise to MeOH (500 mL), and a yellow precipitate forms. The mixture is filtered to obtain **6.12** (1.69 g,72%) as a yellow solid. ^{1}H-NMR δ 7.43, 7.26, 6.97, 4.81, 3.72, 1.66, 1.25, 1.05, 0.88. ^{13}C-NMR 152.29, 147.19, 132.68, 120.39, 118.82, 115.68, 114.26, 101.76, 95.43, 89.84, 84.77, 58.39, 52.26, 31.96, 29.67, 29.41, 27.50, 22.77, 18.62, 14.22, 11.20. MW=7200.

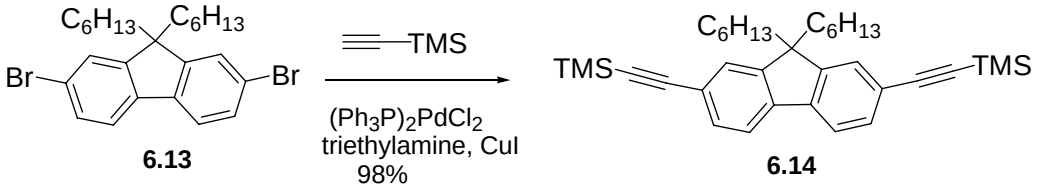

6.13 **6.14**

9,9-Dihexyl-2,7-bis-trimethylsilanylethynyl-fluorene (6.14) In a Schlenk flask under nitrogen atmosphere, **6.13** (4.00g, 8.16 mmol), $Pd(PPh_3)_2Cl_2$ (0.057 g, 0.082 mmol), CuI (0.0156 g, 0.082 mmol), and PPh_3 (0.05 g, 0.082 mmol) are dissolved in triethylamine, and the reaction capped. TMSA (2.00 g, 20.4 mmol) is added via syringe, and the reaction is heated at 85˚C for 24 h. The reaction solution is cooled to room temperature and washed with a 10% NH_4OH solution and extracted with hexane. The hexane extract is washed with a 25% HCl solution and extracted with hexane. This hexane layer is washed with H_2O and extracted with hexane and dried over $MgSO_4$ and filtered. The solvent is removed to yield, and the crude solid is recrystallized from ethanol to yield **6.14** (4.21 g, 98%) as a colorless solid. ^{1}H-NMR δ 7.65 (d, 2H), 7.62 (d, 2H) 7.45 (d, 2H), 7.43 (d, 2H), 7.34 (m, 2H), 2.58, 2.57, 2.56 (t, 2H, alkyl-H), 1.38 (m, alkyl-H), 1.12 (m, alkyl-H), 1.10 (t, 6H, alkyl-H) ^{13}C NMR ($CDCl_3$) δ 150.72, 140.69, 131.09, 126.07, 121.67, 119.73, 106.07, 94.17, 55.22, 40.43, 55.22, 40.43, 31.62, 29.76, 23.69, 22.71, 14.11, 0.18.

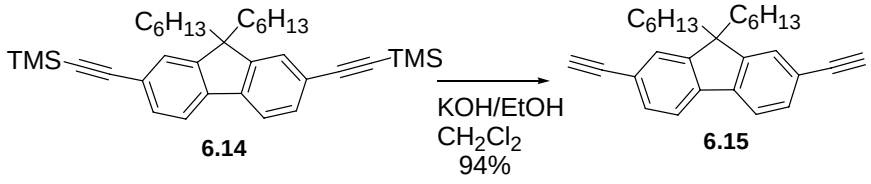

9,9-Dihexyl-2,7-bis-ethynyl-fluorene (6.15) 6.14 (1.5 g, 2.85 mmol) is dissolved in CH_2Cl_2 (20 mL) followed by the addition of a 10% wt solution of KOH in ethanol (2 mL). The reaction is stirred at room temperature for 1h. The solvent is removed and the crude product is dissolved in hexanes and washed 3 times with water (50 mL). The resulting solid is purified over a silica gel plug with hexanes. The solvent is removed in vaccuo to yield **6.15** (1.02g, 94%) as a pale yellow solid. ^{1}H-NMR ($CDCl_3$) δ 7.52, 7.38, 3.02 (s, 2H, ethynyl H), 2.61 (t, 4H, alkyl H), 1.29 (m, alkyl H), 0.85 (m, alkyl H). ^{13}C-NMR ($CDCl_3$) 142.35, 135.83, 130.28, 126.59, 121.34, 120.59, 81.98, 78.94, 55.36, 40.92, 31.53, 30.78, 24.65, 22.34, 14.71.

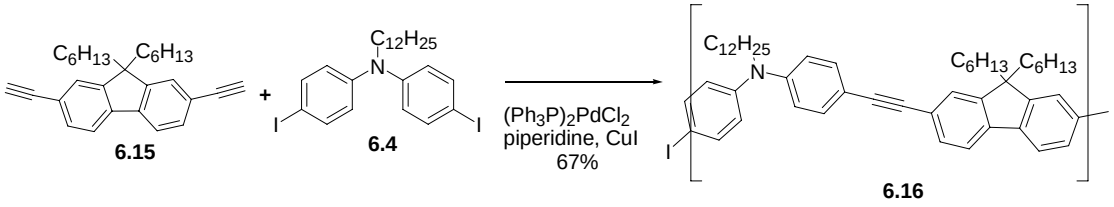

(6.16) 6.4 (1.00g, 1.69 mmol) is dissolved in piperidine (5 mL) in a 25 mL Schlenk flask under nitrogen atmosphere. The catalysts, $Pd(PPh_3)_2Cl_2$ (12 mg, 0.0169 mmol) and CuI (3 mg, 0.0169 mmol) are added, and the reaction is capped. The reaction is stirred for 48 h. at 65˚C. The resulting mixture is added dropwise to MeOH (500 mL). A yellow

precipitate is formed. This precipitate is filtered, and **6.16** is obtained (67%) as a fluorescent yellow solid. ^{1}H-NMR δ 7.35, 7.13, 6.98, 2.53, 2.51, 1.99, 1.97.

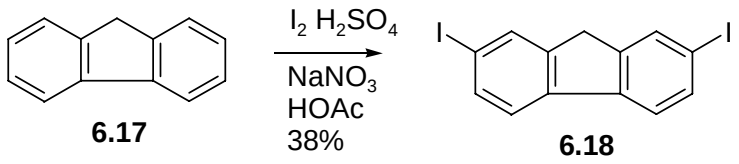

6.17 **6.18**

2,7-diiodofluorene (6.18). Fluorene (**6.17**) (25.0 g, 150 mmol) was dissolved in glacial acetic acid (1500 mL) while stirring in a round bottom flask equipped with a dropping funnel. I_2 (53.3 g, 210 mmol) was ground into a fine powder and added to the solution, followed by the addition of $NaNO_3$ (6.00 g, 70.6 mmol). H_2SO_4 (75 mL) was added dropwise over a period of 30 min. When all the H_2SO_4 had been added, a second portion of $NaNO_3$ (6.00 g, 70.6 mmol) was added followed once again by H_2SO_4 (75 mL). During the addition of this second portion of H_2SO_4, a color change from dark purple to a light red was observed, and a light precipitate was formed signaling that the reaction was complete. The mixture was washed with a concentrated Na_2SO_3 solution, filtered, washed further with cold acetic acid, and finally with copious amounts of H_2O. To the solid was added some warm EtOH and then refiltered, removing some of the monoiodide. The product was recrystallized from isopropanol affording **6.18** (24.1 g, 38 %) as a light yellow solid; m.p. 213-214 °C. ^{1}H NMR ($CDCl_3$) δ 7.86 (s, 2H), 7.70-7.67 (m, 2H), 7.47 (d, 2H, *J* = 8.0 Hz), 3.82 (s, 2H); ^{13}C NMR ($CDCl_3$) δ 144.8, 140.4, 136.0, 134.1, 121.6, 92.4, 36.3.

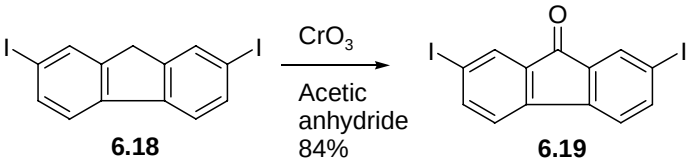

6.18 **6.19**

2,7-diiodofluorenone (6.19). CrO_3 (24.0 g, 240 mmol) was added to a suspension of **6.18** (41.8 g, 100 mmol) in acetic anhydride (600 mL) while stirring at room temperature for 12 h. The reaction mixture was poured slowly into 500 ml of a 2% HCl solution at 0˚C, filtered, and recrystalized from 2-propanol yielding **6.19** (36.2 g, 84%) as yellow needles; Mp.= 209-210 °C. ^{1}H NMR ($CDCl_3$): δ 7.60 (d, 2H), 7.46 (dd, 2H), 7.37 (dd, 2H). ^{13}C NMR ($CDCl_3$) δ = 190.6, 143.4, 142.9, 134.8, 133.5, 122.1, 94.4.

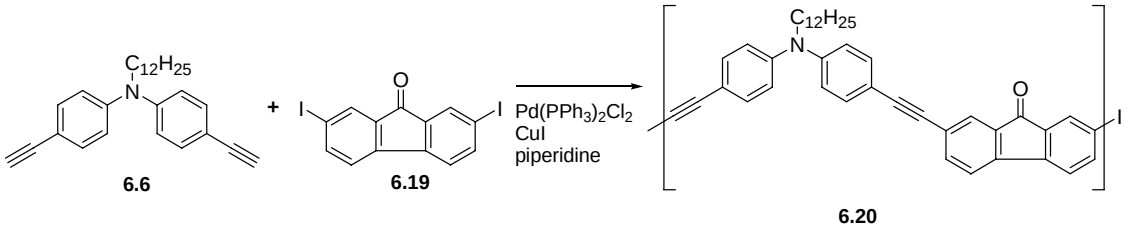

6.6 **6.19** **6.20**

Polymer (6.20) The DPA compound **6.19** (0.222 g, 0.514 mmol) is dissolved in piperidine (2 mL) in a tubular Schlenk flask under a nitrogen atmosphere. The catalyst, $Pd(PPh_3)_2$ (3.4 mg, 0.000514 mmol) and CuI (1.0 mg, 0.000514 mol) are added, and the reaction is capped. The diethynyl compound **6.6 (**0.198g, 0.514 mmol**)** is dissolved in

piperidine (1 mL) and added to the reaction mixture via syringe. The reaction is stirred at 60 ˚C for 48 h. ^{1}H NMR ($CDCl_3$): δ 7.93, 7.77, 7.43, 7.25, 6.99, 3.71, 1.65, 1.25, 0.87.

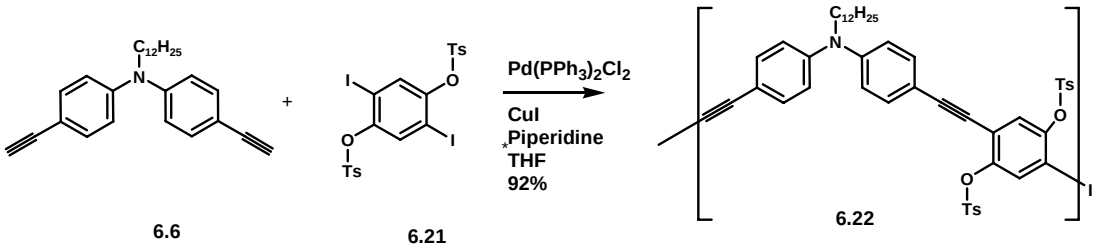

(Polymer 6.22) 6.21 (0.174 g, 0.259 mmol) is added to a tubular Schlenk flask under nitrogen atmosphere and dissolved in piperidine (1 mL) and THF (2 mL). The catalysts, $Pd(PPh_3)_2Cl_2$ (10.8 mg, 0.00259 mmol) and CuI (4.9 mg, 0.00259 mmol) are added and the reaction is capped. **6.6** (4.9 mg, 0.00259 mmol) is dissolved in piperidine (1 mL) and added via syringe. The reaction is heated to 60˚C and stirred for 48 h. The crude mixture is added dropwise to methanol (500 mL). A brownish-yellow solid precipitated. The solution is filtered and the solid is dissolved in CH_2Cl_2 and repriciptated from methanol (500 mL) and filtered to yield **6.22** (92%) as a yellow solid. ^{1}H NMR ($CDCl_3$): 7.36, 7.34, 7.33, 7.15, 3.45, 3.44, 3.43, 2.52, 2.44, 2.41, 2.40.

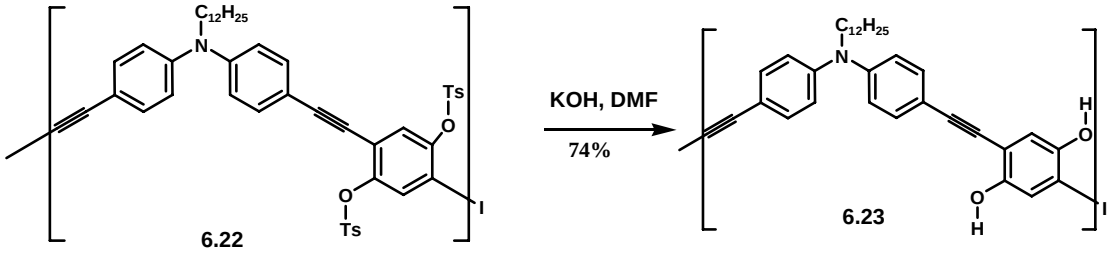

(Polymer 6.23) 6.22 (100 mg, 0.149 mmol) and KOH are dissolved in DMF and the reaction is stirred for 72 h at 50˚C. The reaction mixture is initially yellow and then turns dark brown. The mixture is added drop wise into methanol (500 mL) to give a dark brown solid which is filtered to yield **6.23** (0.054 g ,74%) ^{1}H NMR ($CDCl_3$): δ 7.63, 7.61, 7.58, 7.56, 2.86, 2.50, 1.66, 1.27, 1.24, 0.88.

6.5 References

1. a) Bunz, U. H. F. *Chem. Rev.* **2000**, *100*, 1605; Giesa, R.. b) Bunz, U. H. F. *Acc. Chem. Res.* **2001**, *34*(12), 998-1010. c) Bunz, U. H. F. *Adv. Polymer. Sci.* **2005**, *175*, 1-53. d) Bunz, U. H. F. *Chem. Rev.* **2000**, *100*, 1605-1644.
2. Swager, T. M. *Acc. Chem. Res.* **1998**, *31*, 201.
3. Montali, A.; Smith, P.; Weder, C. *Synth. Met.* **1998**, *97*, 123.
4. Weder, C.; Sarwa, C.; Montali, A.; Bastiaansen, G.; Smith, P. *Science* **1998**, *279*, 835.
5. Samori, P.; Francke, V.; Müllen, K.; Rabe, J. P. *Thin Solid Films* **1998**, *336*, 13.
6. Tang, C. W.; Van Slyke, S. A. *Appl. Phys. Lett.* **1987**, *51*, 913.
7. Adachi, C, Tsutsui, T.; Saito, S.; *Appl Phys. Lett*. **1989**, 55, 1489.
8. Adachi, S.; Tokito, T.; Tsutsui, T.; Saito, S.; *J. Appl Phys*, **1988**, L269.
9. Kim et al. *Synthetic Metals*, **2001**, *122*, 363-368.
10. Yang, J.S; Swager T. M. *J.Am.Chem.Soc*. **1998**,*120*,5321,11864